Doctoral Dissertation
Doctoral Program in Civil and Environmental Engineering (32nd Cycle)

MIX DESIGN AND PERFORMANCE ASSESSMENT OF SELF-COMPACTING CEMENT-BOUND MIXTURES FOR PAVEMENT FOUNDATIONS OF ROAD TUNNELS

Eldho Choorackal Avirachan

Supervisors
Prof. Ezio Santagata
Dr. Pier Paolo Riviera

Politecnico di Torino
February 25, 2020

I hereby declare that, the contents and organisation of this dissertation constitute my own original work and does not compromise in any way the rights of third parties, including those relating to the security of personal data.

…….....

Eldho Choorackal Avirachan

Turin, February 25, 2020

Summary

The road networks play a major role in economic development and social integration, and road tunnels are an integral part of such networks. This doctoral thesis discusses works carried out to develop self-compacting cement-bound mixtures (hereafter indicated as SC-CBMs) specifically designed for the construction of pavement foundations in the road tunnels. The suitability of SC-CBMs was examined for application in pavement foundations through a series of experimental activities. A newly developed mix design procedure for SC-CBMs, assessment of their performance-related properties, incorporation of such mixtures in the design of pavements are described in three parts in this thesis.

In the first part of the thesis, an experimental investigation that focused on self-compacting cement-bound mixtures to be employed for paving applications is described. A significant quantity of secondary raw materials such as Reclaimed Asphalt Pavement (RAP) and mineral sludge was included along with natural aggregates in the formulation of the SC-CBMs. Recipes of the investigated mixtures were defined by optimizing the packing of the aggregate skeleton and by checking the flowability characteristics of cement pastes and composite mixtures. Long-term stiffness and strength properties were evaluated through triaxial and quick shear tests. Based on the obtained results and their interpretation, a mix design procedure was proposed.

Further investigation was conducted focusing on the performance-related characterization of their thermal properties in the second part. In particular, the study was performed to assess the suitability of these mixes in situations that require the backfilling of buried high-voltage transmission cables. The use of SC-CBMs with superior thermal conductivity in the thermal backfills increase the current carrying capacity of cables.

In the third part of the thesis, performance characteristics of the SC-CBMs, which were produced in a concrete batch plant, were studied using laboratory and

field tests. Investigated properties included flowability, compressive strength, resilient modulus and bearing capacity. It was found that mixtures prepared with a cement dosage of up to 100 kg/m^3 possess the required properties of flowability, strength and stiffness. On the contrary, mixtures with higher cement dosages (150 kg/m^3 and 200 kg/m^3) fail to meet all the performance-related requirements as a result of their high long-term strength which jeopardizes excavatability. Obtained results also highlighted the effects of the different components on the properties of the mixtures and led to the definition of acceptance criteria which can be adopted for the quality control in actual construction works. A case study of pavement design in a road tunnel was further conducted, where relevant data about the temperature and traffic was collected from an actual pavement in a road tunnel. In particular, a full-scale test section was constructed with the use of self-compacting cement-bound mixtures in the subgrade and foundation, overlaid by two asphalt layers. The subsequent investigation included Falling Weight Deflectometer (FWD) measurements and laboratory tests, which were carried out for the assessment of volumetric and mechanical properties of laid mixtures. Different pavement cross sections were analyzed by making use of these material properties, the additional advantages related to the greater efficiency of construction operations in tunnels and the lower consumption of virgin aggregates were also discussed.

Based on this research, conclusions were drawn concerning the behavior of self-compacting cement-bound mixtures in pavement foundations, their performance as thermal backfills and the feasibility of incorporating them in the pavement design. Moreover, possible developments of future research were highlighted.

Acknowledgements

I would like to thank my supervisors Prof. Ezio Santagata and Dr. Pier Paolo Riviera for their continuous support and guidance related to all the activities of my research. Working with Prof. Santagata was a great learning experience and I am grateful to him for providing me this opportunity for doing PhD in his research group. I will cherish all the fruitful discussions we had on several topics that were never confined only to my research interests. The help I received from the professor in preparing and reviewing articles for journal publications was significant. Dr. Pier Paolo was a helping hand who was always available for discussions. He was very supportive in trying out new ideas at the laboratory and helpful in the completion of my experimental activities. I will always admire him as a great person. I would also like to thank my thesis examination committee for their valuable suggestions.

I would extend my thanks to everyone in the Road materials laboratory of Politecnico di Torino for their consideration and support during the past years. I would like to specially mention Lucia, Davide, Beppe and my PhD colleagues for their support in and out of the laboratory.

I would like to gratefully acknowledge the financial and technical support of SITALFA S.p.A., ITINERA S.p.A. and SITAF S.p.A. which they provided during different experimental investigations. Special thanks to Arianna for acting as the link between Politecnico and SITALFA which helped in the planning of field trials.

I would also like to acknowledge the help I received from master's students Gabriele Zisa, Andres Albrieu, Michele Airoldi, Maria Cristina, Luigi Dolce, Pietro Perlini in conducting different experiments. I would also like to thank Peppino, Riccardo and Matteo for their help in the laboratory with different testing equipments.

I would like to propose thanks to my friends in Torino and back home for their support in times of need. I would like to specially mention Riyaz and Mahesh with whom I had several discussions about my PhD life. Finally, to my wife Divya and my family, without them, I would not have achieved anything in life. I cannot thank Divya enough for her support and understanding in all these years while we were staying miles apart.

Contents

List of tables

List of figures

List of publications

International journal publications

[1] E. Choorackal, P.P Riviera and E. Santagata, "Mix design and mechanical characterization of self-compacting cement-bound mixtures for paving applications," *Construction and Building Materials*, vol. 229 pp.116894, Dec 2019, https://doi.org/10.1016/j.conbuildmat.2019.116894

[2] E. Choorackal, P.P Riviera, D. Dalmazzo, E. Santagata, L. Zichella and P. Marini, "Performance-related characterization of fluidized thermal backfills containing recycled components," *Waste and Biomass Valorization*, pp.1-12. Mar 2019, https://doi.org/10.1007/s12649-019-00650-9

[3] E. Santagata, E. Choorackal and P.P Riviera, "Self-compacting cement-bound pavement foundations for road tunnels: performance assessment in field trials," Under review in the *International Journal of Pavement Engineering*.

[4] P.P Riviera, G. Bertagnoli, E. Choorackal, and E. Santagata, "Controlled low-strength materials for pavement foundations in road tunnels: feasibility study and recommendations," *Materials and Structures*, vol. 52(4), p.72. Aug 2019, https://doi.org/10.1617/s11527-019-1367-4

International conference presentations

[5] E. Choorackal, P.P Riviera, D. Dalmazzo, E. Santagata, L. Zichella, and P. Marini, "Reuse of recycled asphalt pavement and mineral sludges in fluidized thermal backfills," *6th International Conference on Sustainable Solid Waste Management*, Naxos Island, Greece, 13–16 Jun 2018.

[6] P.P Riviera, E. Choorackal, and E. Santagata, "Performance evaluation of innovative and sustainable pavement solutions for road tunnels," in: *Proceedings of the 5th International Symposium on Asphalt Pavements & Environment (APE)*. ISAP APE 2019. *Lecture Notes in Civil Engineering*, vol 48. Springer, Cham, 11-13 Sep 2019, https://doi.org/10.1007/978-3-030-29779-4_40

Notation list

Acronyms and abbreviations

AASHTO	American Association of State Highway and Transportation Officials
AS	Mineral Sludge
ASTM	American Society for Testing and Materials
CBM	Cement-Stabilized Mixture
CBR	California Bearing Ratio
CLSM	Controlled Low-Strength Materials
CTB	Cement Treated Base
D	Diameter of aggregate particles (in mm),
D_s	Diameter of flow spread
D_{max}	Maximum diameter of aggregate particles (in mm)
D_{min}	Minimum diameter of aggregate particles (in mm)
Ev	Strain modulus
EALFs	Equivalent axle load factors
EWC	European Waste Catalogue
FWD	Falling Weight Deflectometer
FTB	Fluidized Thermal Backfills
ICP	Inductively Coupled Plasma
k	Thermal conductivity (expressed in W/(m·K))
LTPP	Long-Term Pavement Performance
M_r	Resilient Modulus
MEPDG	Mechanistic- Empirical Pavement Design Guide
NM	Neher-McGrath
P(D)	Cumulative percentage passing the sieve D
PSI	Present Serviceability Index

q	Distribution modulus
q_h	Heating power of the needle
RAP	Recycled Asphalt Pavement
RCA	Recycled Concrete Aggregate
R^2	Coefficient of determination
SAPEM	South-African Pavement Engineering Manual
SCC	Self-Compacting Concrete
SC-CBM	Self-Compacting Cement-Bound mixtures
SCM	Supplementary Cementitious Material
SEM	Scanning Electron Microscopy
SG	Specific Gravity
SN	Structural Number
SS-D	Stone cutting sludge (Diamond Disc)
SS-F	Stone cutting sludge (Frame wire saw)
$T_{pav,p}$	Pavement design temperature
UCS	Unconfined Compressive Strength
w/c	Water to Cement ratio
w/p	Water to Powder ratio
XRD	X – Ray Diffraction
Δw_{12}	The percentage of mass loss after 12 cycles
Δl	The percentage of length change

Symbols

σ_3	Confining pressure
σ_d	Deviatoric stress
ε_r	Reversible strain
ε_p	Permanent strain
θ	Bulk stress
Co	Cobalt
Cu	Copper
Fe	Iron
Ca	Calcium
Ni	Nickel
Cr_{tot}	Chromium (total)
Pb	Lead
Zn	Zinc
Mg	Magnesium
Al	Aluminium
Si	Silica

1. Introduction

1.1 Road tunnels

There is an increased demand for underground structures like road tunnels due to the increased mobility needs of a growing population. Road tunnels are complex infrastructures, constructed with large scale financial investment and play an important role in the integration of different regions. Apart from connecting distant locations in the shortest route, they also facilitate passage of different utility lines, high-voltage cables and optical fiber networks through them. Approaching the design of this complex system from only one direction such as that of geology, civil engineering or alignment creates serious issues for their effective service. Control of this system can only be achieved by finding out appropriate solutions which take in to account all the related factors (Figure 1.1) [1]. Lack of realizing the complexities in such projects would lead to the wastage of resources and structures with functional deficiencies [1]. According to the available studies, 60-80% of the relative financial impact during the entire service life of road tunnels is governed by the decisions taken during its planning and design stage [2]. Considering these factors, the development of specific materials and methods suitable for application in pavements of road tunnels would improve the general construction quality and service life.

Pavements are classified into rigid, semi-rigid and flexible based on the materials used for the construction and load transfer mechanism. In particular, rigid pavements constructed with cement concrete are attractive in road tunnels from the fire safety aspects and long life [3, 4]. Countries like Austria have restricted to use only rigid pavements when the length of the tunnel is more than 1000 m [5]. Semi-rigid pavements are constructed with an asphalt surface layer over a chemically stabilized foundation layer. They are less popular than rigid pavements. However, if properly designed and constructed, they can offer a similar service life at lower initial investment [6]. Flexible pavements, which are constituted by bitumen-bound materials in their upper part, offer a good solution in terms of their remarkable riding comfort, lower initial investments, limited noise emission, easy maintenance, and superior skid resistance in comparison to rigid pavements [7, 8]. Easy availability of expert workforce and specialized machinery is another reason for the popularity of flexible pavements. The existing research and available guidelines on pavements in road tunnels are mostly related to the improvement of safety aspects concerning accidents and fire [9, 10, 11, 12, 13, 14]. The research for the development of advanced asphalt flame retardants and the use of nanomaterials to create flame-retardant tunnel asphalt pavements

are also in progress [15]. The contribution of bituminous layers to the total fire load and heat release is insignificant especially in case of fire originated from vehicle crashes [16]. However, porous asphalt pavements are not permitted in the road tunnels as it can cause the spread of flammable liquids to a greater area, in case of any leakage due to accidents. Other factors which may be considered when choosing pavement type include construction and life-cycle costs, availability of materials, local experience with involved technologies, and global impact on the environment [17, 18].

Figure 1.1 Road tunnel as a complex system (PIARC) [1]

The service life of pavements in tunnels is affected not only by the volume and intensity of traffic loading but also by the particular temperature regime which occurs throughout the year. As proven by direct measurements, in comparison to the case of open roadways, temperatures tend to be significantly higher and are characterized by a lower daily and seasonal variability in tunnels [19], thus leading to lower stiffness values of the upper pavement layers whenever they are composed of asphalt concrete (see Figure 1.2). Such an occurrence may be partially compensated by building stiff pavement foundations which contribute to the limitation of pavement deflections under loading and consequently to the enhancement of pavement life.

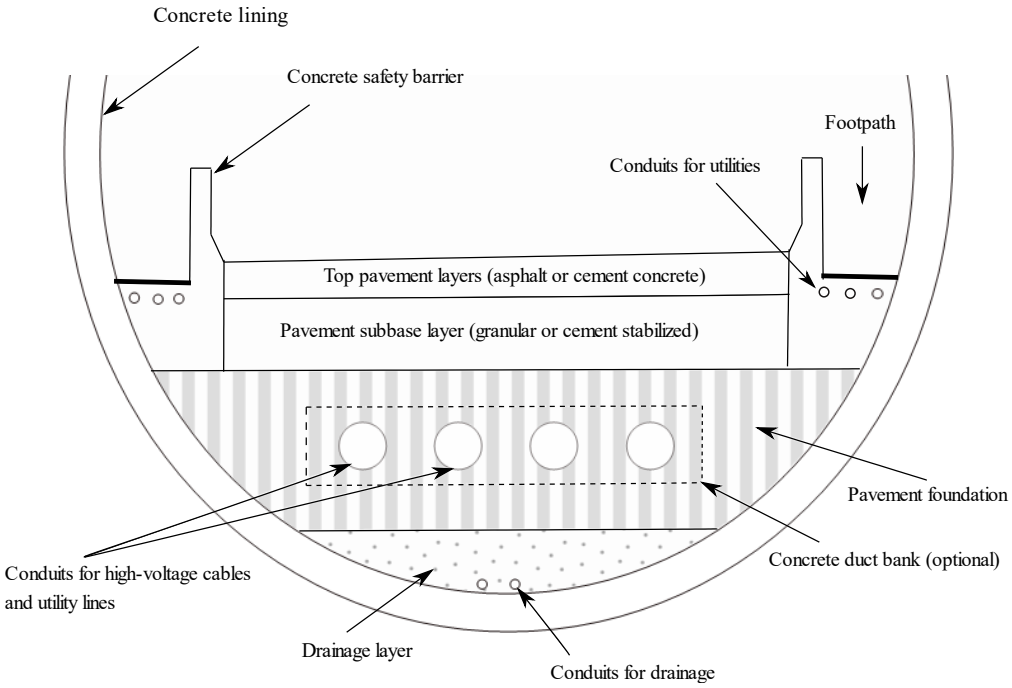

Figure 1.2 Typical cross section of pavement in road tunnel

1.1.1 Pavement foundations in road tunnels

Irrespective of the pavement type, designers have to define the pavement structure in all its details, including the constitution of foundation layers comprised between the base of the tunnel and the pavement, which have the main function of providing adequate bearing capacity [20]. Such a need, which is crucial in order to guarantee satisfactory performance, applies both to the case of tunnels with a rock substrate and those with underlying structural elements (i.e. curved inverts or linear shallow foundations). The subgrade, subbase and the base course together perform the structural functions of a pavement foundation. The main functions include the distribution of stresses from the vehicular loading to the subgrade during its service life with a reduced intensity so that it does not cause any permanent deformation in the subgrade. During construction of surface layers, the foundation layer should also act as an adequate platform for the construction traffic (haul trucks) as well as for placing and compaction of materials that are used for the formation of surface layers. Hence, the loading pattern that comes over the foundation layer is a combination of all these operations. It includes large intensity loading that occurs over directly over the layers for a very short time during the construction traffic, small intensity loading

that continues occur for a very long time during the service life and the relatively large intensity loading that may occur during the compaction of upper layers [21].

The composition of the pavement foundations in tunnels may have a relevant impact on the quality of construction operations, on the service life of the infrastructure, and on maintenance activities which may be necessary over time. With respect to construction operations, one of the key factors which need to be considered in the selection of the foundation material is its compaction behavior [22]. This is especially true in those cases in which road tunnels house important utility lines (e.g. high-voltage transmission cables and optical fiber networks) that are buried below the top pavement layers in sets of conduits which sometimes may be encased in Portland cement concrete duct banks (see Figure 1.2). When placing the foundation material, care should be taken in reaching the required target density and in filling all voids and cavities which are created by the complex arrangement of embedded pipes. However, when applying compacting efforts by means of rollers, such an operation may be of limited efficiency and may also pose the threat of damaging the conduits and the utilities themselves. Furthermore, the use of rollers in tunnels may significantly impact the economics and logistics of construction works.

Another aspect which needs to be considered when analysing the functions of pavement foundations in tunnels is their thermal conductivity, which affects the ampacity of buried high-voltage lines [23, 24]. Ampacity is defined as the maximum current-carrying capacity of a line which is a function of the maximum temperature that can be reached by the cables. In practical terms, the foundation material should have a sufficiently high thermal conductivity in order to efficiently dissipate the heat generated by the current, thereby guaranteeing the long-term integrity of the line.

Typical pavement foundations which are adopted in practice involve the placement of a filling which is constituted in its bottom portion of a coarse-grained unbound material (that ensures proper drainage) and in its upper part of selected soil (that acts as a subgrade) [20]. However, as an alternative option, cement-bound materials can also be employed to form the entire filling. In particular, it may be advantageous to employ self-levelling cement-bound mixtures with high thermal conductivity, which can be placed by simply pumped up to the desired thickness, with no need for compaction, thereafter achieving a homogeneous state even in the presence of buried underground utilities and drainage conduits. Cement-bound pavement foundations in road tunnels are required to achieve a sufficient short-term bearing capacity in order to withstand the loading of construction equipment and hauling trucks within a very short time after their placement. Furthermore, laid mixtures should not develop an excessive long-term strength in order to allow excavations to be easily performed in case of maintenance needs for the buried utilities and in order to reduce the potential for reflective cracking. Maintenance activities may be necessary in the course of time

whenever malfunctioning of the underground utilities occurs or when these need to be upgraded. Thus, it is essential for the pavement foundation to be easily excavatable, thus allowing the conduits to be accessed with the use of limited demolition efforts which should not jeopardize their integrity [25]. After completion of maintenance, repair of the foundation should take place by following procedures which are similar to those of initial construction in which compaction issues once again need to be taken into account.

1.1.2 Cement-treated pavement foundations

Cement, lime or any similar hydraulic binder can be used for the stabilization of foundation layers for creating a stiffer foundation layer, depending on the target properties and availability [26]. Recently attempts have been made to include several waste materials such as recycled concrete aggregate (RCA), reclaimed asphalt pavement (RAP) and other construction and demolition (C&D) wastes into the cement-treated base layers due to the associated economic-environmental benefits and lower expectations from their mechanical properties [27, 28, 29, 30]. Difficulty in obtaining suitable stabilized foundation materials at the site, absence of a construction technique which can produce stabilized foundations with consistently good quality, and the threat of reflective cracking of the upper asphalt layers are some of the factors [31] that prevent pavement engineers from the use of stabilized foundation layers in road tunnels.

Classical cement-treated pavement foundations are constructed through a two-step process. Initially, granular aggregates mixed with cement are placed in layers of designated thickness. Subsequently, layers are compacted at optimum moisture content to achieve the desired density and thickness. When unbound granular layers are replaced by cement stabilized layers of higher strength, there is a shift in the critical strain location under vehicle loading (Figure 1.3). It moves to the bottom of the cement stabilized layer from the bottom of the asphalt layer [32]. Thus, cement-treated granular layers are subjected to fatigue with the generation of tensile cracks. In the case of pavements in tunnels, cement-treated mixtures are also used for invert filling and construction traffic would be passing over it until the completion of other top layers. As a result, compressive strains could develop at the top, leading to rutting and permanent deformation of the layers. This phenomenon can also occur for unpaved roads constructed with cement-bound layers. Load-bearing characteristics of unbound granular materials and chemically stabilized materials change depending on the kind of particle packing, binder content and moisture content. Unbound granular materials and modified granular materials fail in deformation and disintegration through shear, densification and breakdown. Cemented materials with higher cement content fail in cracking due to fatigue, shrinkage and over-stressing [20]. Diligent quality control measures need to be ensured when such materials are used for construction [33].

There are several incidents of premature failure of pavements that had happened when cement-treated layers are used in the pavement foundation. Rutting and alligator cracking due to a weak cement-treated base was observed in a pavement section by Chen [31], ingress of moisture to the base material and further loss of its mechanical properties was noted in this case. Scullion and Harris investigated three cement treated base layers (CTB) that had undergone severe deterioration soon after the construction [34]. Wheel path alligator cracking and severe pumping were the main consequences of failure. The presence of entrapped water and expansive clay minerals within the base layers and use of CTBs with different thermal expansion coefficients and shrinkage coefficients over one another resulted in the debonding of the layers and transverse cracking. Moreover, the use of higher cement and water content than the optimum during compaction would cause premature failures [31].

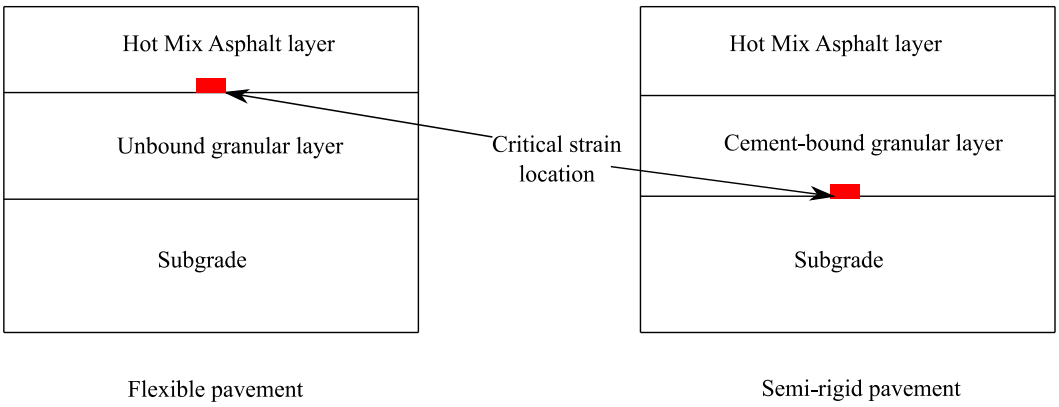

Figure 1.3 Shift in the critical strain location

The integration of good material design practices with sound structural design lead to long-lasting pavements. Mechanistic-Empirical pavement design guides that are used for the design of pavements do not deal with the preparation of cement-bound mixtures or their mix design procedures. However, pavement design guidelines such as SAPEM and Austroads provide presumptive values of elastic modulus for the cement-treated pavement materials based on either their unconfined compressive strength or flexural strength [35, 36, 14]. There is a lack of clarity on the selection of presumptive values when other alternate materials are used in the foundation layers. The tests for the performance assessment of such materials typically consist of UCS, resilient modulus and flexural strength [37]. However, the selection of cement-stabilized pavement foundation materials based only on their unconfined compressive strength is a widely adopted practice.

1.2 Self-compacting cement-bound mixtures

Use of cement-bound or cement-stabilized mixtures in pavement construction are quite common due to the remarkable contribution they can provide to the enhancement of bearing capacity [38, 39, 40, 41]. Past studies have widely discussed their mix design and performance-related characterization, and as a consequence they are included as standard materials in technical specifications and design manuals [42, 20, 43].

Cement-bound mixtures that are conventionally used in pavement foundations are not self-compacting and need laying and compaction similar to unbound materials. There are no specific self-compacting cement-bound mixtures that were developed to construct pavement foundations. Flowable cement-bound mixtures possess abilities of self-levelling and self-compaction. These mixtures can be broadly classified into two, as self-compacting concrete (SCC) and controlled low-strength materials (CLSM) (Figure 1.4).

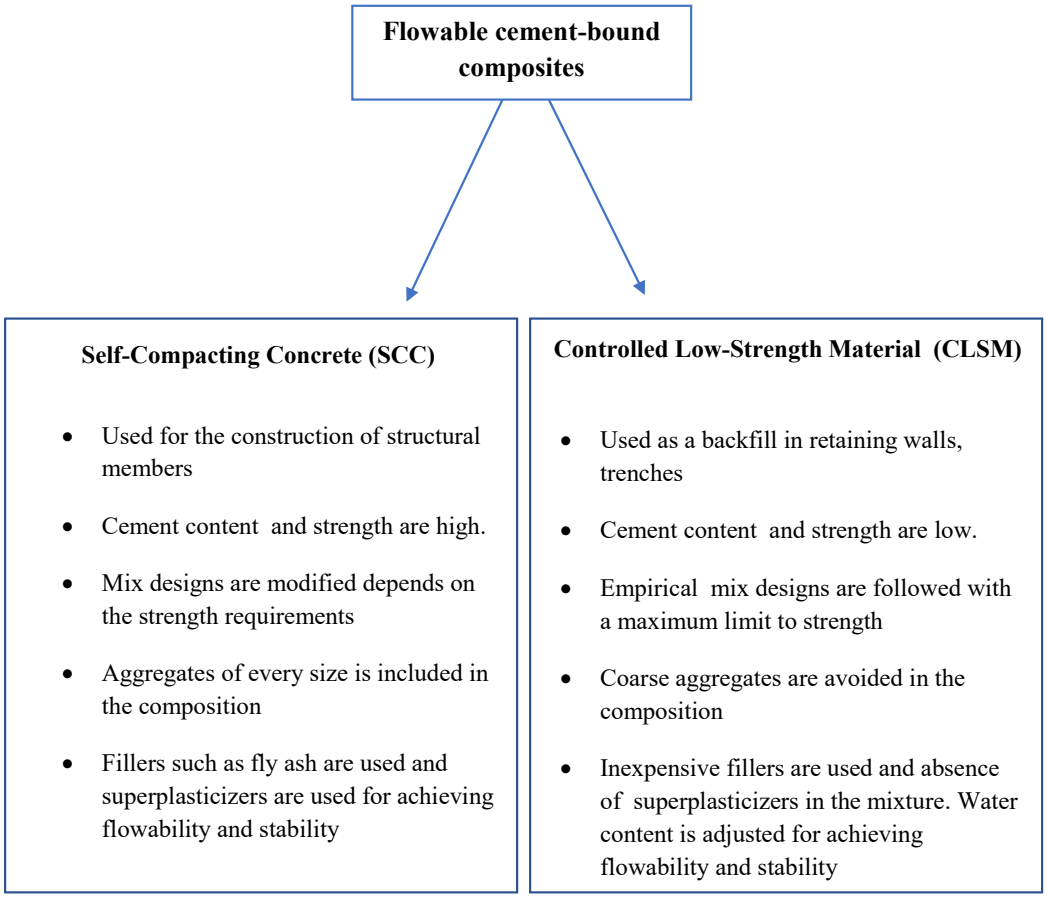

Figure 1.4 Classification of flowable cement-bound mixtures

In the specific case of road tunnels, the use of cement-bound mixtures can be of interest not only for the formation of the sub-base, but also for the construction

of the foundation, which is comprised between the base of the tunnel and the pavement [44, 45]. In particular, it may be attractive to make use of self-compacting cement-bound mixtures which can be quickly laid on site with no need of compaction even in the presence of a congested network of buried utilities [23]. As mentioned before, such mixtures are required to possess a limited strength, which corresponds to an acceptable excavatability, since they should allow easy access to buried conduits in case of maintenance. Furthermore, when designed with the supplementary objective of guaranteeing a low thermal resistivity, they can aid the dissipation of heat produced by high-voltage cables which are embedded in the pavement foundation [23, 46, 24].

Self-compacting concrete (SCC) was developed with a view of creating durable structures. This was especially necessary due to the reduction in the number of skilled workers who can perform compaction of conventional cement concrete. The ability to pass-through a congested reinforcement network increased the popularity of SCCs [47]. CLSMs, which contain a hydraulic binder, mineral aggregates and water, are self-compacting cementitious materials characterized by low binder content and high porosity [48]. They are typically employed for backfilling walls and trenches, for utility bedding, as subbases in bridge approaches, and for void filling applications in sewers, tunnel shafts, basements and other underground structures [25]. Their relatively low strength, which can be tailored by adjusting composition, makes them ideal materials for applications in which it is anticipated that there may be the need of future excavations to be carried out in order to access buried utilities without damaging them [49, 50, 51, 52].

Based on the discussion provided above, it can be concluded that an ideal foundation material for pavements in tunnels should possess several key properties which include self-compaction during construction, sufficient stiffness throughout the pavement service life, high thermal conductivity, thermal stability, and adequate excavatability. However, none of the conventional materials which are employed in typical tunnel construction operations exhibit properties which match the set of listed engineering requirements. Selected soils and granular mixtures, although easily excavatable, require thorough compaction after laying and are limited in stiffnesses. Furthermore, they usually have low thermal conductivity and may undergo undesired dry-out phenomena which further reduce such a property. Standard cement-bound materials (e.g. cement-stabilized mixtures and Portland cement concrete) present advantages in terms of their stiffness and with respect to their thermal properties, which are positively affected by the presence of Portland cement. However, they still require external compaction and may be difficult to remove from the cross section especially in the very long term. This thesis tries to address the above mentioned challenges by introducing a self-compacting cement-bound mixture for the construction of pavement foundations of road tunnels.

1.3 Research questions

The overall aim of this research was to design an innovative self-compacting cement-bound mixture for the construction of pavement foundation in road tunnels that satisfy all the necessary performance requirements. The first task to be completed in this direction was the formulation of a mix design procedure for the self-compacting cement-bound mixtures (SC-CBMs) with adequate mechanical properties and flowability. This led to the formation of the first research question.

i. How to design a self-compacting cement-bound mixture with recycled components as the main constituents, that is suitable for use in the foundation of the pavements in road tunnels?

The second problem to be addressed was related to thermal properties, which are important for the use of SC-CBMs in pavement foundations that contain buried high-voltage cables. This aspect is also relevant for the use of SC-CBMs in other applications like fluidized thermal backfills (FTB). This lead to the following second research question.

ii. How do the thermal properties of the self-compacting cement-bound mixture change with their composition? Is it possible to use them as fluidized thermal backfills for buried electrical cables?

The third task was formulated in order to evaluate the effectiveness of SC-CBMs through a series of field trials. The field trials were planned in such a way to optimize the composition and production procedures of SC-CBMs progressively. The results from the field trials were used to define a guideline for the production and quality control of SC-CBMs as noted in the following research question.

iii. How can production of SC-CBMs be ensured with consistently desired quality and how can guidelines be defined for the quality control of such mixtures to be laid in the field?

Finally, the feasibility of using SC-CBMs in pavement designs need to be demonstrated. This led to the final task of a case study, where the design of pavements with self-compacting cement-bound mixtures in the foundations was performed as pointed out in the following final research question.

iv. How can the developed SC-CBMs be incorporated into the mechanistic-empirical pavement design methods and how can they be compared to traditional pavement cross sections?

1.4 Layout of the work

This thesis is organized into three parts containing four chapters in total. (Figure 1.5). Each of the parts addresses a specific issue related to the self-compacting cement-bound mixtures, through chapters that answer each of the research questions listed in section 1.3. A review of relevant literature is presented in every chapter followed by the chosen research methodology and by the obtained results.

Part I: Mix design

The available research on the mix design of self-compacting cement-bound mixtures is reviewed. Selection of suitable raw materials for the SC-CBMs and formulation of a mix design procedure are described. Based on the mechanical characterization of the mixtures, a detailed flow chart for the mix design of SC-CBMs is provided in Chapter 2 of Part I.

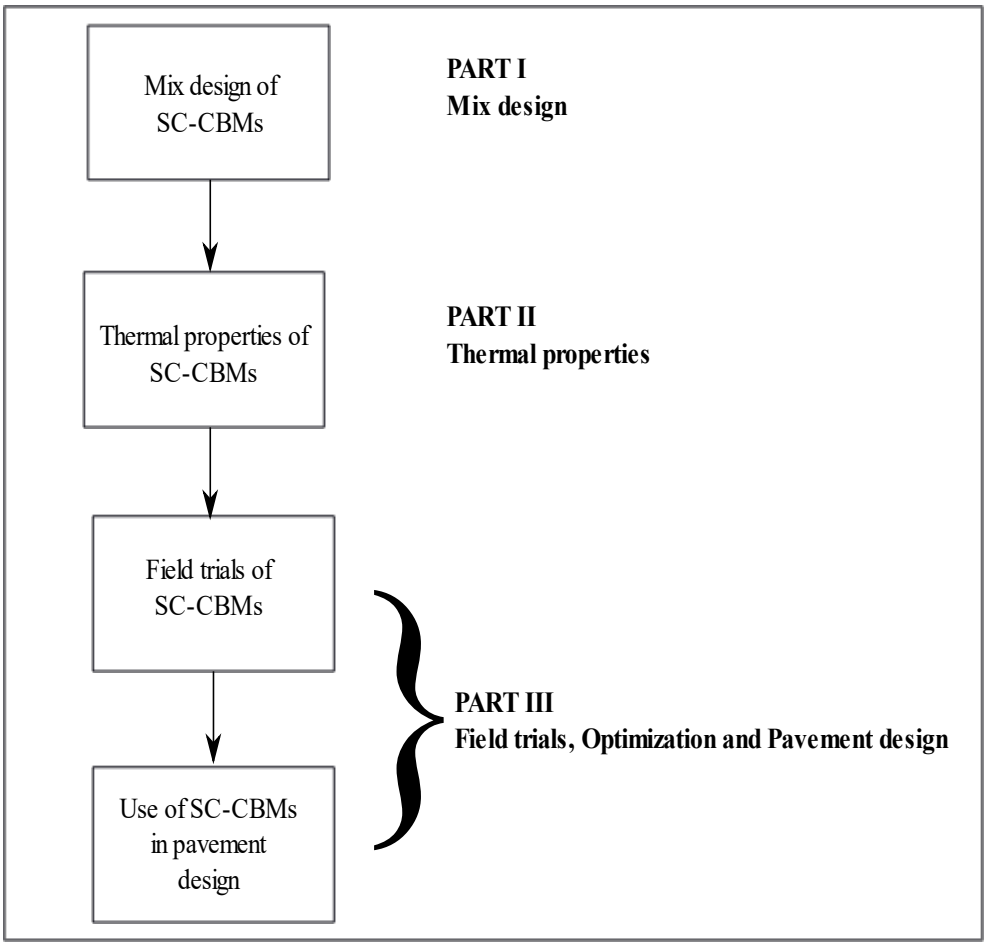

Figure 1.5 Flow chart depicting the scheme of the research

Part II: Thermal properties

The thermal properties of the SC-CBMs are examined in Chapter 3 of Part II. The role of thermal backfills in increasing the current carrying capacity of buried electrical cables is discussed. The performance assessment was conducted to check the feasibility of using SC-CBMs as fluidized thermal backfills and for backfilling underground transmission cables which need to buried in the pavement foundations of road tunnels.

Part III: Field trials, Optimization and Pavement design

An overview of the performance-related characterization of cement-bound mixtures used for pavement foundations is described in detail in this Part. Different field trials were planned progressively in order to optimize SC-CBM production procedures. The steps taken to resolve practical constrains are elaborated in this part of the thesis and finally, design guidelines and acceptance criteria are provided for the field application of SC-CBMs in Chapter 4. The design of pavements incorporating self-compacting cement-bound mixtures is also demonstrated in this part based on the data collection performed on the full-scale trial section. Moreover, a comparison is made with other standard pavement cross sections in Chapter 5. Finally, Chapter 6 of the thesis presents the general conclusions and recommendations for future studies.

Part I: Mix design

Some of the works described in this part has been previously published in the following:

- E. Choorackal, P.P Riviera and E. Santagata, “Mix design and mechanical characterization of self-compacting cement-bound mixtures for paving applications,” *Construction and Building Materials*, vol. 229 pp.116894, Dec 2019, https://doi.org/10.1016/j.conbuildmat.2019.116894

2. Mix design of self-compacting cement-bound mixtures

As the first step, the relevant literature on flowable cement-bound mixtures and pavement foundations was analyzed. The mix design principles of classical self-compacting cement-bound mixtures were learned to develop proposed self-compacting cement-bound mixtures (SC-CBMs) suitable for pavement foundations of road tunnels.

2.1 Mix design approaches

CLSMs were historically designed by following trial and error approaches. The flowability and compressive strength were fixed as the target properties and the composition of the mixtures were modified to reach the desired level of performance. In particular, Janardhanam et al. [53] proposed a mix design method which takes into account workability, setting time, mechanical properties and durability, while Bhat and Lovell [54] suggested a procedure which included the evaluation of unconfined compressive strength. Consideration was also given to the studies carried out by Bouzalakos et al. [55], which employed response surface methods to highlight the sensitivity of mixture behaviour to variations of the different components. Alizadeh [56] proposed a mix design procedure, that requires the combined adjustment of various ratios defining the composition of CLSMs. Recently there have been some attempts for the performance-based design of CLSMs (see Figure 2.1). This new approach still requires several trial and error attempts with different proportions of aggregates to find the optimum packing. Aggregates (A), binder (B) and water to solid ratio (W/s) were identified as the factors that control the performance of CLSMs.

The mix design methodology of SCC was developed with the target of achieving self-compaction under self-weight. This was achieved by limiting the aggregate content, adopting a low water/powder ratio and with the use of a superplasticizer (Figure 2.2). There was a progressive evolution in the mix design methodologies of SCC. Initially, it started as empirical and later became more performance-based focusing on particle packing and paste rheology [57]. The effect of particle size distribution in improving the properties of SCC was later studied in detail by various researchers [58, 59, 60].

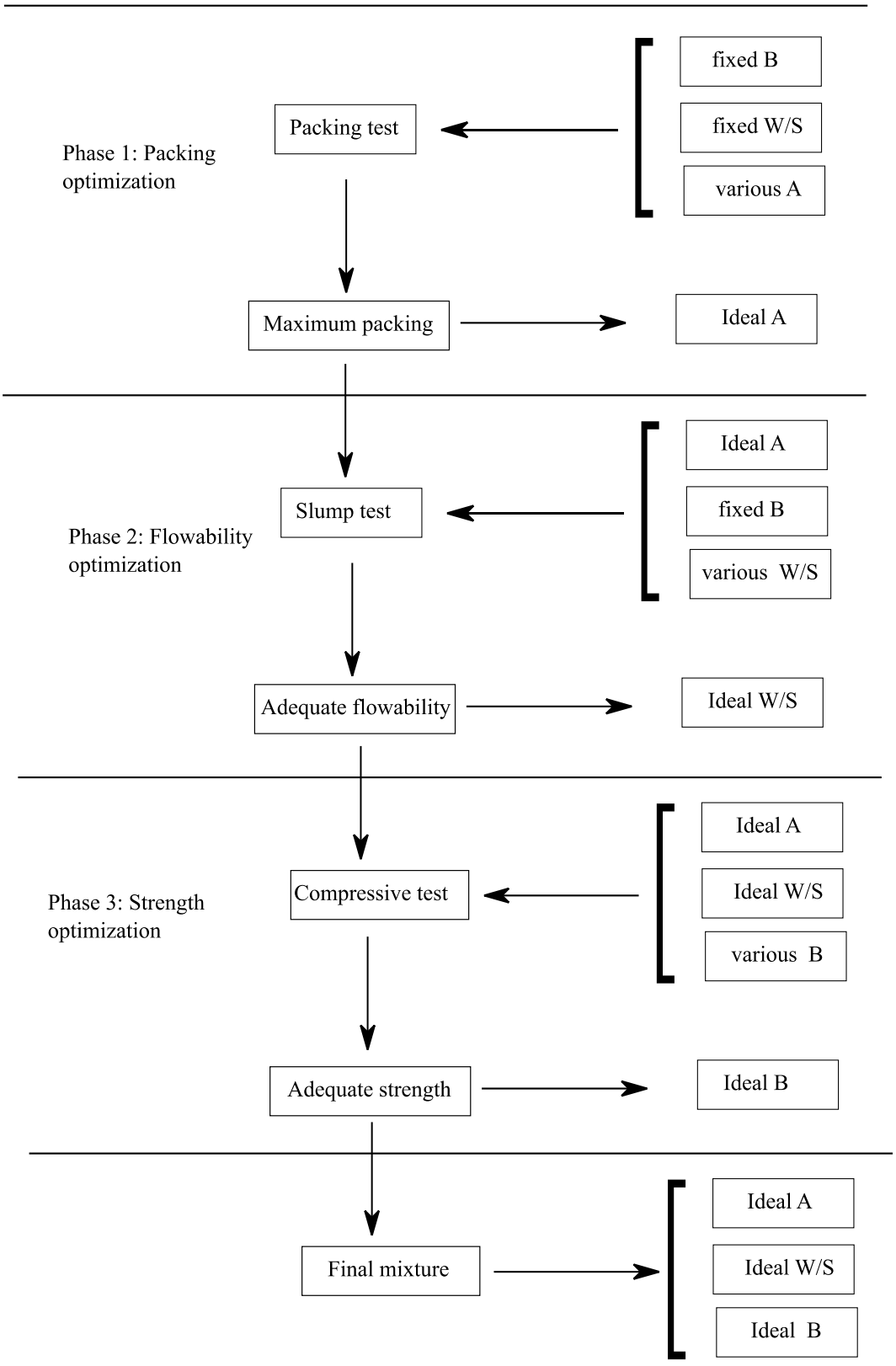

Figure 2.1 Mix design methodology adopted for CLSMs [61]

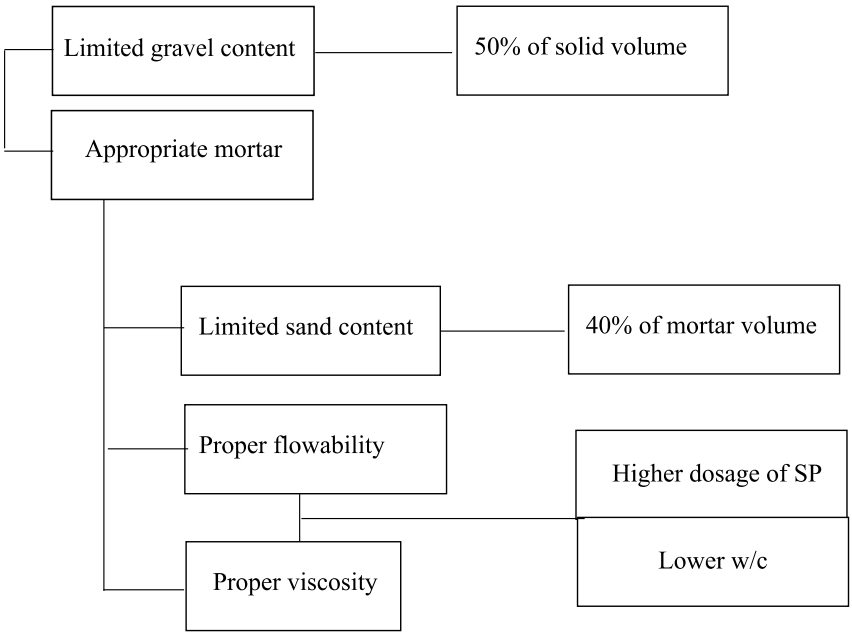

Figure 2.2 Strategies to achieve self-compaction in SCC [47]

The main properties of SCC are the filling ability, passing ability and segregation resistance [62, 63]. Several fillers like fly ash, blast furnace slag, marble dust, quarry dust were used in the composition of SCCs with the target of improving flow properties [64, 65, 66]. The replacement of cement by other pozzolanic fillers resulted in more economical mixtures and enhanced the long term strength by the formation of secondary hydration products, although it had caused a delay in the initial strength development. Other recycled aggregates have also been used in the formulation of SCCs. The use of recycled concrete aggregates in SCCs was reported by several researchers [67, 68, 69] and difficulty in achieving high strength was noted in this case. Reduced elastic modulus and increased strain capacity were reported when recycled tyre particles were used as the aggregates [70]. Inclusion of steel fibers was proposed as a method to improve the fatigue strength of SCCs when recycled shredded tyres were used in their composition [71].

There are different approaches to the mix design of SCC. The basic principle behind the mix design is to pack the aggregate fraction to its maximum dense state, followed by the creation of enough paste in the mix by adjusting the water/cement ratio and the finer fraction of the mix. The superplasticizers and viscosity modifying agents are also used in the mix to reduce the water content to decrease the segregation tendency of constituent materials and to increase the fluidity of the mixtures. Okamura proposed an initial mix design methodology for the SCC [72]. A simplified mix design methodology was later proposed by Su [73]. Several other methods of mix designs were proposed by other researchers [74, 75, 76, 77, 78, 79]. Initially, these mix designs were empirical in their

approach, but later aggregate packing models and rheological properties were considered for the mix design. The main considerations of the different widely used mix design methodologies for SCC are summarized below.

Okamura's and Nan Su' s mix design methods

Okamura's method limited many parameters such as mortar volume and coarse aggregate content for achieving optimum granular skeleton [47, 72]. This is commonly known as the Japanese method of SCC mix design. Nan Su introduced the idea of the packing factor to the mix design (Figure 2.3). The packing factor was defined as a ratio of the density of aggregates in the SCC mix to the density of aggregates in its bulk. This ratio was fixed empirically and the quantity of fine aggregates and coarse aggregates were determined. Cement quantity was fixed based on the strength requirement and powder quantity was determined from volumetric calculations. Water quantity was a function of the required fluidity of pastes [73]. Both the above mix design methodologies did not consider the particle size distributions of the constituent materials in detail while designing the mix.

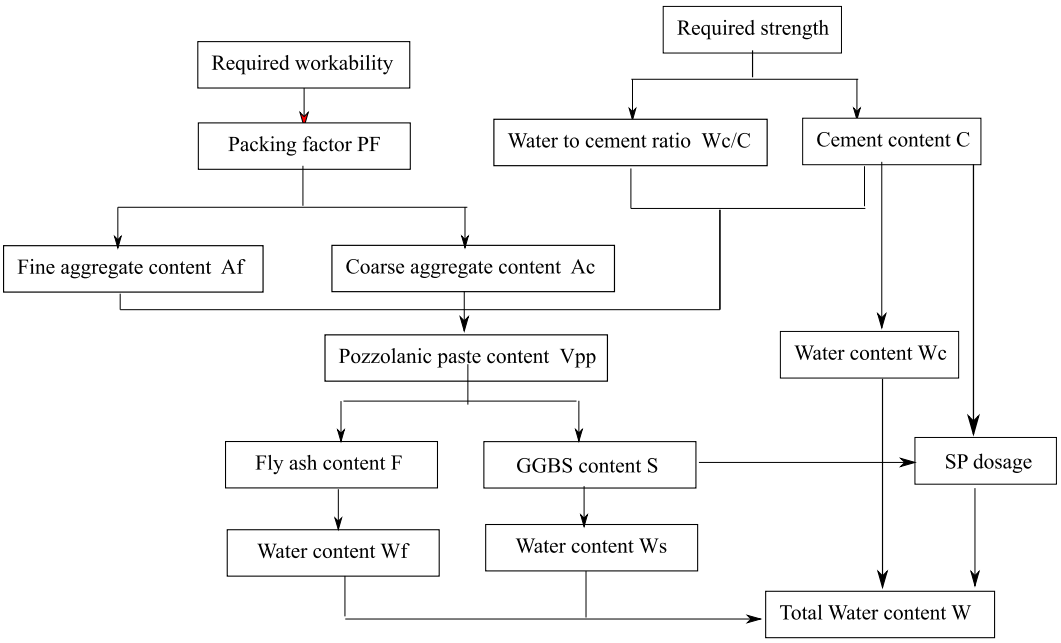

Figure 2.3 Mx design methodology proposed by Nan Su [73, 57]

Brouwers' mix design method

Brouwers suggested a mix design methodology where the particle size distribution of all the constituent materials was integrally considered and optimized to achieve a reference particle size distribution. This method considered water/powder ratio and cement content as a part of the optimization problem. It gave more importance to the particle size distributions of constituent materials in

order to create a self-compacting mix. Andreasen & Andersen (A&A) showed that the void fraction and density depend only on a factor known as distribution modulus (q). Modified A&A equation with a q value of 0.25 is proposed as the reference particle size distribution for the SCC mix. The volume of each constituent material is determined by solving an optimization problem for the target particle size distribution. It is assumed that the densest packing of constituent materials is possible when the reference PSD is followed [59, 58]. As stated before, a good SCC mix design should consider different factors such as the possibility of wide application, robustness in the case of variations in constituent materials, technical requirements, sustainability and cost [57] but there is no single mix design methodology that can satisfy all these considerations.

The proposed mix design method for SC-CBMs combines elements that were drawn from other studies carried out on CLSMs and on SCC, which share with SC-CBMs common flowability characteristics. SCC design methods are well-defined, whereas CLSMs are mostly designed by employing empirical approaches [25, 80]. During the development of a mix design procedure for SC-CBMs, optimal mixture composition is identified as a function of engineering requirements which are expressed in terms of flowability, stiffness and strength. These properties are dependent upon several factors, among which the most relevant are cement content, water content and particle size distribution. A further tailoring of the characteristics of SC-CBMs can be obtained by making use of the various admixtures and by adjusting their dosage.

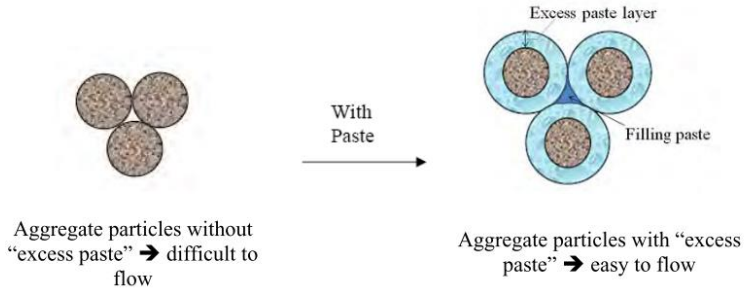

Figure 2.4 Excess paste theory in mix design of cement concrete [83]

A key role in the definition of the optimal mixture recipe was given to aggregate packing, which in the mix design of SCC is addressed by referring to target distributions containing relevant portions of filler [59, 81, 82]. Such a feature was also considered in the investigations carried out on CLSMs by Pujadas et al. [61], who based the choice of optimum proportions of constituents on wet packing tests carried out on a large number of trial mixtures. All the studies in this direction definitely highlighted the role of an excess paste layer in contributing to the flowability and workability of the cement concrete (Figure

2.4). With respect to the assessment of mechanical properties, the main references were taken from research work carried out on CLSMs, which possess low strength characteristics that are similar to those of SC-CBMs. The development of the proposed mix design method was based on a laboratory experimental investigation carried out by considering a given set of component materials. These included virgin aggregates and two granular components of recycled origin. Given that flowability is a prerequisite of SC-CBMs, use was also made of a superplasticizing additive. Experimental results highlighted the effects of several composition parameters on the flowability and mechanical properties of the considered SC-CBMs. As a result, the mix design procedure was rationalized and presented in a form which may be of practical use to designers.

2.2 Use of secondary aggregates

The scarcity of virgin aggregates and the availability of the large quantity of waste materials prompted pavement engineers to devise new strategies for incorporating secondary aggregates in the pavements without affecting their service life. The feasibility of recycling a particular waste material as secondary aggregates and the extent of inclusion is decided based on the expected performance and relevant supporting laboratory characterization. Different types of secondary aggregates are generally used in cement-bound mixtures. Recently aggregates belong to the category of Construction and Demolition wastes (C&D) are preferred as secondary aggregates as they reduce the production costs and global environmental impact. They are produced during the processes associated with construction and demolition of civil infrastructures. Secondary aggregates include Recycled Concrete Aggregate (RCA), Reclaimed Asphalt Pavement (RAP), mineral sludges, quarry dust, steel slag, etc. They are generally used in cement-bound mixtures in addition to their standard components [84]. Katz and Klover [85] reported on the improvement of mechanical properties of CLSMs which can be achieved by employing asphalt dust, coal fly ash, coal bottom ash and quarry waste. Raghavendra and Udayashankar [86] investigated on the effects caused by recovered gypsum powder and fly ash, developing a corresponding mix design procedure which yielded acceptable CLSM formulations. Puppala et al. [87] showed that satisfactory flowability and density can be attained with CLSMs containing clayey soil, while Naganathan et al. [88] observed that the use of quarry dust may have a stabilizing effect on this type of mixtures. Other Authors found that for some specific waste materials, critical issues may need to be considered. When evaluating the incorporation of high volumes of paper sludge, Wu et al. [89] recorded detrimental effects related to its high water absorption, while fluidity concerns were highlighted by Wang and Chen [90] when employing steel slag fillers. Finally, Etxeberria et al. [91] were critical in the analysis of CLSMs containing fine aggregates coming from C&D waste, due to the fact that

significant adjustments in the formulation were needed in order to guarantee adequate flowability and compressive strength.

RAP is the main waste material which is produced as a result of maintenance and rehabilitation activities carried out on distressed road pavements. It is produced from existing infrastructures as part of periodical resurfacing, rehabilitation or reconstruction operations in order to meet given serviceability requirements (Figure 2.5 and Figure 2.6). It is constituted by mineral aggregates covered by thin, aged bitumen films and it is typically employed in substitution of part of the virgin aggregates in the production of cold and hot bituminous mixtures [92, 93, 94, 95, 96]. According to available statistics, approximately 50 million and 69 million tons of RAP material are stockpiled every year in Europe and in the U.S., respectively. As per the recent estimates, in Italy 30% of available RAP is disposed of in landfills [7]. However, the current use of RAP in pavement recycling operations does not absorb these large quantities and as a consequence alternative recycling options need to be devised. However, RAP is also used as replacement of virgin aggregates in bituminous mixtures provided that it is adequately granulated and fractionated before use. Such a practice is encouraged by the fact that as part of the Long-Term Pavement Performance (LTPP) program of the Federal Highway Administration, it has been reported that pavement bitumen-bound layers with up to 30% RAP exhibit a performance which is equivalent or better than that of standard bituminous layers containing exclusively virgin materials [92]. Several other studies have shown that it is possible to reuse RAP in the construction of pavement granular bases or subbases [97, 98] and that combinations of RAP and virgin aggregates stabilized with cement can also be employed in road base construction [99]. RAP has also been used as a replacement of coarse aggregate in cement concrete: however, outcomes of investigations and trials indicate that such a practice should be limited only to non-structural applications due to the difficulty in achieving high strength [100].

Published work on the design and characterization of CLSMs do not document any experience on the use of RAP. This is probably due to the fact that RAP typically contains, in addition to fine aggregates, coarse fractions which are seldom required to supplement virgin aggregates in these mixes. Nevertheless, in recent years some work has been done on Portland cement concrete and cement-stabilized mixtures as part of the general desire of identifying innovative, low-cost and sustainable materials. Huang et al. [101] observed that use of RAP can lead to a reduction of concrete compressive and tensile strength but may also enhance toughness characteristics. This was also reported by Abdel-Mohti et al. [102], who suggested that strength reduction may be mitigated by adding fibres during concrete production. The feasibility of including RAP in cement-stabilized mixtures was demonstrated by Taha et al. [99], who showed that in such cases cement and water content need to be conveniently adjusted and that the use of increasing quantities of RAP may indeed yield a reduction of compressive

strength. On the other hand, Puppala et. al [103], while focusing on resilient modulus testing, found that mixtures containing RAP show good potential for use as sub-base materials.

Figure 2.5 Milling of RAP from the pavement (left) and RAP used in the investigation (right)

Figure 2.6 Large piles RAP visible in production plants (SITALFA plant)

Figure 2.7 Mineral sludge production (SITALFA plant)

In conclusion, the use of RAP in construction materials has been investigated widely and in general, it has been found that it leads to a reduction of construction costs, depletion of virgin aggregates, land-filling and energy consumption. However, there are no studies that document the use of RAP in flowable cement-

bound mixtures like CLSMs, probably as a result of the complexity of the performance-related requirements that are usually referred to in the design of such mixtures. Typical components of CLSMs are fine aggregates, Portland cement, water, and various admixtures. However, their composition can be much more complex since they may also include a wide range of industrial by-products and recycled materials to reduce costs and increase the sustainability of construction operations. Cement kiln dust, fly ash and slag can be used as partial replacements of cement, while virgin aggregates can be substituted by construction and demolition wastes, recycled concrete aggregates, scrap tyre particles and reclaimed asphalt pavement (RAP) [85, 104, 105, 106].

Mineral sludge considered in the study came either from stone cutting operations or from the washing of aggregates employed for production of bituminous mixes and Portland cement concrete (Figure 2.7). In both cases, it was found that they were abundantly available and that several issues were present with respect to their potential reuse. Residual sludge produced during the processing of ornamental stones is considered a waste (EWC code 010413) and according to available statistics, its annual production in Europe is equal to approximately 5 million tons [107]. The main challenges for the management of this type of sludge derive from its huge volume, very fine particle size distribution and high water content. Mineral composition of sludge depends on the parent rock, although the most common minerals are feldspars, quartz, calcite and mica [108]. Metals which derive from wear and tear of cutting tools are also present and this prevents the direct reuse of sludge without any treatment or processing because of its potential contaminating effects. As a consequence, in order to fit into the framework defined by the European Commission for the prevention and recycling of waste, stone cutting companies have tried to identify potential industrial applications in which sludge may be employed in immobilized form, mainly by the inclusion in building materials. Significant examples of such attempts are represented by the use of granite cutting sludge in coloured cement mortars [109], in floor tiles [110] and as partial replacement of sand in cement concrete [111]. The use of limited quantities of granite sludge as a Supplementary Cementitious Material (SCM) was also explored and it was shown that it does not alter the morphological features of cement hydration products and can be used for the manufacture of blended cements [112]. Sludge from the marble cutting industry also found its reuse in different applications of interest for the building and tyre industry [113, 114, 115].

Sludge derived from the industrial washing of aggregates, which may constitute 20-25% of the output of crushing operations carried out in quarries, is also considered as waste. However, some attempts have been made in order to reuse this type of material as part of specific construction operations. According to data available in literature, in combination with soil it may reach satisfactory California Bearing Ratio (CBR) values and as a consequence may be employed in

pavement sub-base layers [116]. Other studies have indicated that quarry dust may have a negative influence on the compressive strength and on other mechanical properties of Portland cement concrete [117]. Finally, it has been found that quarry dust can be used as a raw material in self-compacting concrete in substitution of fly ash and silica fume to reduce the cost of production [118] and as a stabilizing agent in CLSMs [88].

2.3 Materials and methods

Aggregate fractions employed for the mix design of SC-CBMs were crushed silica coarse sand (0-6 mm) and medium-fine gravel (8-16 mm). In addition, for the formation of the aggregate skeleton, two further granular materials were considered: RAP coming from aged and distressed pavement, and mineral sludge obtained from the washing of crushed natural aggregates. It was envisioned that by including these recycled materials in the SC-CBMs, they would lead to the design of mixtures with reduced production costs and enhanced sustainability characteristics.

RAP, which was provided by a local contractor, derived from the milling of dense-graded asphalt wearing courses, but its exact age was unknown. Since SC-CBMs have to satisfy the previously mentioned long-term excavatability requirements, the potential strength reduction due to the presence of RAP in these mixtures was considered as a positive factor. Similar advantages were attributed to the use of mineral sludge, which does not lead to any pozzolanic reactions in the presence of water. Furthermore, the fineness of the mineral sludge was regarded as essential in order to improve the flowability and stability of the SC-CBMs.

The virgin and recycled granular materials indicated above were preliminarily oven-dried until reaching constant weight either at 105°C (as in the case of the aggregate fractions and of the mineral sludge) or at 60°C (in the case of the RAP). A lower drying temperature, which entailed longer conditioning times, was selected for the RAP in order to prevent the softening of residual bitumen to take place.

2.3.1 Characterization of granular components

Results obtained from particle size distribution analyses and specific gravity (SG) tests are provided in Figure 2.8 and Table 2.1, respectively. It was observed that silica sand and RAP were characterized by continuous size distributions which seemed suitable to form most part of the composite skeleton of the SC-CBMs, whereas the available gravel was almost single-sized, and therefore fit for use in order to provide bulk effects to the mixtures. In the case of the mineral sludge, it was recorded that it possessed a very high content of filler, of the order of 60%. Such a characteristic made it a very good candidate to ensure an adequate

filling of the voids structure of SC-CBMs and to guarantee a proper flowability of their cementitious paste.

With respect to SG values, very similar values were recorded for the aggregates and sludge (of similar lithological origin), whereas the RAP fraction presented a significantly lower value due to the presence of oxidized bitumen. Finally, it should be mentioned that ignition tests carried out for the determination of binder content of the RAP fraction yielded an average value (from two replicates) of 4.60% with respect to the total mass of aggregates.

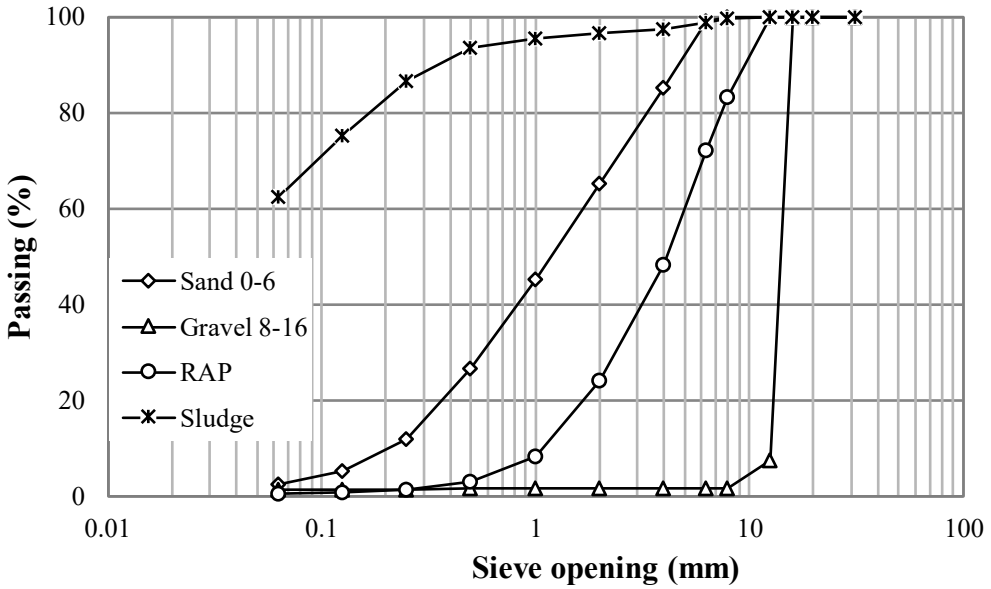

Figure 2.8 Particle size distribution of aggregates, RAP and mineral sludge

Table 2.1 Specific gravity of aggregates, RAP and mineral sludge

Fraction	SG
Sand 0-6	2.745
Gravel 8-16	2.733
RAP	2.527
Sludge	2.785

All the dried components were then subjected to sieve analyses for the determination of particle size distribution as per EN 933-1 [119] and to pycnometer tests for the determination of specific gravity as per EN 1097-6 [120]. RAP samples were also subjected to the determination of bitumen content as per EN 12697-39 [121], which entails the evaluation of the mass loss caused by a high-temperature treatment (at 540°C).

2.3.2 Flowability tests

Cement pastes and trial SC-CBMs were prepared in the laboratory by employing a standard Portland cement and a commercially available superplasticizer. According to the information provided by suppliers, cement was of the CEM I R42.5 type [122], with a specific gravity of 3.150, while the superplasticizer (Advaflow 455, Grace Products) was a liquid polycarboxylate product with a specific gravity of 1.060. Whenever used, the superplasticizer was employed with the dosage suggested by the supplier, equal to 0.5% by weight of cement.

Cement pastes and SC-CBMs were prepared by making use of a mechanical mixer in batches of 200 g and 2000 g, respectively. The superplasticizer was added in the required quantity by preliminarily mixing it with the water to be employed in each batch. Immediately after mixing, both the cement pastes and the trial SC-CBMs were subjected to flowability tests. In the case of SC-CBMs these tests were carried out by following the procedure indicated in ASTM D6103 [123], while for the cement pastes the procedure, although similar to the standardized one, was much simpler.

As indicated in ASTM D6103 [123], the standardized procedure involves the filling with fresh cementitious mixture of an open-ended cylinder (of 75 mm diameter and 150 mm height, with a corresponding maximum theoretical volume of 662.7 cm^3) resting on a horizontal, smooth and non-absorbent surface (Figure 2.9). The cylinder is then quickly lifted, allowing the mixture to spread under the effect of its own weight. Following such an operation, the so-called spread diameter (D_s, expressed in mm) is measured as the average of two readings taken along perpendicular directions. Furthermore, the mixture is visually inspected in order to detect the signs of any undesired phenomenon such as segregation or bleeding.

When considering CLSMs employed for trench filling applications, it is usually required that D_s is comprised between 170 mm and 250 mm in order to ensure a high flowability and simultaneously guarantee the absence of any bleeding or segregation phenomena [48]. In the case of the SC-CBMs, which contain coarse aggregates which are larger than those typically employed in CLSMs, greater values of D_s are expected. Thus, a target range of 200-350 mm was considered more appropriate. Visual verification of a satisfactory mixture stability (i.e. absence of bleeding or segregation) was retained as a fundamental phase of testing. Values of D_s greater than 350 mm did not seem compatible with mixture stability which needs to be absolutely avoided in order not to jeopardize the long-term behaviour of the mixtures in service.

Figure 2.9 The arrangement used for flowability measurements

For the analysis of the flow characteristics of cement pastes, a smaller cylinder was employed, with a volume of 283.7 cm^3. Such a size was found to be adequate with respect to the volume of the batches which could be prepared in a representative manner and compatible with the observed spreads. Rather than measuring D_s values, flowability tests carried out on the pastes only entailed the visual assessment of the uniformity of flow and of the possible occurrence of clear phase separation phenomena. Although such a test is merely qualitative, it was found to be useful in order to discriminate between the flow properties of the various cement pastes.

2.3.3 Determination of mechanical properties

In order to assess the mechanical properties of SC-CBMs in the hardened state, for each trial mixture four specimens were cast in cylindrical moulds (diameter 100 mm, height 200 mm) with no application of any vibration and levelling actions. Specimens were then demoulded after 24 hours and sealed in plastic bags in order to ensure an optimal curing process. Such a process was carried out by storing the specimens at room temperature for 28 days, when it was considered that fully cured conditions were reached. Subsequently specimens were subjected to the determination of their mechanical properties.

Resilient modulus

Hardened SC-CBM specimens were subjected to testing in accordance to AASHTO T 307-99 [124] (sub-base protocol) for the determination of the resilient modulus (M_r). Such a parameter is usually adopted for the description of the stress-strain response of soils and granular materials under traffic loading conditions [125, 126, 127] but has also been employed to assess the mechanical behaviour of cement-stabilized and cold-recycled bituminous mixtures [128, 99, 129]. Tests are carried out by making use of a triaxial apparatus which allows the simultaneous control of confining pressure (σ_3), which is kept constant, and of deviatoric stress applied in the vertical direction (σ_d), which varies in time by following a haversine-shaped function. Corresponding strains (ε), of reversible

and permanent nature (ε_r and ε_p, respectively), are measured in the vertical direction. The testing facility is shown in Figure 2.10. It consists of a tri-axial pressure chamber, a load cell unit and an LVDT arrangement for the measurement of response of the specimen.

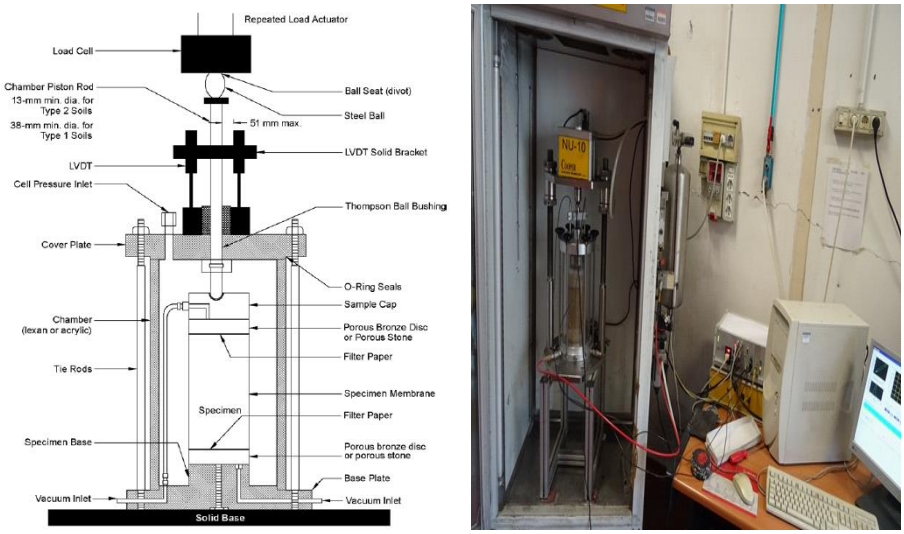

Figure 2.10 Tri-axial testing facility used for the resilient modulus test [124]

According the reference standard, a single specimen is subjected to 15 loading sequences composed of 100 cycles with various combinations of σ_3 and σ_d, which are comprised in the 0.0207-0.1379 MPa and 0.0186-0.2482 MPa, respectively. These stress components lead to values of the bulk stress, given by the sum of the three principal stresses applied to the test specimen, comprised between 0.08 MPa and 0.66 MPa, thereby allowing experimenters to capture the non-linear response of the considered materials (Figure 2.11). According to its definition, for each considered stress condition, resilient modulus is calculated by means of the following expression:

$$M_r = \frac{\sigma_d}{\varepsilon_{r,max}} \qquad 2.1$$

where $\varepsilon_{r,max}$ is the maximum value of the recoverable portion of vertical axial strain recorded in the 100 loading cycles associated to the applied deviatoric stress σ_d. In absolute terms, no threshold values can be fixed for the definition of Mr acceptance requirements in the case of SC-CBMs. This is due to the fact that for each specific application the minimum long-term bearing capacity is inherently dependent upon pavement cross section, expected loading conditions and target design life [44]. Moreover laboratory measured resilient modulus values are also stress sensitive. There are several models available in the literature to identify this

stress-dependency for unbound granular materials [130, 131]. Recently there have been development of many more models suitable for the bound granular materials such as cement stabilized materials. This is explained in detail in section 2.4.4.

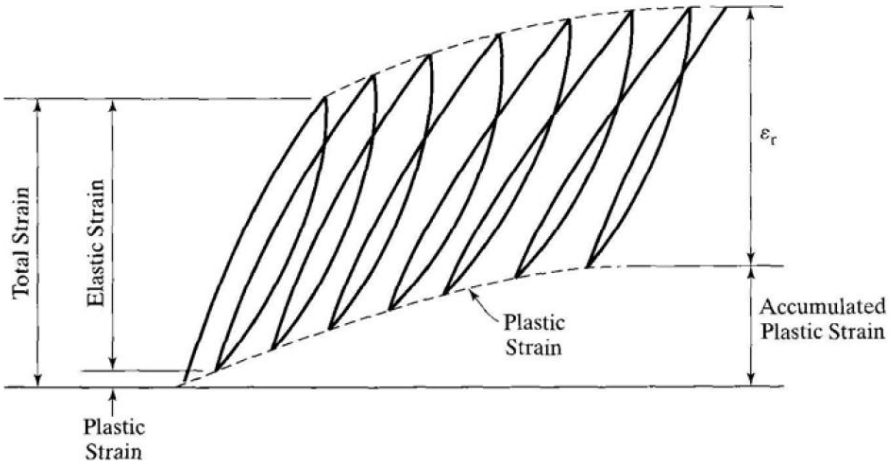

Figure 2.11 Strains under resilient modulus testing [132]

Nevertheless, it may be considered that technical specifications frequently refer to a minimum modulus assumed in pavement design calculations which for roads of primary importance is of the order of 100-120 MPa [20, 133, 134, 135]. In the case of road tunnels, where it may be convenient to reduce the thickness of the upper bound layers as a results of high service temperatures, such a limit may be increased on a project-specific base [44].

After being tested for the evaluation of resilient modulus, and by making use of the same triaxial equipment, SC-CBM specimens were subjected to the so-called quick shear tests [124]. As per the corresponding standard, applied axial load was progressively increased by imposing a vertical strain rate of 1%/min, which approximately corresponds to a displacement rate of 2 mm/min. Although the reference standard requires the application of a confining pressure for subgrade soils and granular subgrades (equal to 27.6 kPa and 34.5 kPa, respectively), in the case of the SC-CBMs tests were carried out by applying vertical loads only. Thus, the adopted procedure is similar to the one described in ASTM D1633 [136] for the determination of compressive strength of soil-cement, which requires a slightly lower displacement rate (equal to 1.3 mm/min). In quick shear tests, values of applied load are recorded by a load cell and can be converted into normal vertical stresses (σ_1), while average axial strains induced in the specimens (ε_1) can be calculated from imposed vertical displacements. As a result, stress-strain curves can be obtained, and the values corresponding the peak load may be indicated as quick shear strength (σ_{qss}) and strain at failure (ε_f).

When considering the failure properties of SC-CBMs, excavatability requirements need to be taken into account. In such a context, upper limits have been defined for CLSMs by referring to a maximum compressive strength

determined on cylindrical specimens equal to 2.1 MPa [137, 138] Such a limit was maintained when analyzing the results of tests carried out with the quick shear protocol in the absence of confining pressure.

2.4 Results and discussion

2.4.1 Flowability of cement paste

Cement paste in SC-CBMs not only controls the time-dependent development of stiffness and strength, but also has a direct effect on their flowability characteristics in the fresh state. Thus, identification of the optimal composition of cement paste was carried out by means of the simple flowability tests described in section 2.3.2. Tests were performed on water-cement pastes prepared with and without superplasticizer. Obtained results indicated that for w/c values increasing up to 0.60, regardless of the presence of the superplasticizer, the pastes did not reach sufficiently fluid conditions in order to evenly spread under their own weight (Figure 2.12). Satisfactory flow was observed when starting to consider w/c values equal to or higher than 0.70. Thus, as explained in detail in section 2.4.3, such a threshold value was employed as a reference for the preparation of SC-CBMs which were subjected to flowability tests carried out in accordance to ASTM D6103 [123].

2.4.2 Identification of target particle size distribution

The optimal combination of the available granular materials composing the aggregate skeleton of the SC-CBMs was identified by considering their combined particle size distribution and by minimizing its deviations from a reference curve. Such a curve, which is also known as the "modified Andersen and Andreasen curve", was proposed by Funk and Dinger [139] for the design of SCCs and is given by the following expression:

$$P(D) = 100 \cdot \frac{({D_{max}}^{q} - D^{q})}{({D_{max}}^{q} - {D_{min}}^{q})} \qquad 2.2$$

where D is the diameter of aggregate particles (in mm), P(D) (expressed in %) is the cumulative percentage passing the sieve with opening equal to D, D_{max} is the maximum diameter of aggregate particles in the mixture (in mm, fixed at 16 for all mixtures and corresponding to a P(D) equal to 100%), D_{min} is the minimum diameter of aggregate particles in the mixture (in mm, assumed to be equal to 5 μm for all mixtures), q is the so-called distribution modulus.

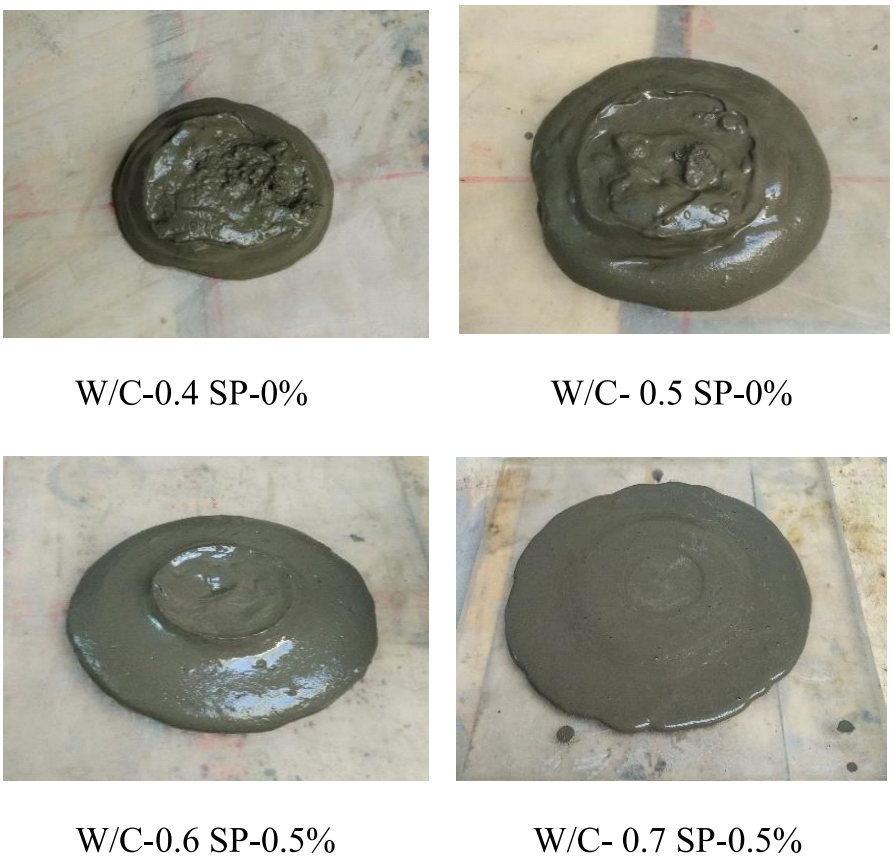

Figure 2.12 Flowability of cement paste

The distribution modulus q defines the balance of coarse and fine aggregates within the lithic skeleton. As reported in literature [59], smaller values of q are required in order to increase the volume of fines, thus obtaining a more suitable packing of the aggregate structures. The values of q can vary between 0 and 1 depending upon workability requirements, even though for highly flowable mixes values lower than 0.23 are usually adopted [140].

It should be underlined that in the definition of the particle size distribution of the SC-CBMs, the effects associated to the presence of the cement particles was not considered. This approximation is reasonable since the cement dosage adopted in SC-CBMs is generally comprised between 30 kg/m^3 and 100 kg/m^3. As indicated in section 2.4.3, cement dosage of the SC-CBMs prepared during the investigation was fixed at 60 kg/m^3.

Results obtained by optimizing the composition of the aggregate skeleton of the SC-CBMs are given in Table 2.2. These are listed as a function of the distribution modulus, for which three different values were considered (equal to 0.21, 0.23 and 0.25), centred on the previously mentioned reference value of 0.23. Corresponding particle size distributions are displayed in Figure 2.13.

Table 2.2 Composition of the aggregate skeleton of selected SC-CBMs

Fraction	Percentage by weight (%)		
	q = 0.21	q = 0.23	q = 0.25
Sand 0-6	34	33	33
Gravel 8-16	10	11	11
RAP	28	30	32
Sludge	28	26	24

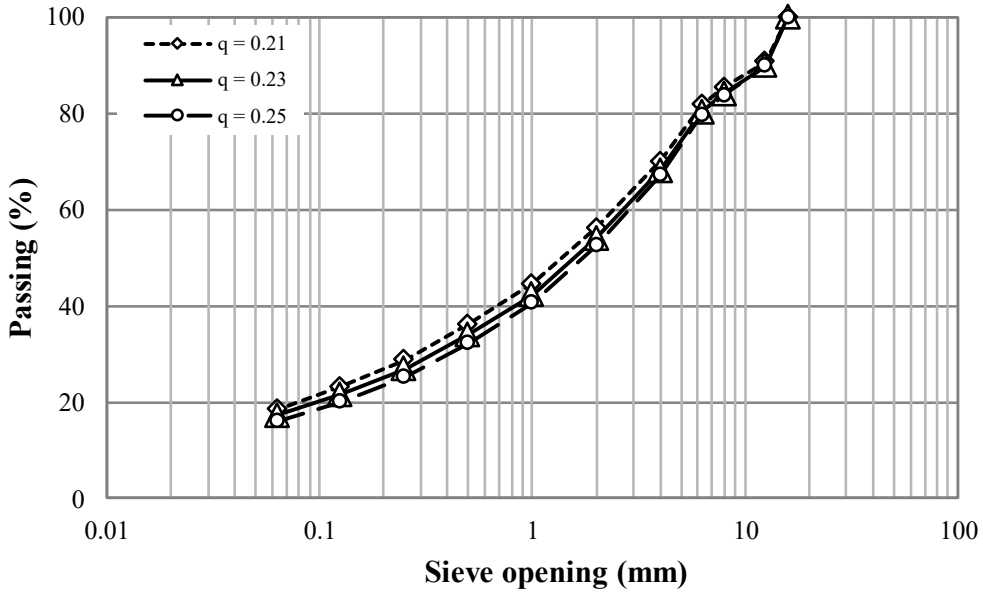

Figure 2.13 Particle size distribution of the aggregate skeleton of SC-CBMs

2.4.3 Flowability of SC-CBMs

Composition of the SC-CBMs subjected to flowability tests as per ASTM D6103 [123] contained optimized aggregate skeletons identified as indicated in section 2.4.2 and a reference Portland cement dosage of 60 kg/m^3. With respect to cement paste, results obtained from flowability tests carried out as described in section 2.4.1 indicated that a minimum w/c equal to 0.70 was necessary in order to achieve satisfactory flowability characteristics. However, in SC-CBMs, which are characterized by a significant quantity of particles passing the 0.075 mm sieve, rather than referring to w/c, it was considered more appropriate to base the definition of paste composition on an alternative and more meaningful parameter, the so-called water-to-powder ratio (w/p) [57]. In this case, "powder" is the term which is used to collectively indicate Portland cement and the filler fraction, which for the considered SC-CBMs mainly derives from the contribution of mineral sludge. As a result of this rationale, when defining the composition of trial SC-CBMs, it was postulated that the previously identified w/c threshold (equal to 0.70) could be employed to estimate the corresponding value

of w/p. For such a purpose, the different specific gravity of Portland cement and powder (equal to 3.150 and 2.785, respectively, see Table 2.1) were taken into account by converting the w/c value into a ratio by volume and by thereafter translating it into a w/p ratio by weight. This simple calculation led to a reference value of w/p equal to 0.80, to be employed for the definition of the composition of SC-CBMs. Nevertheless, it was considered essential to directly evaluate the flowability of SC-CBMs as a function of the variations of this parameter. Since in the tests carried out on cement pastes the benefits of using the superplasticizer were appreciated in terms of stability and uniformity, all SC-CBMs subjected to testing were prepared by employing such an additive with its standard recommended dosage (equal to 0.5% by weight of cement).

Table 2.3 Results of flowability tests carried out on SC-CBMs

Mixture	D_s (mm)
0.21-0.80	300
0.23-0.80	320
0.25-0.80	350
0.25-0.75	260
0.25-0.70	150

In order to capture the effects of variations of both q (which dictates the quantity of cementitious paste in the mixture) and w/p (which controls the consistency of the mixture in the fresh state), five different mixtures were prepared. Three were characterized by a constant w/p value, equal to 0.80, and a variable q, equal to 0.21, 0.23 and 0.25 (previously identified as discussed in section 2.4.2). The other two possessed a constant q value, equal to 0.25, and a variable w/p, equal to 0.75 and 0.70. In rest of the chapter various mixtures are associated to a code which combines q and w/p values (e.g. “0.21-0.80”).

q = 0.21 w/p = 0.80 | q = 0.23 w/p = 0.80 | q = 0.25 w/p = 0.80 | q = 0.25 w/p = 0.75 | q = 0.25 w/p = 0.70

Figure 2.14 SC-CBM specimens subjected to flowability tests

Results obtained in this second stage of flowability tests carried out on the SC-CBMs are shown in Table 2.3, while images of the specimens after spreading are provided in Figure 2.14. When considering the results obtained on the first three SC-CBMs listed in Table 2.3, it was observed that for a given value of w/p (equal to 0.80), the progressive increase of q, which corresponds to a reduction of

the content of fines, led to an enhancement of flowability, with increasingly high values of D_s. However, visual observations made on the SC-CBM samples indicated that such a change in behaviour in terms of flowability was coupled with a slight reduction of homogeneity displayed after spreading (see Figure 2.14). These outcomes are due to the fact that when the consistency of the paste remains constant (i.e. with a constant w/p), as its volume is reduced (i.e. with an increasing q), its overall lubricating effect within the bulk structure of the mixture tends to decrease. For the explored range of q values, variations of D_s were quite limited, all the measured values being contained within the previously defined target range of acceptance (200-350 mm, see section 2.3). Physical expectations suggest that the reduction in D_s associated with the decrease in q could be compensated by an increase of w/p, which would reduce paste consistency. However, trials carried out in the laboratory indicated that such modifications could not to be operated since the corresponding SC-CBMs showed clear signs of bleeding and segregation.

When focusing on the last three mixtures listed in Table 2.3, experimental results indicated that by keeping the q value constant (equal to 0.25) and by reducing w/p, a significant reduction of flowability was obtained. These results are in line with those discussed above, since they can be explained by referring to the progressive increase of paste consistency (i.e. reduction of w/p) associated to the presence of smaller quantities of free water in the given volume of powder paste (i.e. with a constant q), which leads to a reduction of lubricating effects. Obtained results showed that the SC-CBMs were extremely sensitive to variations of w/p, D_s being reduced to 260 mm in the case of w/p equal to 0.75, and to 150 mm for the mixture with w/p equal to 0.70. The first mixture met the D_s requirements, while the second one was not acceptable from such a viewpoint. It can be postulated that adjustments to the flow behaviour of these last two mixtures could be obtained either by increasing w/p (and therefore going back to the formulation of the third mixture listed in Table 2.3) or by increasing the content of fines by means of an adequate reduction of q (e.g. by assuming values of the order of 0.21-0.23).

2.4.4 Assessment of mechanical properties

Results of triaxial tests carried out on the SC-CBMs after 28 days of curing are shown in Figure 2.15, where the logarithm of resilient modulus, expressed in MPa, is plotted as a function of the logarithm of bulk stress (θ), also expressed in MPa. As per the sub-base protocol adopted for testing, bulk stress, which is given as the sum of the three principal stresses applied to the test specimen, varied between 0.08 MPa and 0.66 MPa in each of the 15 loading sequences composing every test. Minimum and maximum M_r values recorded for each mixture are given in Table 2.4.

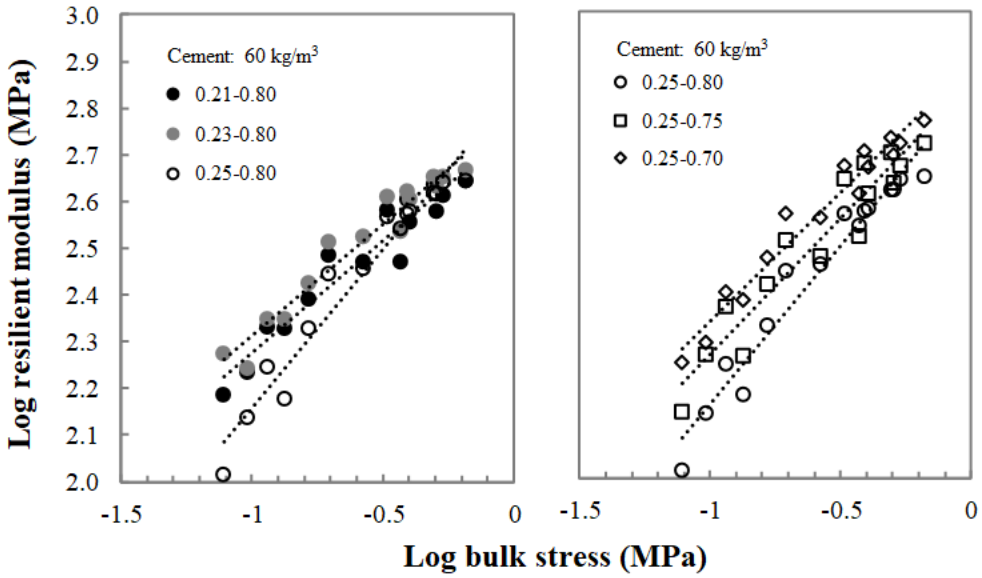

Figure 2.15 Resilient modulus experimental data and typical range for granular sub-base materials

Table 2.4 Resilient modulus ranges of the SC-CBMs

Mixture	$M_{r,min}$ (MPa)	$M_{r,max}$ (MPa)
0.21-0.80	153	441
0.23-0.80	175	467
0.25-0.80	104	443
0.25-0.75	139	524
0.25-0.70	177	584

Recorded resilient modulus ranges synthesized in Table 2.4 are in line with those reported for high-quality sub-base granular materials and stiff subgrade soils [141, 142, 143, 144, 145]. However, as mentioned in section 2.3, they cannot be compared to any fixed acceptance threshold since the structural suitability of SC-CBMs should be established on a project-specific basis [44]. It was found that the effects caused by variations of q for a constant value of w/p (equal to 0.80) were non-negligible. Such an outcome highlights the fact that the resilient response under loading of the SC-CBMs with a composition of the aggregate skeleton defined as indicated in section 2.4.2 is not only related to their bulk structure and to the stiffness of cementitious paste, but is also dependent upon the content of fines and on the corresponding volume of cementitious paste. It was observed that the highest stiffness values were obtained for an intermediate value of q (equal to 0.23), thus indicating that the filling effect provided by the fines and by the

associated paste can lead, beyond a certain limit, to a reduction of the packing of the coarser aggregate particles.

Significant variations of the resilient modulus were recorded when reducing the w/p ratio as the value of q (equal to 0.25) was kept constant. Quite intuitively, this is due to the fact that as the volume of water decreases, during the hardening process the microstructure of the SC-CBM, as that of any other cementitious component, is characterized by decreasing porosity [146]. Such an evolution is beneficial in terms of stiffness since micropores, as a function of their size, distribution and total volume, can act as points of weakness under the application of external loads.

Results displayed in Figure 2.15 indicate that all considered SC-CBMs displayed a non-linear stress-hardening behavior, with M_r values which significantly increased as a function of θ. Such a behavior is consistent with other findings documented in literature on similar cement-stabilized materials and on granular sub-bases [147, 148, 149]. It is interesting to observe that the stress-sensitivity of the mixtures was affected by the aggregate packing and content of fines as indicated by the recorded variations of the slope of interpolation lines as a function of q. The influence on stress-hardening of variations of paste stiffness was less evident, with similar slopes of the interpolation lines recorded for all mixtures regardless of their w/p value.

For a more detailed assessment of the stress sensitivity of the SC-CBMs, experimental data were modelled by means of the three-parameter function proposed by Puppala for the evaluation of lime-treated soils and cement-stabilized pavement base layers [150, 103]. This function is provided in the following:

$$M_r = k_1 \cdot p_a \cdot \left(\frac{\sigma_3}{p_a}\right)^{k_2} \cdot \left(\frac{\sigma_d}{p_a}\right)^{k_3} \qquad 2.3$$

where p_a is the reference atmospheric pressure (equal to 0.10133 MPa) and k_1, k_2 and k_3 are non-dimensional material-dependent constants. The results of regression analyses carried out by referring to Equation (2.3) are shown in Table 2.5, which contains the calculated values of the fitting constants and coefficients of correlation between measured and modelled data (R^2).

Values of parameter k_1, which can be considered as an indicator of the overall magnitude of the resilient modulus, showed non-negligible changes as a result of variations of the q parameter (while keeping w/p constant at 0.80) and of the w/p ratio (for q equal to 0.25). Such an outcome was already discussed when considering the M_r ranges given in Table 2.4 and can be explained by referring to the same physical phenomena mentioned in such a context. Although the overall stress dependency of the SC-CBMs was qualitatively assessed by referring to the slope of interpolations lines provided in Figure 2.15, more interesting observations could be made when analysing the individual effects of confining

pressure and deviatoric stress. As the content of fines decreased (i.e. as the value of q increased), k_2 and k_3 tended to increase and decrease, respectively, thereby showing an increased dependency upon confining pressure coupled with a reduced dependency upon deviatoric stress. These trends are consistent with the change in structure of the SC-CBMs, which with the increase of q progressively tend towards coarser aggregate skeletons that reflects into a greater display of volumetric effects and a lower occurrence of shear strains. In the case of the first mixture listed in Table 2.5, k_2 was smaller than k_3, while the opposite was observed for the following two coarser mixtures, with k_2 greater than k_3. Observed trends are similar to those which have been reported for other types of materials subjected to resilient modulus testing [145].

Table 2.5 Results of resilient modulus modelling

Mixture	k_1	k_2	k_3	R^2
0.21-0.80	3535.1	0.19	0.27	0.971
0.23-0.80	3903.8	0.25	0.20	0.954
0.25-0.80	3633.6	0.38	0.21	0.949
0.25-0.75	3940.7	0.29	0.24	0.953
0.25-0.70	4521.5	0.26	0.26	0.979

As the value of w/p decreased with a constant q value, k_2 and k_3 tended to decrease and increase, respectively, displaying variations which were opposite to those discussed above. The decrease of volumetric effects can be explained by referring to the enhancement of the stiffness of the powder paste, while the increasing occurrence of shear effects can be related to the gradual embrittlement of the cementitious powder paste. The first two SC-CBMs considered in the analysis of the effects of w/p variations exhibited k_2 values greater than k_3 values, while the two parameters were equal in the case of the third mixture. The reliability of the model employed for data fitting is proven by the high values of the coefficient of correlation which are given in Table 2.5. The overall reliability of the model can also be appreciated by considering the plot provided in Figure 2.16, where M_r values calculated by means of Equation (2.3) ($M_{r,calc}$) are displayed as a function of measured values ($M_{r,meas}$). For the entire set of data, the total coefficient of correlation was equal to 0.961.

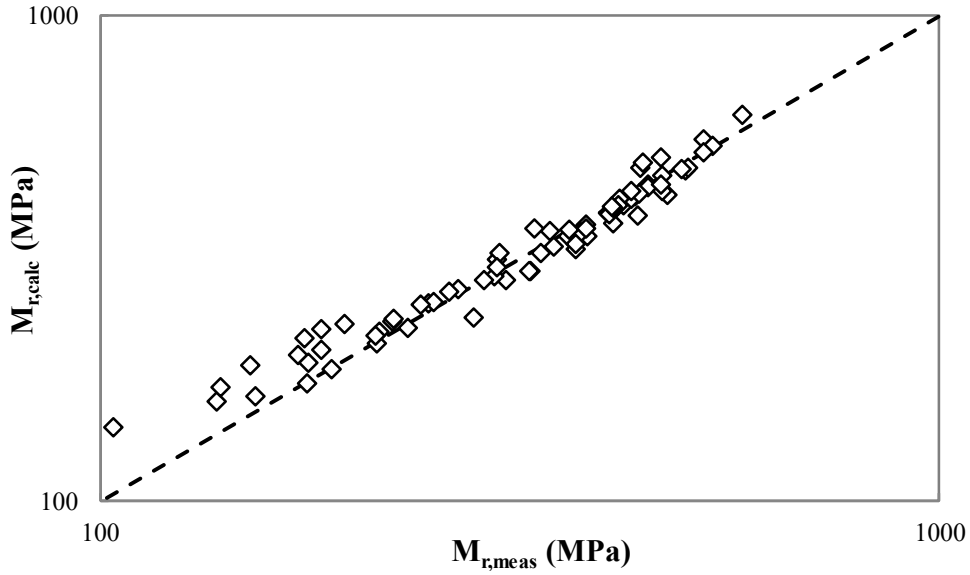

Figure 2.16 Reliability of resilient modulus modelling

As mentioned in section 2.3.3, after triaxial testing the SC-CBMs were subjected to failure tests carried out in accordance to the quick shear protocol [124]. Experimental results are synthesized in Table 2.6, which lists the values of quick shear strength (σ_{qss}) and strain at failure (ε_f), calculated from the experimental data recorded for each set of 4 tested specimens. Stress-strain curves exhibited by the SC-CBMs during testing are shown in Figure 2.17.

Table 2.6 Stress and strain at failure of SC-CBMs subjected to quick shear tests

Mixture	σ_{qss} (MPa)	ε_f (%)
0.21-0.80	0.404	0.603
0.23-0.80	0.416	0.459
0.25-0.80	0.405	1.038
0.25-0.75	0.449	0.662
0.25-0.70	0.609	1.123

Experimental results given in Table 2.6 and in Figure 2.17 indicate that with the progressive increase of q, the SC-CBMs did not exhibit any relevant changes in strength, with σ_{qss} values very close to each other. On the contrary, recorded values of ε_f varied significantly, with the lowest value associated to the stiffer mixture (see Table 2.5) characterized by a q value equal to 0.23. These results are consistent with the composition of the SC-CBMs and with the discussion of resilient modulus test results provided previously. As expected, strength seems to be controlled by the w/p ratio (which did not change for the first three mixtures

listed in Table 2.6), while ductility at failure is influenced by the variable packing of the aggregate skeleton and by the variable content of fines.

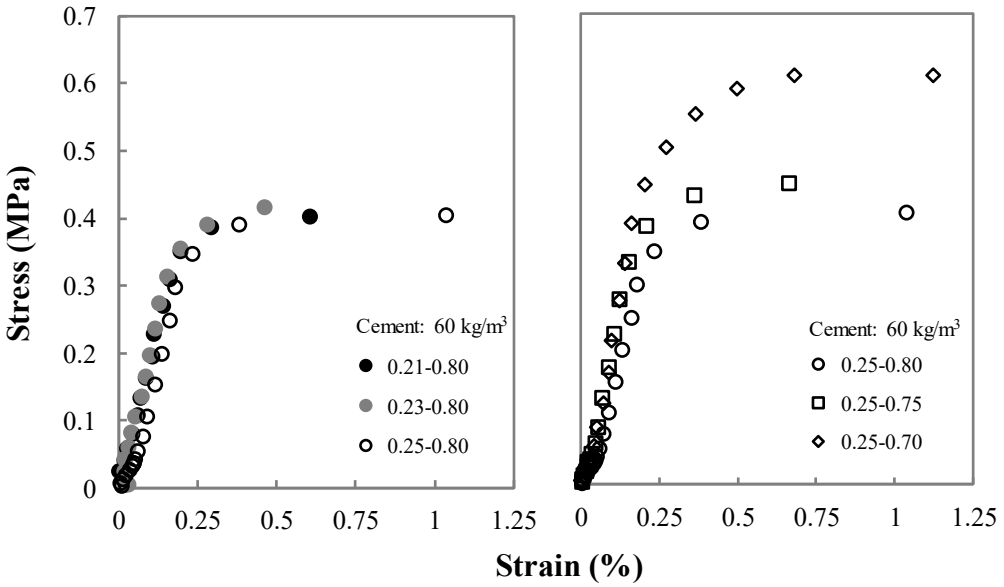

Figure 2.17 Stress-strain curves obtained from quick shear tests

When considering the results obtained on the last three mixtures, characterized by a progressive decrease of w/p, σ_{qss} was found to increase as a result of the gradual reduction of micropores in the cement paste that can trigger microcracking phenomena under loading. However, ε_f did not display a clear trend, and as a consequence it was not possible to confirm that the degree of brittleness of the SC-CBMs is mainly controlled by q (which did not change for these mixtures).

As mentioned in section 2.3, for the purpose of acceptance of the SC-CBMs, reference can be made to the maximum allowable limit defined for excavatable CLSMs, equal to 2.1 MPa [137, 138]. Thus, the results given in Table 2.6 indicate that from the viewpoint of exacavatability all the considered SC-CBMs can be considered fit for purpose.

2.5 Proposed mix design procedure

Based on the results presented in section 2.4, a mix design procedure for SC-CBMs can be proposed. Such a procedure is presented in the flowchart of Figure 2.18, in which the component blocks are grouped into a sequence of 6 conceptual stages. Four of them (numbered from 2 to 5) include activities which are analogous to those which were carried out in the described experimental investigation. The scheme also displays a preliminary stage of preparation (stage 1) and a final stage of mixture selection (stage 6) which completes the decision process. Employed shapes have the usual meaning that is assigned to flowchart

blocks in the representation of algorithms (ovals for beginning and ending conditions, rectangles for straightforward processes, diamond for questions which employ two possible outcomes).

In order to provide a tool readily available for use in most practical applications, the procedure illustrated in Figure 2.18 has been limited in width, with the objective of reaching the final design SC-CBM with minimum efforts. Nevertheless, it can be expanded in order to allow designers to have a more thorough understanding of the effects of all the variables considered in the formulation of SC-CBMs on a wider set of performance-related properties.

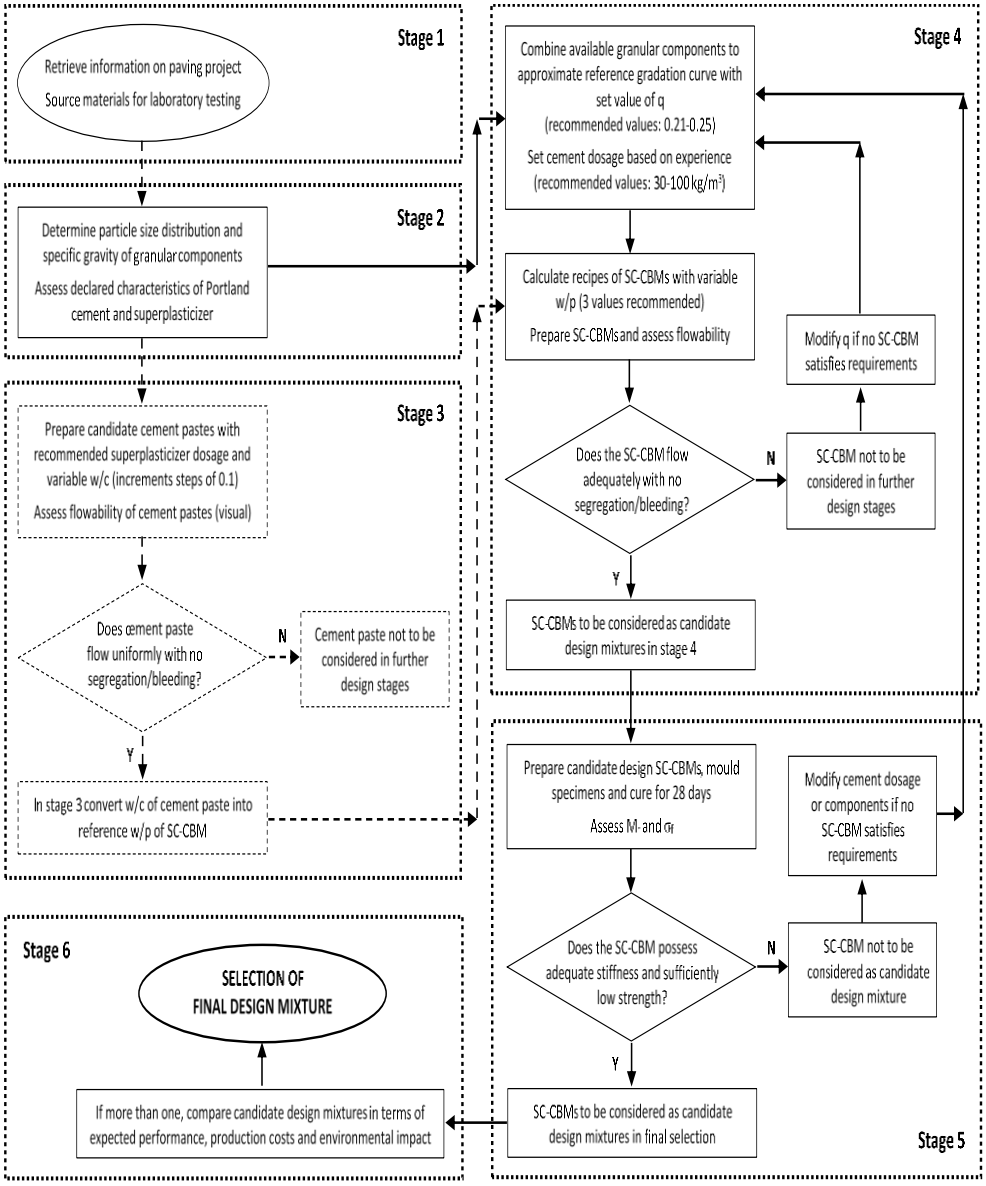

Figure 2.18 Flow chart of the proposed mix design procedure

2.5.1 Stage 1 – Preliminary data collection

The preliminary stage of design (stage 1) is dedicated to the retrieval of information relevant for the paving project and to the sourcing of materials for laboratory activities. Information which may be of interest for the purposes of mix design is related to pavement cross section, local constraints, available materials, expected design life, technical specifications, production costs, and estimated environmental impacts. However, other data not included in this list may be crucial for specific paving projects. From the list of available materials, the SC-CBM designer needs to select those which may be of interest for the production of the SC-CBM. Consequently, these have to be made available to the laboratory in order to carry out the subsequent stages of the mix design procedure.

2.5.2 Stage 2 – Characterization of component materials

The second stage of design is focused on the characterization of component materials. In such a context, it should be underlined that required tests are quite limited and in the case of granular components they are those which are carried out as part of routine quality control procedures (determination of particle size distribution and specific gravity). Furthermore, for Portland cement and superplasticizing additives, tests are not mandatory as they can be replaced by the assessment of data sheets provided by manufacturers. Although the investigation described in this chapter considered a limited number of component materials, whenever possible and if justified by the extent and importance of the construction project, a wider the set of materials may include in this stage of design. This may allow the identification, in the following stages (3 and 4), of several alternative optimized cement pastes and aggregate skeletons, which may thereafter lead to significantly different SC-CBMs. As in the case of the performed investigation, it is recommended to include recycled materials in the evaluation in order to identify design mixtures the production of which can be attractive also in terms of enhanced sustainability and limited environmental impact.

2.5.3 Stage 3 – Identification of optimal cement paste

The third stage of design has the goal of identifying an optimal cement paste, the composition of which can then be converted into an optimal powder paste (which includes water, cement and filler). The underlying decision-making process is based on the outcomes of simple, quick and low-cost flowability tests which exclusively require visual observations. Results presented in section 2.4.1 indicate that although such an approach is empirical in nature, it leads to the identification of cementitious pastes which can perform properly, both in the fresh and hardened state, in the SC-CBMs in which they are included. As previously

mentioned, for projects which deserve such an extension, analyses can be performed on several combinations of cementitious binders and additives. Although manufacturers usually suggest the recommended dosage of superplasticizer, it may also be of interest to explore the effects on flowability deriving from its variation. In the scheme of Figure 2.18, the activities composing stage 3 are enclosed in dashed blocks since it is envisioned that when considering only one pair of cement and superplasticizer, the designer may decide to skip such stage of design, directly moving to stage 4. In such a case, values of investigated water-to-powder ratios may be assumed on the basis of previous experience or investigated during stage 4 by means of a trial-and-error approach.

2.5.4 Stage 4 – Optimization of aggregate skeleton

The fourth stage of design addresses the optimization of the aggregate skeleton of SC-CBMs. As illustrated in the chapter, use can be made of the reference Andersen and Andreasen gradation curve, which leads to gradations in which the presence of a bulk structure and of a relevant quantity of fines is adequately balanced, thus ensuring adequate packing and flowability. The latter property can be measured with the standardized ASTM tests which are similar in simplicity, speed and cost to those which are carried out in stage 3 on cement pastes. It is required to perform such tests on trial SC-CBMs in which the water-to-powder ratio can be drawn from the previous stage of design, but such a parameter should also be conveniently varied in order to directly assess the effects of its variation. Target values of flowability have been proposed for the specific application which inspired the investigation, but these can be conveniently adjusted based on the requirements of specific projects. For direct application of the procedure in its basic form, designers are required to start with set values of cement dosage and distribution modulus and by terminating the stage when achieving the desired flowability characteristics with a single value of the water-to-powder ratio. However, for a more comprehensive design, several options can be kept open by choosing several alternative values of the distribution modulus and of the water-to-powder ratio.

2.5.5 Stage 5 – Mechanical characterization of SC-CBMs

The fifth stage of design deals with the mechanical characterization of the SC-CBMs which, as a result of the outcomes of the previous design stages, have been identified as suitable candidates for the considered application. Requirements which in this phase can be employed for the acceptance of the candidate mixtures are expressed in terms of minimum stiffness and maximum strength achieved in fully cured conditions. In the investigation described in section 2.4.4 these characteristics were assessed by referring to AASHTO standards, but they may also be evaluated by means of other test procedures. When the requirements are

not met, the procedure entails a new iteration which starts with the assumption either of a new set of granular components or of a modified cement dosage. The initial value of distribution modulus may also be changed.

2.5.6 Stage 6 – Selection of design SC-CBM

The sixth and final stage of design is concentrated on the selection of the design SC-CBM. If more than one of the candidate mixtures satisfy the requirements, they need to be compared to one another. Factors which may be kept into account to identify the best mixture are expected performance, production costs and associated environmental impact. In such a context, knowledge of engineering details of the project in which the SC-CBM will be used are vital, and the involved analyses may require the application of specific models. Even in the case of a single candidate mixture successfully coming through the previous stages, it is recommended to carry out the abovementioned analyses in order to corroborate the outcome of the mix design procedure.

2.6 Example application of the mix design procedure

As a proof of the feasibility of the proposed method, the experimental results presented in section 2.4 can be placed within its decision process for the identification of the design SC-CBM.

The results of flowability tests carried out in stage 4 would limit the choice to the mixtures with a w/p value equal to 0.80, excluding the ones with w/p values equal to 0.75 and 0.70. Among these three mixtures, preference should be accorded to the two with a finer aggregate skeleton, associated to q values equal to 0.21 and 0.23, which appeared more homogeneous and exhibited D_s values not too close to the maximum allowable value (equal to 350 mm). This second aspect may be of practical interest since it is expected that in full scale production operations there may be physiological variations of composition which should be accounted.

The two mixtures shortlisted in stage 4 (0.21-0.80 and 0.23-0.80) exhibited mechanical properties, assessed in stage 5, that satisfied hypothesized acceptance requirements. Such an outcome would indicate that both can be considered as candidate design mixtures. As part of stage 6, the two candidate mixtures seem to be practically equivalent in terms of their production costs and associated environmental impact as a result of their common percentage of recycled components, equal to 56% by weight of all granular components. However, when comparing them in terms of expected performance, a slight preference can be accorded to the mixture with q value equal to 0.21, as a result of its higher strain at failure since it may be less prone to cracking in service. Such a phenomenon may be detrimental because of its possible consequences in terms of initiation of reflective cracks which can propagate through the overlying pavement.

Based on the discussion provided above, as a result of the investigation described in section 2.4, and in the absence of any further details related to a specific paving project, the final design SC-CBM which may be selected for the formation of pavement foundations in road tunnels would be the one with w/p equal to 0.8 and q equal to 0.21. When SC-CBMs has to be used in practical applications, depends on the project specific requirements, the compositions can be tailored in the way as proposed in the mix design procedure.

Part II: Thermal properties

Some of the works described in this part has been previously published in the following:

- E. Choorackal, P.P Riviera, D. Dalmazzo, E. Santagata, L. Zichella and P. Marini, "Performance-Related Characterization of Fluidized Thermal Backfills Containing Recycled Components," *Waste and Biomass Valorization*, pp.1-12. Mar 2019, https://doi.org/10.1007/s12649-019-00650-9

- E. Choorackal, P.P Riviera, D. Dalmazzo, E. Santagata, L. Zichella, and P. Marini, "Reuse of recycled asphalt pavement and mineral sludges in fluidized thermal backfills," *6th International Conference on Sustainable Solid Waste Management*, Naxos Island, Greece, 13–16 Jun 2018.

3. Thermal properties of self-compacting cement-bound mixtures

The mix design procedure for self-compacting cement-bound mixtures was developed by considering only the mechanical and flowability properties as discussed in Chapter 2. Thermal properties of these mixtures are worth investigating for their application in pavement foundations of road tunnels, which also house buried high-voltage cables. These mixtures can also be used for other applications like in Fluidized Thermal Backfills (FTBs) if they possess adequate thermal conductivity. This chapter of the thesis explores the thermal properties of SC-CBMs.

3.1 Thermal backfills for transmission cables

The construction of new tunnels and road networks is often combined with the placement of utility lines such as high-voltage transmission cables which in most cases are buried underground to ensure safe and reliable power transfer. Their current carrying capacity depends on several factors, among which temperature of the conductor plays a crucial role. Hence, heat dissipation capacity of the material surrounding cables should be ensured by employing the so-called thermal backfills [151, 152, 153, 154]. If needed, these can be designed as FTBs, which are self-levelling and self-compacting flowable mixes constituted by a proper combination of hydraulic binder, aggregates, fly ash and water [155, 156, 157]. Their formulation can be adjusted to include several recycled components which contribute to the reduction of costs and environmental impact associated with construction operations [154, 155, 158].

Underground transmission cable networks are designed to deliver a particular power. However, the thermal resistivity of the surrounding medium affects its transmission. Heat is generated during power transmission due to the electrical resistance of conductor, sheathing and insulation of the buried cables. Thermal properties of their surrounding medium further control the heat dissipation. Thermal resistivity can be defined as the capability of materials to allow heat transfer through it. The reciprocal of thermal resistivity is the thermal conductivity. As the thermal resistivity of the surroundings increases, heating losses increase for the cables which result in a reduction of its current carrying capacity. The maximum current carrying capacity of a conductor in amperes

under its service conditions without exceeding the maximum limit on temperature is called as its ampacity. Ampacity depends on the ability of the cable installation system in dissipating the temperature to its surrounding soil and atmosphere. The maximum limit to the thermal resistivity of the surrounding environment is specified in design documents depends on the safe operating temperature of the cables and the required current carrying capacity. The effect of soil thermal resistivity on the ampacity for a typical directly buried cables is shown in Figure 3.1. The knowledge of thermal conductivity of the surrounding backfill is important for the calculation of the ampacity of cables with confidence [159].

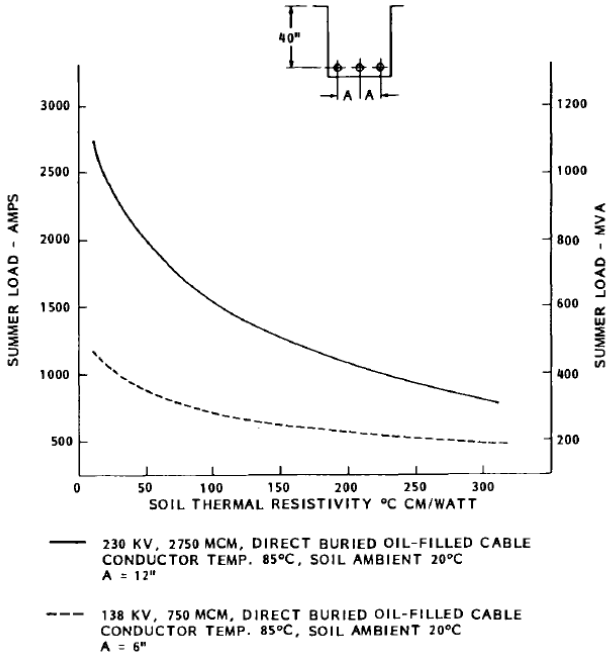

Figure 3.1 Effect of soil thermal resistivity on the on the cable ampacity [159]

To enhance the thermal conductivity of cable system, in-situ soil can be replaced with special thermal backfills. One of the essential feature of underground cable thermal backfills is their resistance to the migration of moisture and thermal drying during the occurrence of extreme conditions. Moreover, their mechanical strength should be sufficient to facilitate other services in the area such as sewers, water lines, roadways and railway tracks in addition to the erosion resistance. It should also have the ability to be placed in confined areas such as trenches and tunnels. Finally, it should be acceptable from environmental aspects without any harmful effects [159]. The qualities of a good thermal backfill prescribed by the Electric power research institute [160] include a high thermal conductivity over the range of operating conditions, lower critical moisture content, ease of installation, low materials costs and formulation using locally available materials. If SC-CBMs developed in Chapter 2 can satisfy all the

above-mentioned requirements, they can be used in Fluidized Thermal Backfills (FTBs).

FTBs are significantly different from conventional backfill materials like soils [49, 161, 162] due to their pumpability, improved thermal conductivity and remarkable thermal stability. The latter aspect is of special relevance since it refers to the capability of the material to guarantee constant thermal properties despite drying phenomena which may occur in proximity of the cables as a result of their high in-service temperature [155, 161]. Although mechanical properties of FTBs may vary significantly depending upon project-specific configurations and needs, their stiffness and strength need to be sufficient for the protection of buried cables from the effects of traffic loads. However, limitations to the maximum strength achieved in long-term conditions are frequently introduced as additional design requirements in order to facilitate the removal of such materials in the case of post-construction maintenance operations.

There are several procedures for the calculation of the ampacity of underground cable networks. Neher-McGrath (NM) equations for the ampacity calculations is one such method, still widely used for this purpose [163]. NM equations are useful in calculating both temperature rise and current carrying capacity of the cables. They use thermal equivalents of Ohm's and Kirchoff's laws for a cable system where the thermal resistivities of different cable-layers and surrounding medium are used as influencing factors. They work on the thermal-electrical analogy. For underground cables, thermal resistivity of the earthen portion and backfills are also taken into account [164].

As mentioned before recycled materials used for the formulation of SC-CBMs were Recycled Asphalt Pavement (RAP) and mineral sludge. Both are typically available in abundant quantities and they are usually treated either as waste materials, to be transported to landfills, or as potentially recyclable materials, for which adequate technological solutions need to be sought depending upon the intended end-use. As in the case of RAP, no studies have considered the potential use of mineral sludge in the production of FTBs. However, as mentioned also in the previous chapter, it was envisioned that sludge can provide added value to these composites as a result of two main characteristics. On one hand, its fine particle size distribution may be of aid in guaranteeing an adequate flowability, improving their stability and preventing segregation and bleeding [165, 76]. On the other hand, depending upon its mineralogical composition sludge may contribute to the increase of the thermal conductivity. In particular, it should be noted that while water and air have thermal conductivity values equal to 0.6 and 0.024 W/(m·K), respectively, minerals which constitute mineral sludge may have significantly higher values as in the case of quartz (7.69 W/(m·K)), calcite (3.59 W/(m·K)), chlorite (5.19 W/(m·K)) and muscovite (3.48 W/(m·K)) [166]. The presence of air and organic matter increase the thermal resistivity of materials, while water and clay minerals like quartz decrease.

In the experimental investigation described in this chapter, the main focus was on the design and performance assessment of SC-CBMs containing significant quantities of Reclaimed Asphalt Pavement (RAP) and mineral sludges produced by the crushing of mineral aggregates and by the cutting of natural stones. Consistently with the intended end-use of considered SC-CBMs as thermal backfills, relevant properties which were measured in the laboratory included flowability, thermal conductivity and thermal stability. The effect of thermal conductivity of the SC-CBMs on the ampacity of a high-voltage transmission line was also discussed.

3.2 Materials and methods

3.2.1 Granular components

Aggregates used for the formation of the lithic skeleton of SC-CBMs were obtained from a road construction contractor and were preliminarily characterized by evaluating their particle size distribution and specific gravity (SG) as per corresponding EN standards [119, 120]. Employed aggregate fractions included coarse gravel (indicated as 8-18 mm), coarse sand (designated as 0-8 mm) and RAP (preliminarily treated to reduce its maximum particle size to 12.5 mm). Use of RAP was considered to be compatible with the low strength requirements of the SC-CBMs, while it was assumed that its effects on fluidity and thermal properties could be directly assessed during design.

In order for SC-CBMs to exhibit a fluid behavior and achieve a dense state after setting, it is necessary to include in their formulation a relevant amount of fines. In such a context, possible use of three recycled mineral sludges of different types and origin was considered in the study. One sludge, referred to as “mineral sludge” (AS), was retrieved from the crushing and washing operations of the abovementioned natural aggregates (coarse gravel and coarse sand). The others were obtained as by-products of the cutting and polishing of granite stones in two different plants: depending upon the respective cutting process, they were indicated as “sawmilling sludge - diamond disc” (SS-D) and “sawmilling sludge - frame saw” (SS-F).

At the moment of sampling all sludges were characterized by a very high water content (of the order of 20-30%), but during the preparation of SC-CBMs they were used in their oven-dried state. Preliminary characterization of the sludges was carried out by means of the same procedures employed for aggregate fractions (determination of particle size distribution and specific gravity).

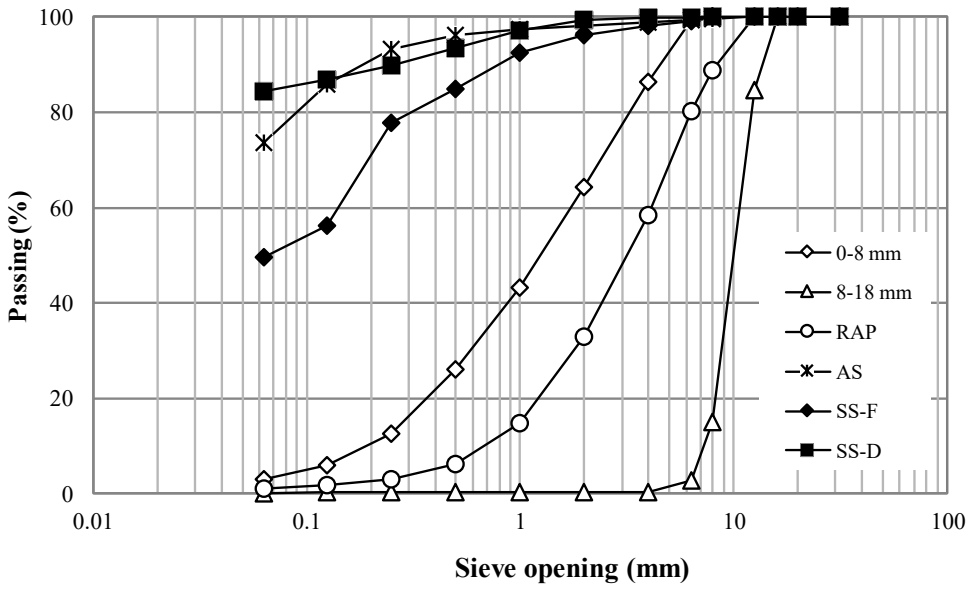

Figure 3.2 Particle size distribution of employed aggregates, RAP and mineral sludge

Results obtained in the preliminary characterization of component materials are synthesized in Figure 3.2 and Table 3.1, while Table 3.2 lists the data obtained from the chemical analyses performed on the mineral sludges.

Table 3.1 Specific gravity of employed components

Fractions	SG
0-8 mm	2.745
8-18 mm	2.733
RAP	2.527
AS	2.785
SS-F	2.954
SS-D	2.666
Portland cement	3.150

With respect to the results of sieve analyses, it was found that the RAP material was characterized by a continuous particle size distribution which makes it a good candidate for inclusion in SC-CBMs. Significant differences were recorded when comparing the three sludges. In particular, while sludges AS and SS-D were almost entirely passing the 0.25 mm sieve, sludge SS-F proved to be definitely coarser.

As expected, it was observed that the specific gravity of AS sludge was close to those recorded for the aggregate fractions from which it was derived, while RAP exhibited a relatively low SG value due to the presence of aged bitumen

films covering individual particles. Finally, SG values measured on the SS-F and SS-D sludges confirmed their different origin in terms of cutting operations and mineralogical composition.

3.2.2 Chemical analysis of the Sludge

Furthermore, since it was expected that sludges would be contaminated due to the wear and tear of crushing, cutting and sieving tools, chemical analyses were performed by means of an ICP (Inductively Coupled Plasma) mass analyzer in order to determine their heavy metals and iron content (as per EPA 3051A/2007 and EPA 6020A/2007). Microstructure of the mineral sludges was also characterized by means of Scanning Electron Microscopy (SEM) using FEI model Quanta Inspect 200 LV and Energy Dispersive X-Ray (EDX) using EDAX Genesis with the SUTW detector. In order to identify crystalline phases, mineral sludges were also examined by means of X-Ray powder Diffractometry (XRD) using Rigaku model Geigerflex.

Inductively coupled plasma mass analyzer is an elemental analysis technique which is capable of detecting elements which are present in very less quantities in a sample. It uses an inductively coupled plasma to ionize the sample. It decompose the samples into constituent elements and transforms those elements to ions and further detects them. In Scanning Electron Microscopy (SEM), a high energy beam of electrons are focused to a surface of a solid object. Interaction of the electrons with the sample reveal various features of the sample surface including its morphology and texture. SEM is also capable to extract information about specific points with the help of EDX. When accelerated electron beam touches the sample, it gets decelerated and the interaction creates dissipation of energy in the form of secondary electrons, backscattered electrons, heat, photons and visible light. Secondary electrons are useful for revealing the topography and morphology of the samples whereas the backscattered electrons depict the contrast in the composition of samples when different phases exist in the sample. The collision of the high energy electrons with the electrons in the outer shells of the sample excites the outer electrons which comes back to its original state with the emission of characteristic X-rays for that particular element. EDX typically work with the SEM system, where it typically collects the system of characteristics X-rays produced during the operation and analyses this energy spectrum to find out the presence of specific elements [167]. XRD is used for the characterization of crystalline materials. An incident beam of X-rays interfere with one another due to the presence of atomic planes in the crystalline sample. XRD pattern of a sample is the intensity of the X-rays scattered at different angles. The detector position is recorded as the angle (2θ). The detector records number of x-rays observed at each angle 2θ. Each phase produce a unique diffraction pattern, a

phase is specific chemistry and atomic arrangement. Amorphous materials do not produce sharp patterns.

Further component materials employed in the SC-CBMs included cement, belonging to class CEM II/A-L R42.5 as per EN standard [122], potable water, totally exempt from impurities, and a commercially available polycarboxylate-based superplasticizer used to improve fluidity.

Table 3.2 Chemical composition (heavy metals and iron) of mineral sludges

Sludge	Co [mg/kg]	Ni [mg/kg]	Cu [mg/kg]	Cr tot [mg/kg]	Zn [mg/kg]	Pb [mg/kg]	Fe [%]
AS	23.9	88.7	43.1	143.9	89.7	19.8	27.2
SS-D	20.2	0.4	<0.1	3.0	17.5	28.9	4.1
SS-F	21.3	69.5	96.7	88.0	85.3	17.5	29.9

Differences in the composition and origin of sludges were also reflected by the results of chemical analyses. Given that in standard aggregate processing there is no use of sharp cutting tools it can be hypothesized that metals detected in the AS sample are mainly derived from the parent rock. The SS-D sample showed high concentrations of Co, which is part of the diamond segment used for cutting, while other metals were all found in very low concentrations. The SS-F sample was characterized by higher concentrations of Fe, Cr, Cu and Zn which come from the blades and metal grit used during cutting. Regardless of origin and type, for all sludge samples the concentration of heavy metals was found to be lower than the legal limits defined by Italian legislation for use in industrial and commercial applications [168, 169, 170]. In such a context it should be emphasized that when including the considered sludges in SC-CBMs, a reduction of their free leaching potential is also expected due to the immobilizing effect induced on heavy metals by cement stabilization [171, 172]. Results obtained from the detailed microstructural characterization of sludge samples are shown in Figure 3.3 (SEM and EDX) and Figure 3.4 (XRD). Gathered information was considered as a useful supplement to the simple preliminary characterization illustrated above.

Sludge derived from the washing of quarried aggregates (AS) as investigated by means of SEM revealed a morphology characterized by a sheet-like arrangement of minerals, while the corresponding results from EDX analyses suggests the potential presence of quartz, dolomite, muscovite and chlorite. SEM and EDX results obtained for the diamond disc stone sludge (SS-D) and the frame saw stone sludge (SS-F) indicated the presence of metallic grains, possibly due to the wear and tear of cutting tools. In the specific case of the SS-D sample, obtained results highlight the presence of Co and Cu which derive from the employed diamond cutting tools. In the case of the SS-F sample, the highlighted

presence of Fe and Ca are respectively due to the employed cutting tool and to the antioxidant used during this processing.

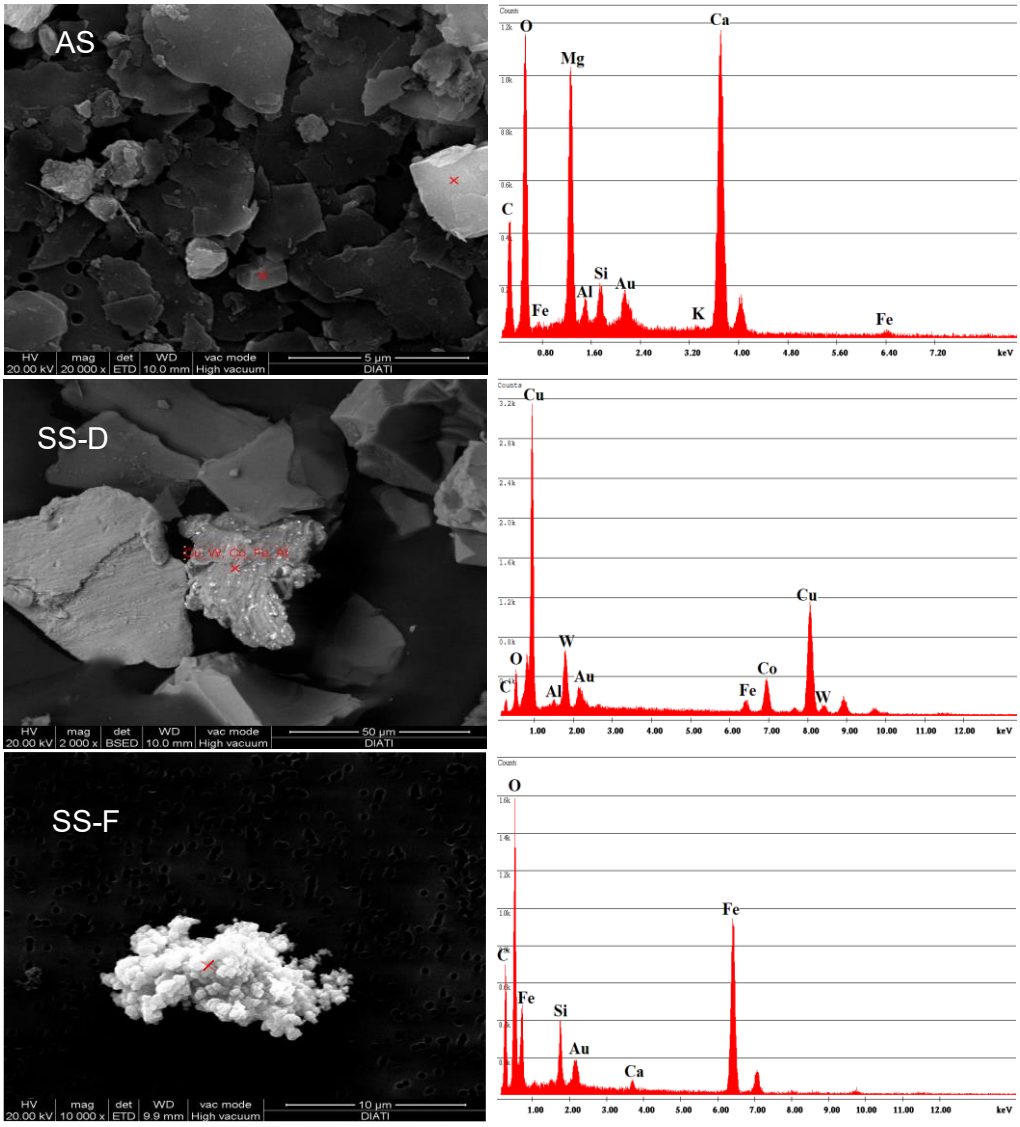

Figure 3.3 Results of SEM and EDX analyses performed on sludge samples

XRD peaks identified in the case of the AS sludge were associated to the presence of quartz, calcite, dolomite, chlorite and muscovite, thus confirming the findings coming from the SEM-EDX analyses. Results obtained on the SS-D and SS-F samples showed similar peaks corresponding to quartz, feldspar and mica (not highlighted in Figure 3.3), while no peaks associated to metals were identified as a result of their very low quantity.

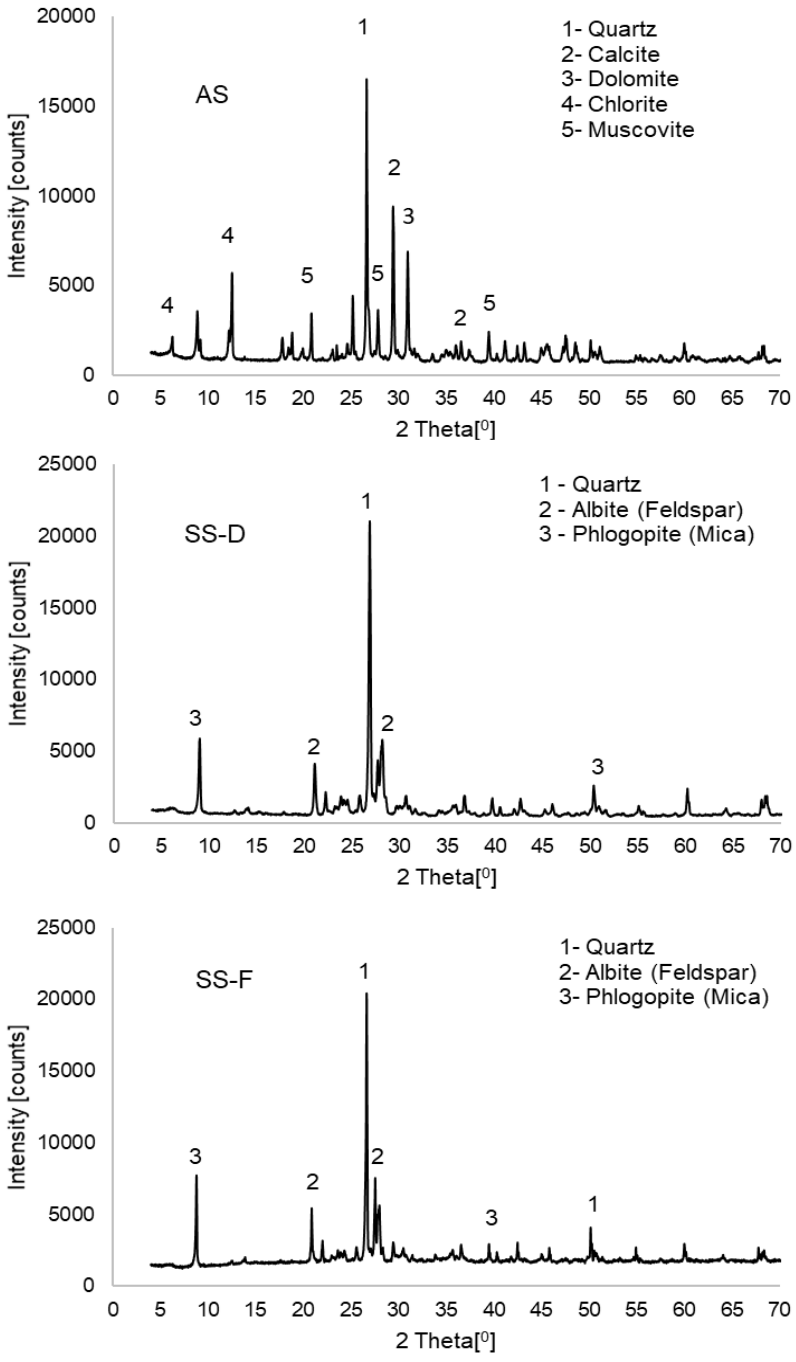

Figure 3.4 Results of XRD analyses performed on sludge samples

3.2.3 Formulation of the mixtures

It is well recognized that flowability and self-compacting ability of these cement-based composites can be achieved by optimizing the particle packing of the aggregate skeleton and by varying water content [57]. Thus, in the investigation described in this chapter, available components were combined in

order to yield a total size distribution that would replicate as closely as possible the following target one suggested by Funk and Dinger for self-compacting concrete, known and the "modified Andersen and Andreasen model" [139]: This is the same mix design procedure that is adopted in Chapter 2 but to account for the variations in the raw materials received from the producers, the mix designs were updated as follows.

$$P(D) = 100 \cdot \frac{({D_{max}}^{q} - D^{q})}{(D_{max}^{q} - D_{min}^{q})} \quad 3.1$$

where D is the diameter of aggregate particles (in mm), P(D) (expressed in %) is the cumulative percentage passing the sieve with opening equal to D, D_{max} is the maximum diameter of aggregate particles in the mixture (in mm, corresponding to P(D) equal to 100% and equal to 16 for all mixtures), D_{min} is the minimum diameter of aggregate particles in the mixture (in mm, assumed to be equal to 5 μm for all mixtures), q is the so-called distribution modulus (assumed equal to 0.21 in the investigation). The target size distribution adopted in the investigation is shown in Figure 3.5, where for the same maximum particle size (equal to 16 mm) it is compared to the classical Fuller curve adopted for the design of dense-graded mixes [173].

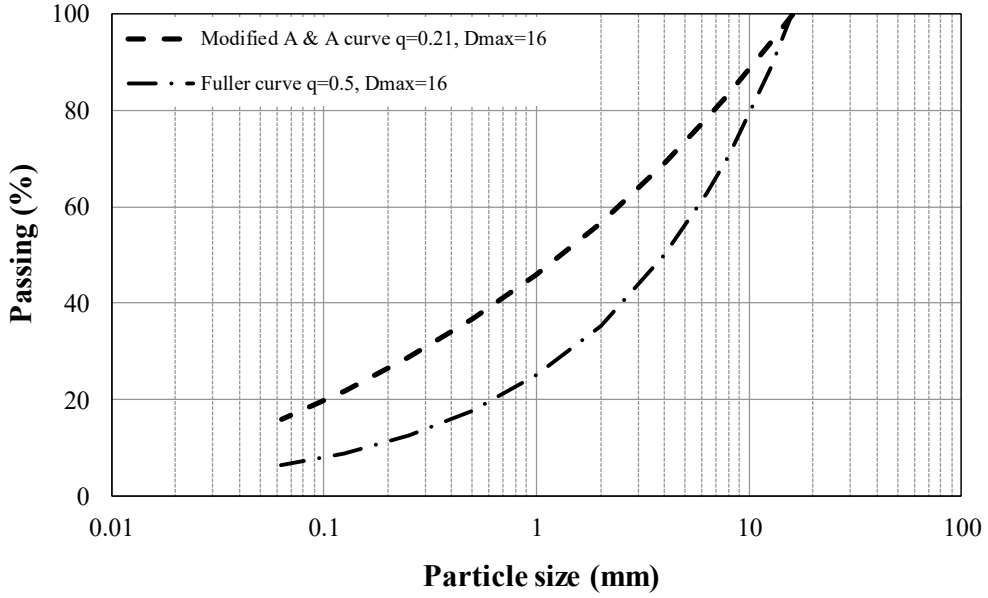

Figure 3.5 Target and Fuller particle size distribution

Composition of the laboratory-prepared SC-CBM mixtures included in the investigation was defined by considering, for each type of sludge, variable cement content (equal to 60, 80 and 100 kg/m^3), RAP content (equal to 0, 15, 20 and 30%), and water-to-powder ratio (W/P, equal to 0.70, 0.75 and 0.80). The dosage

of superplasticizer was kept equal to 0.5% by weight of cement for all mixtures. The term powder is herein used to collectively indicate cement and sludge, which jointly contribute to paste fluidity and void filling. The full-factorial testing matrix stemming from the combination of the factors indicated above was reduced to a more manageable test plan in which the effects of each variable could still be highlighted. In particular, RAP content was varied only in the case of the SC-CBMs containing sludge AS, while it was fixed at 20% in the case of SC-CBMs containing sludges SS-D and SS-F.

Percentages of the various components constituting the aggregate skeleton of the mixes (virgin aggregates, RAP and sludge) were identified by minimizing the differences between the total particle size distribution and the reference one defined in equation 3.1. To avoid biasing effects stemming from the combined use of components with different specific gravities, size distributions were expressed in volumetric terms. As indicated in Figure 3.6, in all cases the corresponding residual deviations were found to be extremely small.

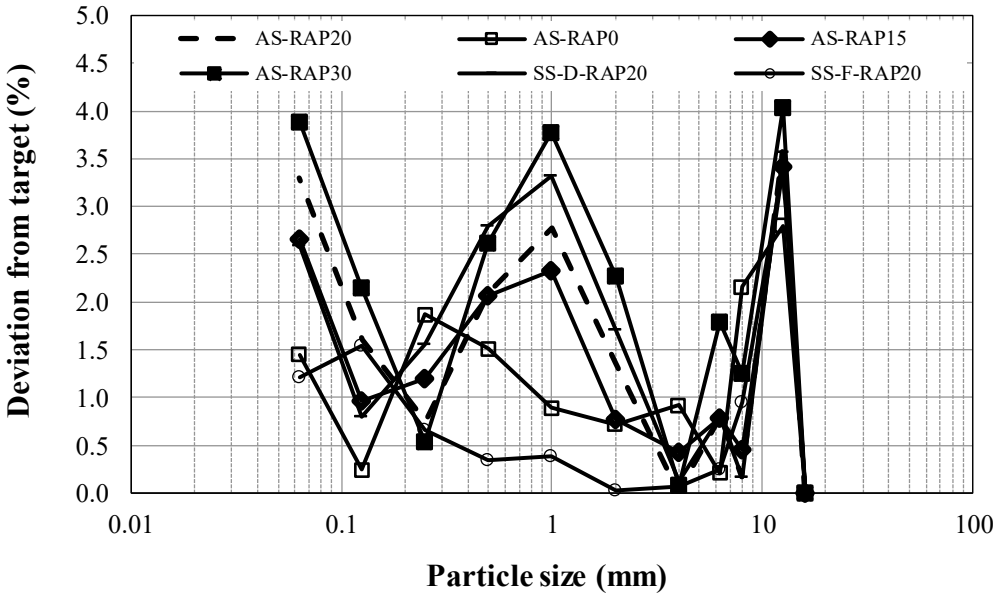

Figure 3.6 Residual deviations from target particle size distribution

Table 3.3 lists the composition of all the SC-CBMs considered in the investigation. They were all prepared by making use of a laboratory mortar mixer and by adopting a protocol which consisted of preliminary mixing of dried aggregates and cement, followed by addition of premixed solutions of water and superplasticizer additive, and completed by continuous mixing until achievement of a homogenous composite.

Flowability of the investigated mixtures was evaluated by making use of the flow consistency test described in ASTM D 6103 [123]. As prescribed by the standard protocol, an open-ended cylinder of 75 mm diameter and 150 mm height is filled with SC-CBM which is thereafter allowed to spread over a non-absorbent

flat surface by lifting the cylinder. The spread diameter (D_s) is then measured and the test sample is visually observed to identify any segregation or bleeding phenomena. It is reported that a flow spread of 170-250 mm can be considered adequate for trench filling applications [48].

Table 3.3 Composition of SC-CBM mixtures

SC-CBM mixture	Cement [kg/m3]	W/P [-]	Composition of aggregate skeleton			
			RAP [%]	Sludge [%]	0-8 mm [%]	8-18 mm [%]
AS-RAP20-C60-0.8	60	0.8	20	24	39	17
AS-RAP20-C80-0.8	80	0.8	20	24	39	17
AS-RAP20-C100-0.8	100	0.8	20	24	39	17
AS-RAP0-C100-0.8	100	0.8	0	21	57	22
AS-RAP15-C100-0.8	100	0.8	15	23	44	18
AS-RAP30-C100-0.8	100	0.8	30	25	31	14
AS-RAP20-C100-0.75	100	0.75	20	24	39	17
AS-RAP20-C100-0.7	100	0.7	20	24	39	17
SS-D-RAP20-C100-0.7	100	0.7	20	23	40	17
SS-D-RAP20-C100-0.8	100	0.8	20	23	40	17
SS-F-RAP20-C100-0.7	100	0.7	20	32	30	18
SS-F-RAP20-C100-0.8	100	0.8	20	32	30	18

3.2.4 Thermal conductivity measurements

Precise knowledge of the thermal conductivity of materials are necessary to use them in applications involving backfilling of electric cables. This data is needed for the design and loading of such cables. A needle probe (Figure 3.7) which works on the principle that temperature rise in a line heat source is dependent on the meadium in which it is placed [162]. In case of soils, thermal conductivity is mainly influenced by the moisture content and density. As these factors increases, the thermal conductivity also increases. Migration of moisture from the vicinity of the measurement location due to heating or gravity can also influence the test results.

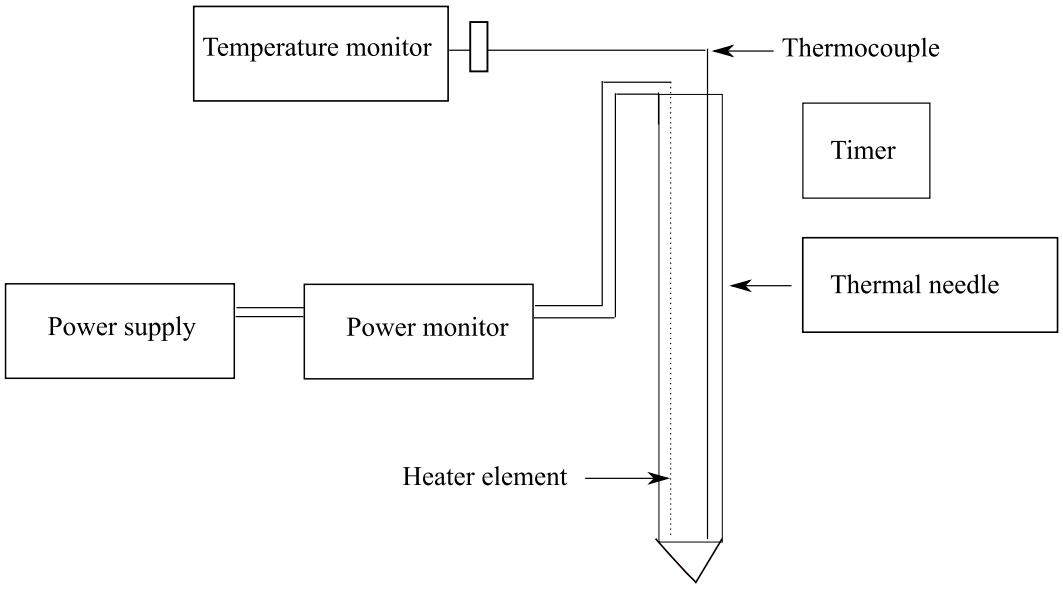

Figure 3.7 Schematic representation of thermal needle probe [162]

Thermal conductivity of the SC-CBMs were measured as per ASTM D 5334 [174] by employing a thermal needle probe (KD2 Pro Thermal Properties Analyzer of Decagon Devices Inc.) which has been extensively used by different researchers for the evaluation of thermal conductivity of soils and cement composites [156, 175, 174]. In the present study, thermal conductivity tests were performed on cylindrical specimens 100 mm in diameter and 200 mm in height which were cured at room temperature (Figure 3.8). Three holes were drilled on the top surface of each specimen before hardening in order to allow the later introduction of the needle probe (100 mm long and 2.4 mm in diameter). To avoid any misreading in measurements, a sufficient free clearance was kept between adjacent holes and between the holes and the lateral specimen surface.

The needle probe acts both as a transient line heating source and as a temperature sensor. Temperature measurements are recorded, at the same intervals, after heating the needle for a fixed duration and during cooling. Thermal conductivity is consequently assessed according to the following equation:

$$k = \frac{q_h}{4\pi a} \qquad 3.2$$

where k represents the thermal conductivity (expressed in W/(m·K)), q_h the heating power of the needle and a indicates the slope of the straight line which models temperature as a function of the logarithm of time.

Figure 3.8 Thermal conductivity measurements

Tests were carried out at different curing times (7, 14 and 28 days). Furthermore, after 28 days of curing, specimens were oven-dried at 60 °C for 48 hours in order to obtain further thermal conductivity measurements which are believed to be representative of low-moisture conditions which may occur during the service life of SC-CBMs. Such measurement conditions are referred to as "lab-dried". As a supplement to all the performance-related tests described above, selected analyses were carried out on SC-CBMs by means of SEM and EDX by using the same equipment described in section 3.2.1.

3.2.5 Ampacity of high-voltage lines embedded in SC-CBMs

As part of the performance-related evaluation of the SC-CBMs considered in the investigation, calculations were performed in order to assess the ampacity of a reference high-voltage transmission line. Ampacity represents the maximum current-carrying capacity of a line which is defined as a function of the limiting conditions in terms of maximum allowable heating of the cables [46]. Such a heating is affected not only by the line characteristics and configuration, but also by the thermal properties of the employed backfill materials. As discussed in literature, use of properly designed thermal backfills can enhance the ampacity of the cables as well as reduce the construction time and overall cost due to the assured quality and quick installation [24].

As shown in Figure 3.9, the reference high-voltage line considered as a reference consists of a four-cable 320 kV arrangement in which the cable contained in conduits are buried directly in the SC-CBMs without any protective

duct banks. The target ampacity of this particular line was considered equal to 600 MW. Since this specific case was referred to a tunnel, air temperature was fixed at 40 °C, while the maximum allowable temperature for the safe operation of cables was set at 70 °C. Ampacity calculations were carried out by making use of the model proposed by Neher and McGrath [176].

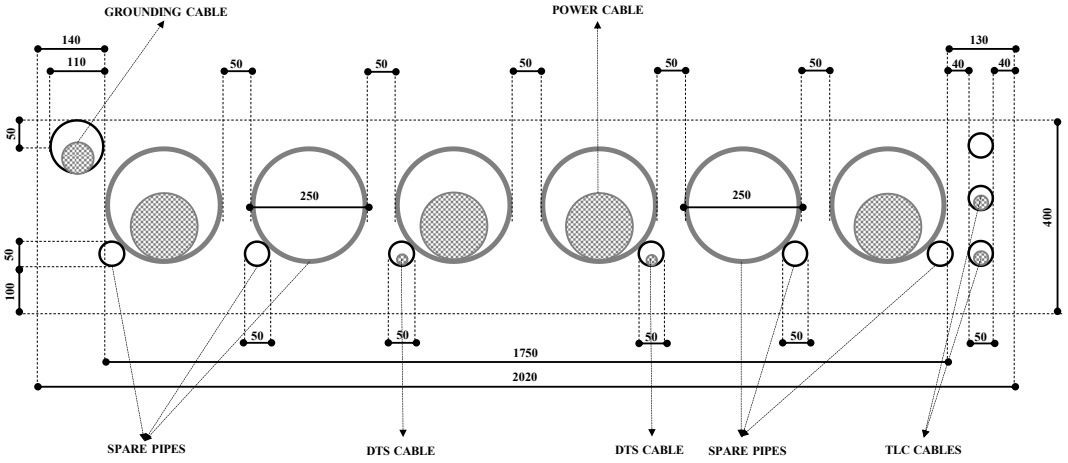

Figure 3.9 Reference high-voltage transmission line used for ampacity calculations

3.3 Results and discussion

Table 3.4 contains the experimental results obtained during the investigation. Spread diameter (D_s) was derived from measurements performed along two orthogonal directions after specimen spreading. Thermal conductivity (k) was calculated as the average of the readings obtained from the three measurements performed on each specimen.

As shown in Table 3.4, all the investigated SC-CBMs exhibited flow spreads greater than 200 mm, thus satisfying the requirements suggested in ACI guidelines [48]. However, bleeding and segregation phenomena occurred in mixtures manufactured with SS-D and SS-F sludges when the W/P ratio reached a value of 0.8, thus preventing the measurement of flow spread. These effects, which probably derive from the specific water absorption properties of employed sludges, do not allow the use of the corresponding SC-CBMs as trench filling materials since a non-homogeneous distribution of air voids and moisture can lead to unacceptable thermal properties. Mixes with 30% RAP also showed similar segregation and bleeding and therefore were not considered in subsequent thermal conductivity analyses.

With respect to thermal conductivity, results were analyzed to identify the effects of variations of curing time, cement content, RAP dosage, W/P ratio and

sludge type. Furthermore, results obtained in lab-dried conditions were considered in order to have information on thermal stability. Figure 3.10 shows the results obtained on SC-CBMs prepared with variable cement content and by employing the AS sludge with 20% RAP and W/P equal to 0.8. In agreement with other studies [177, 178, 179], it was observed that curing time has a negligible effect on thermal conductivity, probably as a result of the presence of a densely packed aggregate skeleton which results in a low void content. Furthermore, cement content has a significant influence on thermal conductivity, which increases by 20% (passing from 1.475 to 1.745 W/(m·K)) when changing cement content from 60 to 100 kg/m3. Such a variation is due to the thermal conductivity of the products formed during the hydration process of cement, which is higher than that of water (equal to 0.604 W/(m·K)) and lower than that of dry cement powder (1.55 W/(m·K)) [175]. Moreover, experimental outcomes can also be explained by considering the porosity reduction induced by making use of higher cement dosages [177, 180].

Table 3.4 Synthesis of experimental results

SC-CBM mixtures	D_s [mm]	k (W/(m·K)) 7 days	14 days	28 days	lab-dried
AS-RAP20-C60-0.8	213	1.512	1.627	1.475	0.820
AS-RAP20-C80-0.8	225	1.661	1.662	1.697	1.022
AS-RAP20-C100-0.8	235	1.809	1.865	1.745	1.068
AS-RAP0-C100-0.8	204	1.670	1.549	1.386	0.863
AS-RAP15-C100-0.8	222	1.869	1.775	1.639	1.017
AS-RAP30-C100-0.8	-	-	-	-	-
AS-RAP20-C100-0.75	225	1.609	1.514	1.371	0.902
AS-RAP20-C100-0.7	210	1.632	1.635	1.333	0.864
SS-D-RAP20-C100-0.7	240	1.652	1.519	1.620	0.794
SS-D-RAP20-C100-0.8	-	-	-	-	-
SS-F-RAP20-C100-0.7	260	1.908	1.675	1.450	0.873
SS-F-RAP20-C100-0.8	-	-	-	-	-

Effects due to other composition variations are represented in Figure 3.11, which refers to thermal conductivity measurements carried out on selected sets of SC-CBMs after 28 days of curing. It can thus be noticed that all considered factors may have an impact on the thermal properties of SC-CBMs.

In the case of RAP, observed variations may be attributed to the concurring change in dosage of the other components (such as sludge) and to the associated effect on particle size distribution, porosity and cement paste volume. A 22% difference was observed between the SC-CBM with only virgin aggregates and

the one containing 20% RAP (mixtures with 100 kg/m^3 cement, AS sludge and W/P equal to 0.8).

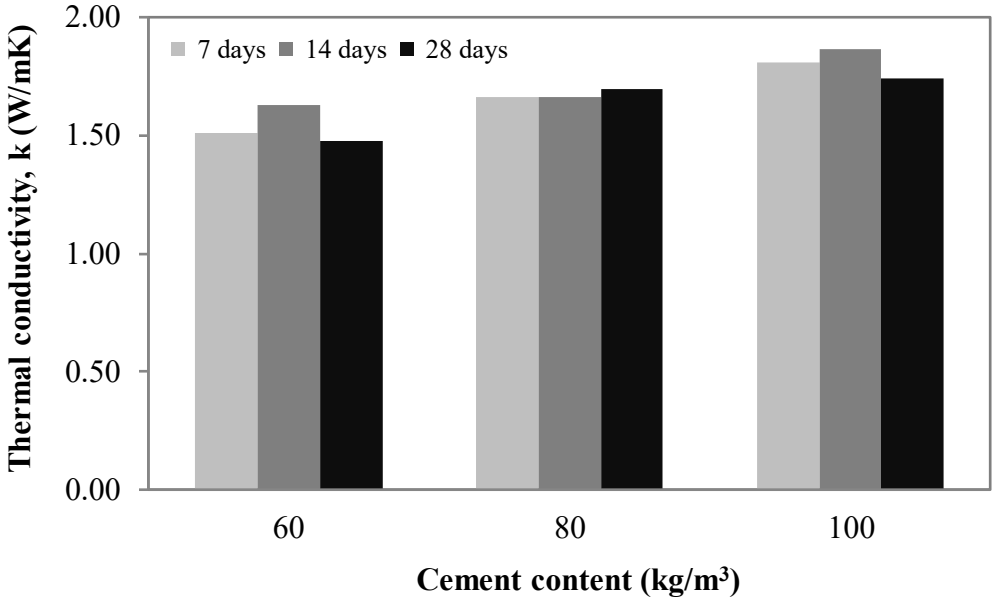

Figure 3.10 Effect of cement content and curing time on thermal conductivity

Recorded effects due to W/P variations were also non-negligible. In particular, thermal conductivity increased significantly (by approximately 30%) when W/P reached the highest value considered in the investigation (equal to 0.8, for mixtures prepared with 100 kg/m^3 cement, AS sludge and 20% RAP). Such an occurrence can be explained by considering that water has a higher conductivity than air, and that mixtures characterized by an excess moisture are prone to be highly conductive.

Finally, effects related to variations of sludge type were also apparent as a result of their variable mineralogical and chemical composition (already discussed in section 3.2.1). In particular, this is shown in Figure 3.11 by considering mixtures prepared with 100 kg/m^3 cement, 20% RAP and W/P equal to 0.7. As mentioned in section 3.1, thermal stability is an essential requirement of SC-CBMs in the case of buried high-voltage cables which continuously transfer heat to the surrounding backfilling material, causing a progressive reduction of moisture. Thus, in the present study assessment of SC-CBM thermal stability was carried out by comparing thermal conductivity measured in lab-dried conditions to that recorded after 28 days of curing. In general terms it was observed that the very low moisture content reached in lab-dried conditions led to a significant reduction of thermal conductivity. However, values recorded in these limiting conditions were still compatible with typical design requirements, which indicate 0.8 W/(m·K) as the recommended minimum limit. This is once again due to the

dense packing of the aggregate skeleton comprised in the considered SC-CBM mixtures and to the presence of a highly conductive hydrated cement paste.

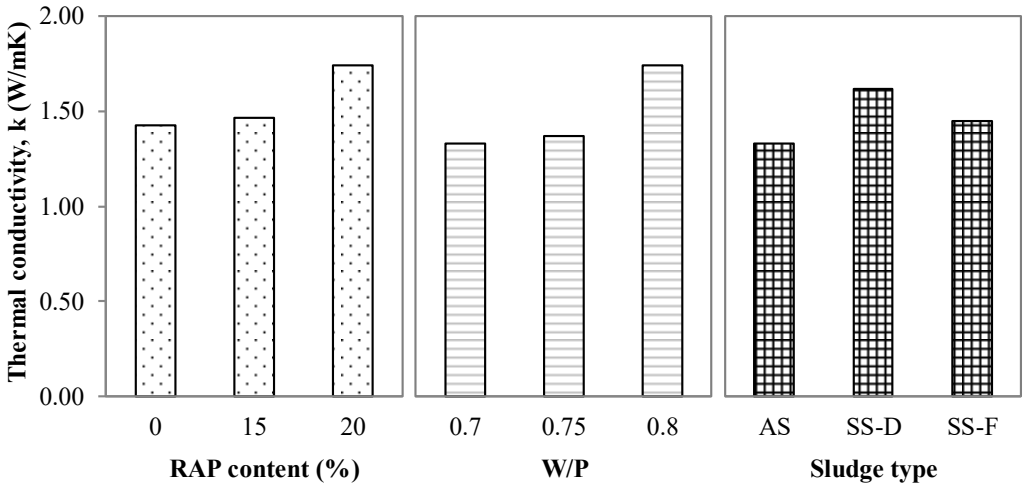

Figure 3.11 Effects of composition variations on thermal conductivity

Examples of the results obtained during the investigation are provided in Figure 3.12, which refers to mixtures prepared with variable cement content and by employing the AS sludge with 20% RAP and W/P equal to 0.8. It can be observed that for these mixtures the thermal conductivity reduction was in all cases of the order of 40%.

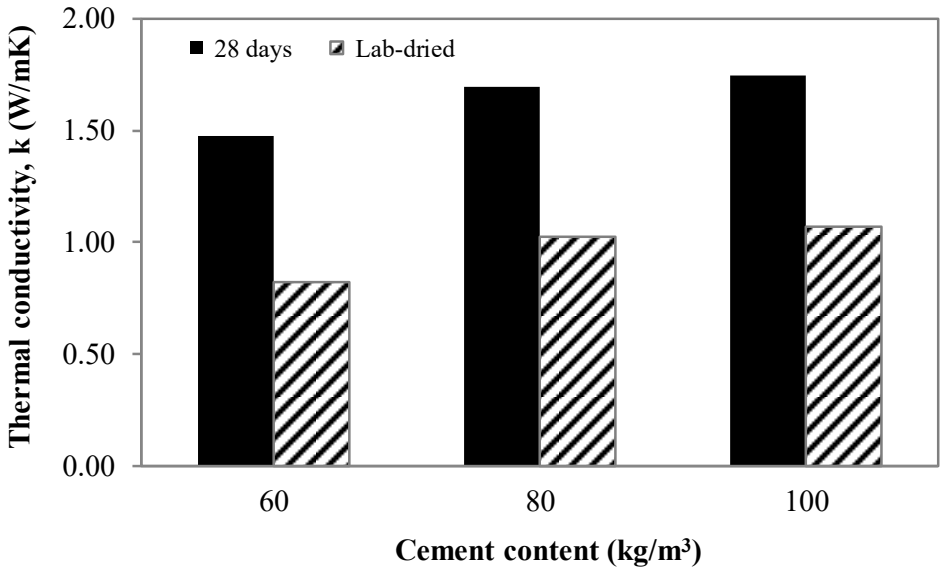

Figure 3.12 Thermal stability of selected SC-CBMs

Results obtained from SEM and EDX analyses carried out on SC-CBMs are shown in Figure 3.13, which refers to a mixture prepared with AS sludge and 20% RAP. The purpose of the analyses was to verify the immobilization of heavy metals which is a desired effect in the context of waste reutilization in cement-bound composites [181]. Obtained results confirm the expected formation of calcium-silicate-hydrates (CSH), characterized by a poorly crystalline structure with different morphologies, by the presence of impurities such as Al, Mg and Fe, and by a binding affinity towards metals [182]. It was also observed that the microstructure of the prepared SC-CBM is characterized by void spaces and weak interfaces between aggregates and cement paste. This may be due to the high water content and low cement dosage adopted during the mix design.

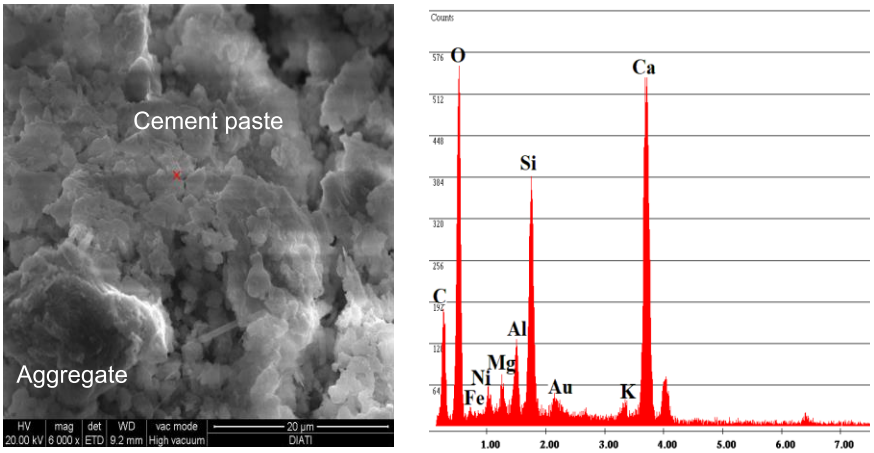

Figure 3.13 SEM and EDX analyses performed on a selected SC-CBM

The ampacity calculations performed as indicated in section 3.2.5 were based on the experimental results listed in Table 3.4, and were carried out in by considering both short-term and long-term conditions. In the first case, thermal conductivity values employed as input data to the Neher and McGrath model were those measured after 7 days of curing. In the second case data used for calculations were those obtained in lab dry conditions in order to account for the dry-out phenomena which take place in materials surrounding high-voltage cables. In both cases the thermal properties were expressed in terms of thermal resistivity (ρ) which by definition is the inverse of thermal conductivity (k).

Table 3.5 shows required the range of resistivity values considered in calculations in short-term and long-term conditions, together with the calculated ampacity values. In short-term conditions, ampacity was found to be significantly higher than that of the targeted value of 600 MW for the entire range of thermal conductivity measured at the laboratory. In the long term, line ampacity was found to be very close to target with some values below the 600 MW threshold associated to the higher SC-CBM resistivity values.

Table 3.5 Ampacity calculations

Short- term		Long- term	
$\rho_{SC\text{-}CBM}$ (K·m/W)	Ampacity (MW)	$\rho_{SC\text{-}CBM}$ (K·m/W)	Ampacity (MW)
0.524-0.661	764.9-718.1	0.936-1.220	644.8-588.0

The main quality control parameters for SC-CBMs are their flow and mechanical strength. Thermal properties are not always measured at the field due to the practical difficulties but with proper selection of materials and production procedures sufficient thermal properties can be ensured [159]. Based on the thermal conductivity studies, it was seen that SC-CBMs under investigation can be successfully used in pavement foundations even in presence of buried high-voltage cables. This also opens up another area for the use of SC-CBMs as fluidized thermal backfills (FTB). As the results are promising from these performance aspects, large scale field trials were planned in the next part of the research.

Part III: Field trials, Optimization and Pavement design

Some of the works described in this part has been submitted/published as:

- E. Santagata, E. Choorackal and P.P Riviera, “Self-compacting cement-bound pavement foundations for road tunnels: performance assessment in field trials,” Under review in the *International Journal of Pavement Engineering*.

- P.P Riviera, E. Choorackal, and E. Santagata, “Performance evaluation of innovative and sustainable pavement solutions for road tunnels,” in: *Proceedings of the 5th International Symposium on Asphalt Pavements & Environment (APE)*. ISAP APE 2019. *Lecture Notes in Civil Engineering*, vol 48. Springer, Cham, 11-13 Sep 2019, https://doi.org/10.1007/978-3-030-29779-4_40

4. Field trials of self-compacting cement-bound mixtures

Laboratory investigations described in Chapters 2 and 3 discussed the potential of SC-CBMs to be used in the pavement foundation of road tunnels. Encouraging results obtained in the laboratory led to the organization of field trials. This part of the thesis describes the field trials conducted for the further optimization of these mixtures. It also describes the development of performance-based criteria for their quality control.

4.1 Scheme of field trials

As a follow-up to initial laboratory investigations described in Chapters 2 and 3, further research studies were carried out by means of full-scale field trials which entailed the plant production and laying of several SC-CBMs. As described in this chapter, the mixtures were subjected to field and laboratory tests for a comprehensive assessment of their performance-related properties. Hence, the performance investigation considered both the tests which are recommended in international guidelines available for CLSMs [25, 48] and typical tests that are used for conventional unbound foundation materials [133]. Tests which belong to the first group focus on characteristics of the CLSMs in the fresh and hardened state, thereby measuring flowability and compressive strength. Additional tests, usually employed for the assessment of the bearing capacity characteristics of pavement sub-bases and subgrades, were those which measure resilient modulus in the laboratory by means of a triaxial equipment and deformation modulus in the field by means of the classical plate loading procedure. Finally, since pavement foundations are usually subjected to construction traffic within a short period after laying, such a situation was simulated during the investigation by subjecting the constructed slabs to the passage of heavy vehicles.

The investigation included four field trials. Field trial 1 had the main objective of verifying the feasibility of mass production and laying of the SC-CBMs and to assess their sensitivity to variations in particle size distribution and cement dosage. As a supplement to this first trial, field trial 2 considered the use of mixtures with higher cement dosages which also included the use of an accelerating agent for the achievement of rapid hardening properties. Field trial 3 was similar to the previous one, except for the fact that it was actually performed inside a road tunnel in order to assess the effect of curing conditions on the in-place characteristics of this specific type of mixture. Finally, field trial 4 was

carried out by considering a laying geometry which more closely replicated that of a road tunnel and by focusing on cement-bound mixtures characterized by optimized formulations identified as a result of the previous experimental activities. Results of laboratory and field tests were interpreted with the objective of identifying the effects of the different components on the properties of the mixtures. These outcomes led to performance-related acceptance criteria which may be adopted during actual construction works which involve the use of SC-CBMs in road tunnels.

4.2 Materials and methods

4.2.1 Mixture components

Components which were available for the formation of the aggregate skeleton of the SC-CBMs were coarse sand (0-8 mm), gravel (8-18 mm), RAP (0-12.5 mm) and mineral sludge. These were subjected to preliminary characterization tests for the determination of particle size distribution and specific gravity (SG) as per corresponding EN standards [119, 120]. Obtained results are shown in Figure 4.1 and Table 4.1. It can be observed that the results refer to two distinct sampling operations which were carried out during the progress of the investigation and that only minor changes were recorded in the characteristics of the various components. Nevertheless, these variations were taken into account in the formulation of the mixtures produced as part of each field trial (see section 4.2.3). Materials retrieved during the first sampling session were employed only in trial 1; those which were collected in the second phase of operation were used in field trials 2 to 4.

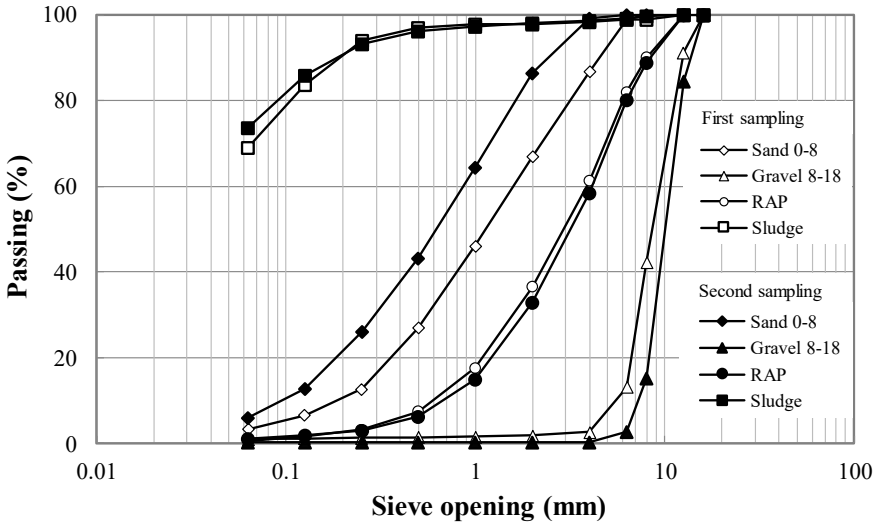

Figure 4.1 Particle size distribution of components.

Table 4.1 Specific gravity of aggregate fractions, RAP and mineral sludge.

Fraction	SG	
	First sampling	Second sampling
Sand 0-8	2.745	2.786
Gravel 8-18	2.744	2.716
RAP	2.530	2.485
Sludge	2.786	2.810

RAP material employed in the investigation was derived from the milling of aged, dense-graded asphalt mixtures. Bitumen content of the single RAP fraction which was made available, determined as per [121], was found to be equal to 4.57% and 4.42% (by weight of aggregates) for the material collected in the first and second sampling session, respectively. It was considered that, due to its aged conditions, residual bitumen contained in RAP would act as an inert component, with no expected diffusion through the adjacent cement paste. Nevertheless, it was not excluded that it could have some effects on the mechanical properties of the SC-CBMs [183, 184].

Mineral sludge employed in the investigation was collected from the stockpiles of an aggregate crushing plant. As a result of its origin (i.e. aggregate washing) and of its fineness, in the natural state it was characterized by a very high water content, of the order of 20%. In the initial phases of the research project (i.e. in field trials 1 and 2), the presence of such a high quantity of water was taken into account by reducing the quantity of water added during the plant production of the SC-CBMs. Nevertheless, as illustrated in the following, efforts were placed in trying to devise an appropriate system for sludge drying in order to ensure a better control of water content during mixture production and to avoid problems related to the tendency of the wet sludge to clog the feeding lines.

At first, sludge drying was attempted by simply spreading it over an open area and by periodically subjecting it to light mixing by means of a wheel loader. However, such a procedure, which was followed in preparation of field trials 1 and 2, proved to be unsuccessful, with a residual water content which remained quite high, of the order of 15%. Furthermore, it was observed that final water content was non-uniform throughout the sludge and that such a non-homogeneity had a negative impact on the production consistency of the corresponding SC-CBMs.

A significant improvement in the drying process was achieved in the second part of the research project, when it was carried out by subjecting the mineral sludge to mechanical pulverization in the presence of added quicklime. As suggested by the wide international literature on lime stabilization of soils

[185, 186, 187], it was envisioned that with such an operation a significant reduction of water content would be obtained as a result of the consumption of water through its reaction with quicklime and of water evaporation caused by the heat released during quicklime hydration.

Figure 4.2 Sludge drying at the field using pulvimixer

Definition of the optimal dosage of lime to be employed for sludge drying was carried out by means of a dedicated trial carried out on a sludge bed of 50 m length, 3 m width and 50 cm thickness which was characterized by an initial water content equal to 22%. On the first half of the section, quicklime was spread over the sludge bed with a dosage of 3% (by weight of the wet sludge), while in the second half the dosage of quicklime was increased to 6%. Sludge-quicklime mixing was thereafter carried out by making use of a pulvimixer (see Figure 4.2). Temperature measured in the sludge bed after treatment was observed to increase significantly and reached values of the order of 40 °C, with a corresponding air temperature of 9 °C. The treated sludge was then left to cool for 1 day and the effectiveness of the considered treatments was thereafter assessed by evaluating water content. Final values of this parameter were equal to 15% and 8% for the 3% and 6% quicklime dosage, respectively. It was therefore concluded that sludge pretreatment with 6% quicklime would be recommended for the remaining field trials. Higher quicklime dosages were not investigated in order to contain processing costs. Although adjustments to the quantity of water added during plant production were still needed even when employing pretreated sludge, they were definitely smaller than those necessary in the first two trials and an improvement of production consistency was clearly observed.

Although quicklime pretreatment was considered with the only purpose of reducing water content, it was expected that composition and microstructure of sludge would be affected by hydration reactions. Furthermore, it was envisioned that such reactions could also have some effect on the mechanical properties of the SC-CBMs in which the pretreated sludge would be included. In order to

address these issues, sludge samples retrieved from the site before and after treatment with quicklime were subjected to X-Ray powder Diffractometry (XRD) tests, performed by making use of a Rigaku model Geigerflex, with the objective of identifying the presence of crystalline phases. Furthermore, the untreated and treated sludge was subjected to observations with a Scanning Electron Microscope (SEM), FEI model Quanta Inspect 200 LV, and to Energy Dispersive X-Ray analyses (EDX), carried out by means of a EDAX Genesis with SUTW detector. Obtained results are displayed in Figure 4.3 and Figure 4.4. Results of XRD tests are expressed in the form of spectra which display the intensity (I) measured by the X-ray detector as a function of its position, defined by the angle 2θ. Results of EDX tests, which were performed by targeting specific points of the samples subjected to SEM observations, are given as spectra which show the counts recorded by the detector as a function of their energy level, expressed in kiloelectron volts (keV). This is similar to the chemical analysis performed in section 3.2.2.

The results of XRD analyses (Figure 4.3) showed that mixing with quicklime caused a remarkable increase of the peak associated to calcite (identified with code “2”), while the characteristic peaks of other minerals (quartz, dolomite, chlorite and muscovite) remained almost unchanged. Outcomes of the EDX analyses (Figure 4.4) were consistent with the results of XRD tests, indicating the presence in the treated sludge of hydrated compounds of Ca, Mg, Al and Si, which are similar to those which are formed as products of Portland cement hydration [186]. Finally, SEM observations (Figure 4.4) indicated that the mineral sludge initially possessed a morphology characterized by a sheet-like arrangement of minerals; after the addition of quicklime, microstructure increased in complexity, with the supplementary presence of amorphous hydrated precipitates.

All SC-CBMs considered in the investigation were produced by making use of Portland cement of the CEM II / A-L 42.5 R type [122] and by employing a commercially available polycarboxylate superplasticizer (Advaflow 455, supplied by Grace Products). According to the information obtained from the manufacturers, specific gravity of these two components was equal to 3.150 and 1.060, respectively. For most of the SC-CBMs produced and laid in field trials, the time-dependent hardening effects of Portland cement were tuned by making use of a hardening accelerator (Polarset, supplied by Grace Products). Its specific gravity, as declared by the producer, was equal to 1.250. Water employed for the plant production of the SC-CBMs was drawn from the local supply network and was declared to be exempt from impurities.

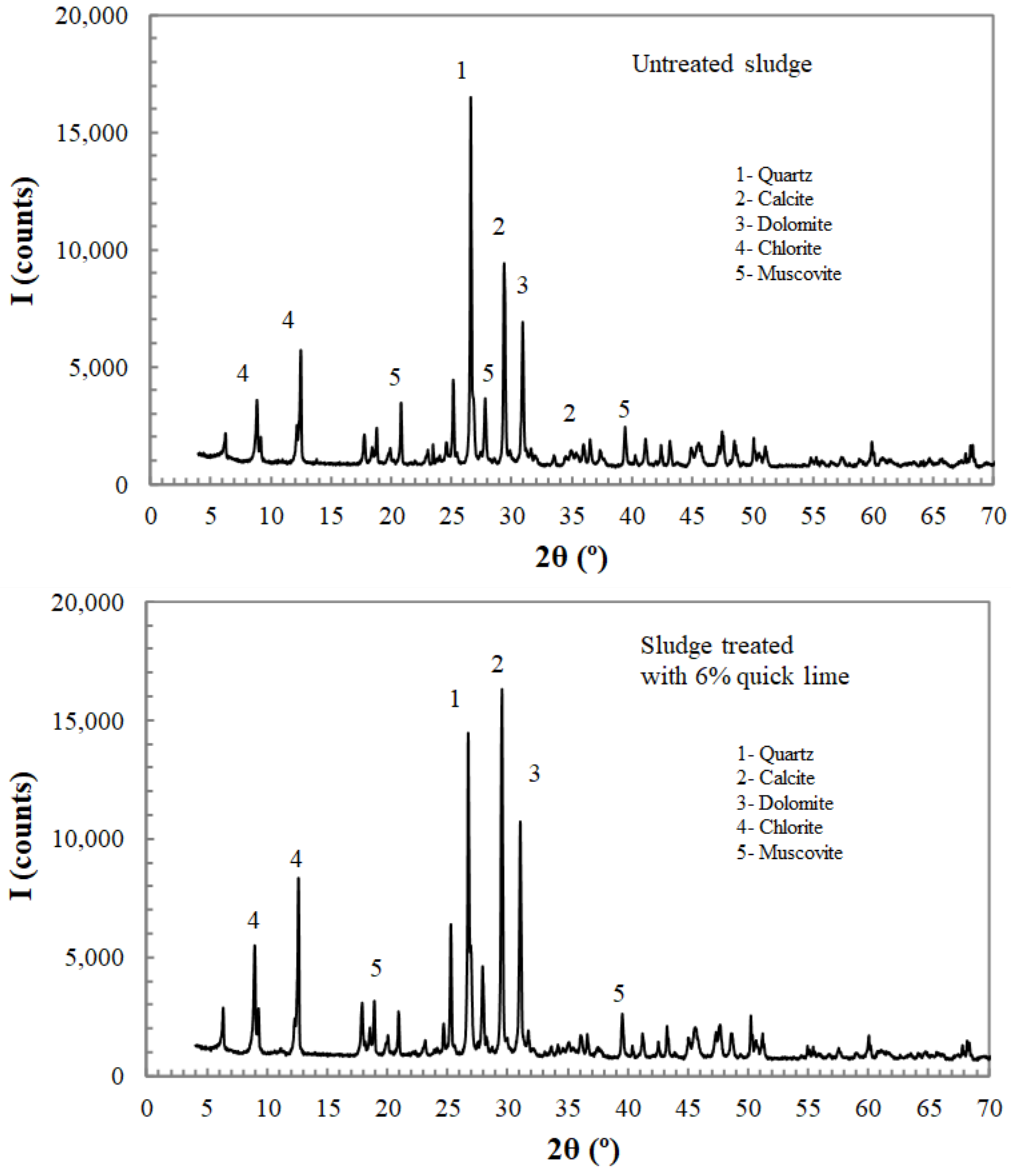

Figure 4.3 XRD spectra of mineral sludge (untreated and treated with 6% quicklime)

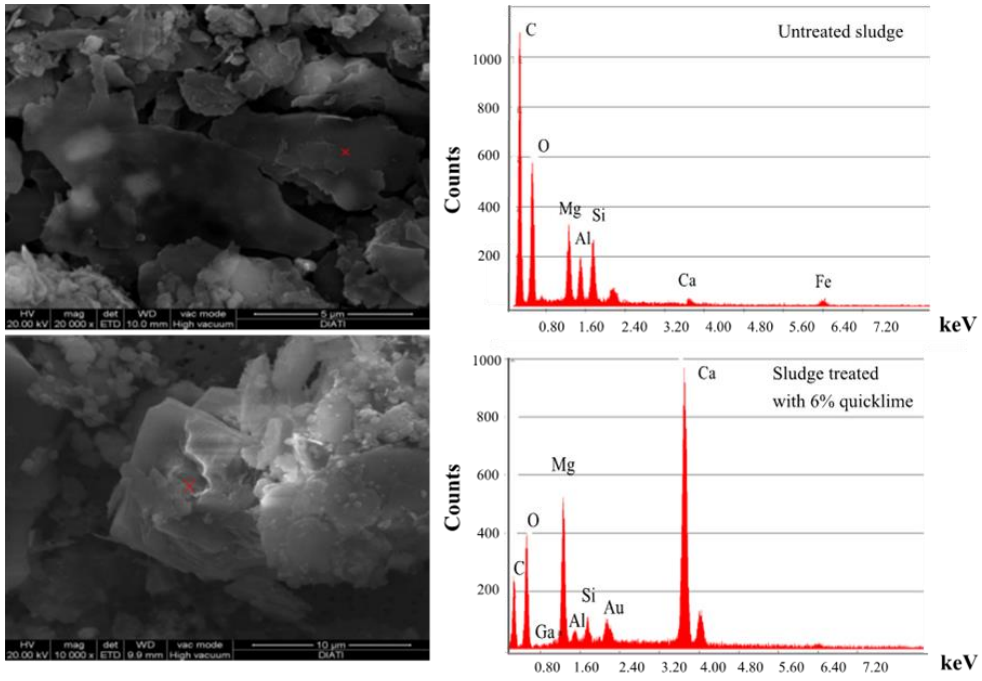

Figure 4.4 SEM images and EDX spectra obtained on mineral sludge (untreated and treated with 6% quicklime)

4.2.2 Mixture recipes

Recipes adopted for the production of the SC-CBMs laid in the field trials were defined by following a procedure previously developed in Chapter 2 [188]. Such a procedure entails the definition of a target size distribution of the particles constituting the aggregate skeleton (aggregate fractions, RAP and sludge) and the selection of appropriate dosages of Portland cement, water and function-specific additives (e.g. superplasticizers and hardening accelerators).

The reference size distribution used in the mix design procedure is described by the so-called "modified Andersen and Andreasen equation" proposed by Funk and Dinger [139] for flowable composites and widely adopted for the mix design of SCCs research [58]. Such an equation is provided in the following: This is same as the procedure adopted in sections 2.4.2 and 3.2.3 in the previous chapters.

$$P(D) = 100 \cdot \frac{({D_{max}}^{q} - D^{q})}{(D_{max}^{q} - D_{min}^{q})} \qquad 4.1$$

where D is the diameter of aggregate particles (in mm), P(D) (expressed in %) is the cumulative percentage passing the sieve with opening equal to D, D_{max} is the maximum diameter of aggregate particles in the mixture (in mm, corresponding to P(D) equal to 100% and equal to 16 for all mixtures), D_{min} is the

minimum diameter of aggregate particles in the mixture (in mm, assumed to be equal to 5 μm for all mixtures), q is the so-called distribution modulus (set equal to 0.21 and 0.23 in the first field trial and thereafter fixed at 0.21 for all the other trials).

The above described reference particle size distribution is shown in Figure 4.5, where it is compared to the classical maximum density curve defined by the well-known Fuller model [173], expressed by the following equation:

$$P(D) = 100 \cdot \left(\frac{D}{D_{max}}\right)^{0.5} \quad 4.2$$

It can be observed that the distribution defined by Equation (4.1) in comparison to the classical Fuller curve is characterized by a significantly higher content of fines. As proven by past research [59, 189], this is considered necessary for the achievement of the desired flowability of cementitious composites while still guaranteeing an adequate stability of their paste (i.e. limited risks of segregation and bleeding) even in the presence of high water contents.

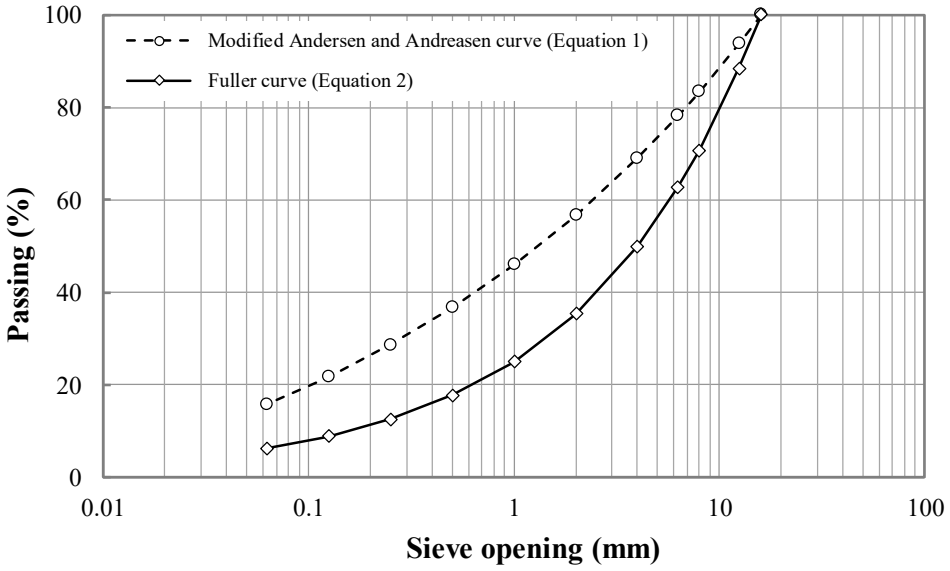

Figure 4.5 Reference particle size distribution and Fuller model.

Percentages of the components constituting the aggregate skeleton of the SC-CBMs were defined by minimizing deviations between their composite particle size distribution and the reference one indicated in Equation (4.1) and by fixing RAP content at 20% by weight of the sum of all the mineral fractions (aggregates, RAP and sludge). Calculated percentages were only marginally affected by variations of the distribution modulus q and were adjusted during the investigation to take into account changes in the composition of employed fractions (see Figure

4.1). Obtained results are listed in the upper part of Table 4.2. It can be observed that 42-44% by weight of the aggregate skeleton of the considered SC-CBMs was composed of recycled components (RAP and sludge). Thus, it can be hypothesized that in comparison to mixtures containing only virgin aggregates, the wide-scale production of SC-CBMs may occur with a reduction of costs and environmental impact.

Since it was expected that cement dosage could have a relevant impact on the properties of the mixtures, during the investigation it was varied in a wide range (comprised between 60 kg/m^3 and 200 kg/m^3). In the SC-CBMs which required the use of the hardening accelerator, the dosage of such an additive was set equal to 1.5% by weight of cement as per suggestion of the manufacturer.

Water-to-cement ratio of the mixtures was defined by referring to a surrogate parameter, the water-to-powder ratio (w/p), which is more frequently used in the design of SCC mixtures which contain a relevant quantity of very fine particles [57]. In the case of the SC-CBMs, "powder" is the term which is used to collectively indicate Portland cement and mineral sludge, which jointly contribute to paste fluidity and void filling effects. As proven by the mix design studies previously carried out in chapter 2, in order to achieve satisfactory flowability characteristics while guaranteeing an adequate stability, it is recommended to use w/p values of the order of 0.75-0.80. This optimal range was identified by referring to powder pastes containing the same polycarboxylate superplasticizer employed in the previous chapters and also described in this chapter (with a dosage of 0.5% by weight of cement). For the SC-CBMs produced and laid in the field trials, the value of w/p was fixed at 0.80 except for the case of the mixtures with 200 kg/m^3 cement, for which it was reduced to 0.75. The dosage of superplasticizer was in most cases fixed at 0.5% by weight of cement although it was increased to 0.75% for the mixtures laid in field trials 3, characterized by cement dosages of 150 kg/m^3 ad 200 kg/m^3.

A summary of the design and composition parameters of all the SC-CBMs considered in the investigation is provided in Table 4.2, while Table 4.3 contains the detailed list of all the 14 mixtures which were produced and laid, together with their identification codes which were used in this chapter. The code is of the alphanumeric type and in sequence contains the values of distribution modulus (e.g. "0.21"), cement content (e.g. "60"), water-to-powder ratio (e.g. "0.80") and two additional codes which indicate the presence or absence of the hardening accelerator (NA when not used, YA when used) and the type of sludge employed during mixture production (NP for sludge in its natural state with no pretreatment, YP for sludge preliminarily treated with 6% quicklime).

Table 4.2 Design and composition parameters of SC-CBMs laid in field trials.

	Trial 1		Trial 2	Trial 3	Trial 4
Distribution modulus, q	0.21	0.23	0.21	0.21	0.21
Coarse sand 0-8 (%)	39	40	36	36	36
Gravel 8-18 (%9	17	18	20	20	20
RAP (%)	20	20	20	20	20
Sludge (%)	24	22	24	24	24
Cement (kg/m^3)	60-100	60-100	100-150-200	150-200	60-100
Water-to-powder ratio, w/p	0.80	0.80	0.80 - 0.75	0.80 - 0.75	0.80
Accelerator (% by weight of cement)	-	-	1.5	1.5	1.5
Superplasticizer (% by weight of cement)	0.5	0.5	0.5	0.75	0.5

Table 4.3 SC-CBMs laid in field trials.

Trial	q	Cement content (kg/m3)	w/p	Accelerator	Pre-treatment of sludge	Identification code
1	0.21	60	0.8	No	No	0.21-60-0.80-NA-NP
	0.23	60	0.8	No	No	0.23-60-0.80-NA-NP
	0.21	100	0.8	No	No	0.21-100-0.80-NA-NP
	0.23	100	0.8	No	No	0.23-100-0.80-NA-NP
2	0.21	100	0.8	Yes	No	0.21-100-0.80-YA-NP
	0.21	150	0.8	Yes	No	0.21-150-0.80-YA-NP
	0.21	150	0.8	No	No	0.21-150-0.80-NA-NP
	0.21	200	0.75	No	No	0.21-200-0.80-NA-NP
3	0.21	150	0.8	No	Yes	0.21-150-0.80-NA-YP
	0.21	150	0.8	Yes	Yes	0.21-150-0.80-YA-YP
	0.21	200	0.75	No	Yes	0.21-200-0.75-NA-YP
	0.21	200	0.75	Yes	Yes	0.21-200-0.75-YA-YP
4	0.21	100	0.8	Yes	Yes	0.21-100-0.80-YA-YP
	0.21	60	0.8	Yes	Yes	0.21-60-0.80-YA-YP

4.2.3 Field trials

Field trials entailed the plant-production of several SC-CBMs and the consequent construction of rectangular slabs. Mixing of aggregate fractions, cement, water and additives (if any) was carried out in a cement concrete batching plant, while the addition of RAP and mineral sludge was directly made into the transit mixer which was used to transport the material to the laying site. Transfer of the mixtures into the timber formwork was thereafter performed by means of either a concrete pump (for the first 3 field trials) or a chute (in field trial 4). No compaction or vibration was carried out on after filling the formwork.

In the first three field trials the slabs had a thickness of 60 cm and plan dimensions of either 3 m × 3 m (in the case of trial 1) or 4 m × 3 m (in trials 2 and 3, in which the width was increased to avoid edge effects when subjecting the slab to the transit of a heavy vehicle). The slab constructed as part of trial 4 was larger in size, with a height of 1.2 m and plan dimensions equal to 4 m × 14 m. It was constituted in its lower part (1 m thickness) of a SC-CBM containing 100 kg/m^3 of cement, while its upper part was made of a mixture with a cement dosage of 60 kg/m^3. The bottom layer was left to cure for a period of 7 days, after which it was overlaid with the second mixture. With respect to the bottom layer, this particular geometry was defined in order to better replicate the thickness of the foundation filling expected in actual road tunnels. The second layer was added on top of it with a reduced thickness (20 cm) in order to gather data on an additional SC-CBM.

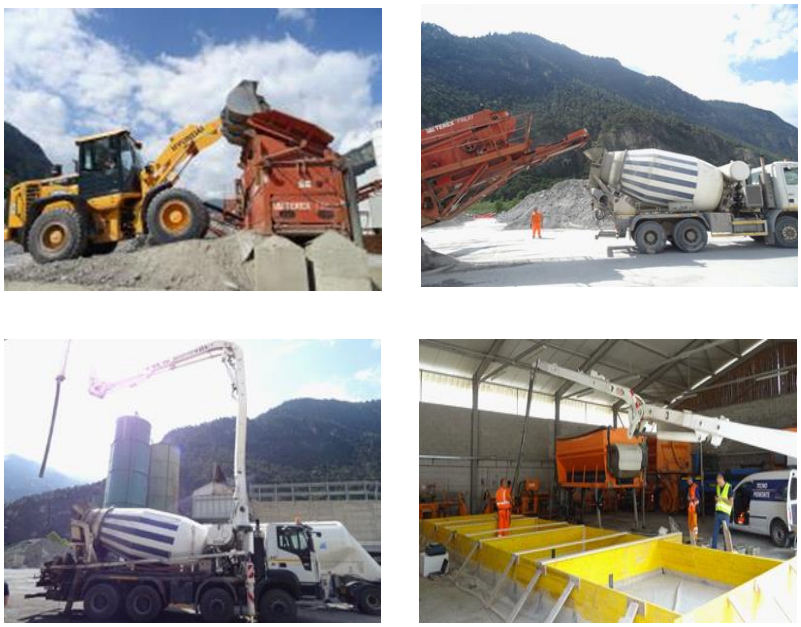

Figure 4.6 Preparation for the site trials

Trials 1, 2 and 4 were carried out in the premises of the production plant, while trial 3 was performed inside a road tunnel in order to assess the effect of the curing conditions expected during pavement construction on the in-place characteristics of the mixtures. It should be mentioned that in the case of road tunnels of significant length, curing conditions may be characterized by a very high temperature which can enhance the hardening of cement-bound foundation materials. Field trial 3 included the placement within the timber formwork of a set of conduits which were buried underneath the laid mixtures and were subsequently inspected after allowing vehicles to transit on top of the slabs. In all cases side shuttering of the slabs were removed after one day of curing and before starting field tests. Photographs taken during the preparation of site trials and construction of the slabs in the four field trials are shown in Figure 4.6 and Figure 4.7.

Figure 4.7 Construction of slabs in field trials.

4.2.4 Mixture properties

Field and laboratory tests carried out on the SC-CBMs employed in the various field trials focused on properties which were considered relevant for the evaluation of their suitability in road tunnel pavement foundations. Field tests assessed the flowability and void content of the mixtures in their fresh state and the bearing capacity of constructed slabs (Figure 4.8). Laboratory tests, which were carried out on specimens casted on site, provided information on the mechanical properties of the mixtures in the hardened state as a function of curing time.

Flowability was considered as a key property to be checked since it is vital for the creation of a homogeneous pavement foundation in tunnels even in the presence of buried conduits. Furthermore, it is essential in order to allow a mixture to be easily pumped for long distances during construction operations with no occurrence of bleeding or segregation phenomena. Determination of void content was also considered relevant in the context of this investigation since such a parameter provides a measure of the actual packing reached by the cement-bound composite, in which settlements in time should be prevented in order to guarantee a stable behavior as a pavement foundation.

Flowability was determined as per the ASTM standard [123], which requires the measurement of the spread diameter (D_s) obtained by allowing a sample to flow under its own weight after being released from a standard cylinder (75 mm in diameter and 150 mm in height). At the time of diameter measurement, visual observations are also carried out in order to detect the occurrence of any bleeding or segregation phenomena. Air content (A_s) was assessed as per [190] (pressure method), which requires samples to be subjected to the action of air pressure in a sealed vessel.

Figure 4.8 Production of SC-CBM at the batching plant (left) air content measurement (right)

Bearing capacity of the constructed slabs was assessed by performing static plate loading tests on their surface after 1, 3, 7 and 28 days of curing, as per

German standard [191]. The test procedure involves the application of vertical loads to a circular plate with 300 mm diameter following a predefined sequence which includes two loading phases with an intermediate unloading. Based on the recorded values of applied vertical stress and measured vertical settlements, the so-called strain modulus E_v (indicated as E_{v1} or E_{v2} when associated to the first or second loading cycle, respectively) is calculated by means of the following expression:

$$E_v = 1.5 \cdot r \cdot \frac{1}{a_1 + a_2 \cdot \sigma_{0max}} \quad 4.3$$

where r is the radius of the loading plate (in mm), σ_{0max} is the maximum applied stress (in MPa, usually equal to 0.50 MPa but reduced to lower values when vertical settlement reaches the maximum allowable limit of 5 mm), a_1 and a_2 are fitting constants which derive from the modelling of the stress-settlement data according to the following equation:

$$s = a_0 + a_1 \cdot \sigma_0 + a_2 \cdot {\sigma_0}^2 \quad 4.4$$

where s is the measured vertical settlement (in mm), σ_0 is the applied stress (in MPa), a_0, a_1 and a_2 are fitting constants.

Results obtained from plate loading tests are usually employed as part of quality assurance procedures for the assessment of the bearing capacity and of the state of compaction of earthworks. Typical acceptance criteria which are adopted in practice establish that E_{v2} should be greater than 45 MPa or 120 MPa for tests carried out on the surface of soil embankments (or subgrade) and on the top of the overlying granular capping layer, respectively [134]. Furthermore, it is usually required that the ratio E_{v2}/E_{v1} be less than 2.5 in order to guarantee the achievement of satisfactory compaction levels. As an alternative, minimum threshold limits may also be fixed for E_{v1}, which is often expected to be greater than 20 MPa for soil embankments.

During the investigation carried out on the SC-CBMs laid in the field trials, results obtained from plate loading tests were analyzed by mainly focusing on E_{v1} in the early phases of curing (up to 7 days) and on E_{v2} in fully cured conditions (after 28 days). In fact, E_{v1} was related to the ability of the mixtures to resist to the action of construction traffic, while E_{v2} was considered as an indicator of the bearing capacity guaranteed during the service life of the pavement. Assessment of the E_{v2}/E_{v1} parameter was not considered to be of any interest since the SC-CBMs are self-compacting by definition.

Supplementary information on the potential resistance of newly-laid SC-CBMs to the loading of construction equipment was obtained by means of a further test, which involved subjecting the constructed slabs to the slow passage

of a 40 tons truck in the early phase of hardening (after either 1 or 3 days of curing). Loads were applied by means of a front single axle with single wheels and a rear tandem axle with dual wheels, while tire inflation pressure was fixed at 0.55 MPa. After the transit of the vehicle, the surface of the slabs was inspected for the identification of induced permanent deformations or damage, if any.

Mixtures in the hardened state were subjected to testing in the laboratory for the measurement of compressive strength and resilient modulus at given curing times. Compressive strength of the mixtures was evaluated after 1, 3, 7 and 28 days of curing by making use of standard 150 mm cubes as per [192, 193]. Results obtained in the early stages of curing (up to 7 days) were analysed in combination with the outcomes of the traffic simulation tests described above in order to gain information on the resistance of the SC-CBMs to the action of construction equipment. Results obtained in full curing conditions (after 28 days) were considered with the purpose of evaluating the excavatability of the mixtures.

Resilient modulus (M_r) of the SC-CBMs was determined after 28 days of curing by means of tests carried out in a triaxial cell as per [124] (sub-base protocol). These tests were considered fundamental within the research project since they yield data which can be employed as part of pavement structural analyses. Although they are more commonly employed for the characterization of subgrade soils and granular sub-bases, they have also been used for the evaluation of different types of materials which include cement-stabilized and cold-recycled mixtures [99, 128, 194]. Test specimens were prepared by filling cylindrical moulds 100 mm in diameter and 200 mm in height. As per its definition, resilient modulus was calculated in the various stress conditions imposed during the test (obtained by changing both confining pressure and deviatoric stress) by making use of the following equation:

$$M_r = \frac{\sigma_d}{\varepsilon_r} \tag{4.5}$$

where σ_d is the repeated deviatoric stress applied along the vertical direction and ε_r is the corresponding recoverable portion of vertical axial strain.

4.3 Results and discussion

4.3.1 Field tests on fresh mixtures

Results of flowability and air content tests obtained on SC-CBMs produced and laid in the field trials are shown in Table 4.4, which also contains the values of parameter V_p/V_g, defined as the ratio between the volume of the components constituting the cement-sludge-water paste (V_p) and the volume of the granular fraction constituted by virgin aggregates and RAP (V_g). As indicated in a previous

study [45], such a parameter can be meaningful in the assessment of flow properties of cement-bound mixtures. In those cases in which V_p/V_g is too low, it can be associated to mixtures in which the coarse fraction is not lubricated enough by the paste; on the contrary, when V_p/V_g is too high, it can correspond to mixtures in which phase separation can occur in the form of bleeding or segregation.

It can be observed that all considered SC-CBMs exhibited a very low air content which was contained within a narrow range (1.4-2.5%). Such an outcome is consistent with the composition of the mixtures, which were designed as self-levelling composites with an excellent particle packing and very high percentage of fines. Furthermore, they were all characterized by similar values of the water-to-powder ratio (w/p), equal to 0.75 or 0.80, which dictates the consistency of the cement-sludge-water paste in the fresh state.

The effectiveness of the approach adopted for the formulation of the SC-CBMs was confirmed by the results of the flowability tests, which in all cases yielded values of the spread diameter (D_s) greater than 200 mm. In such a context it should be mentioned that CLSMs for trench filling operations are usually required to exhibit a D_s greater that 170 mm, while it is recommended that it should be less than 250 mm in order to reduce the risk of segregation or bleeding [25]. In the case of the considered SC-CBMs it should be underlined that these undesired phenomena did not occur even in those cases in which D_s was greater than 300 mm (i.e. for 5 mixtures out of 14). This is due to the soundness of the adopted mix design approach, which for all mixtures guaranteed an acceptable balance between the cement-sludge-water paste and the granular skeleton of the mixture.

Table 4.4 Flowability and air content of SC-CBMs laid in field trials.

	Identification code	**D_s (mm)**	**A_s (%)**	**V_p/V_g**
Trial 1	0.21-60-0.80-NA-NP	210	2.0	1.13
	0.23-60-0.80-NA-NP	220	2.1	1.02
	0.21-100-0.80-NA-NP	280	2.0	1.24
	0.23-100-0.80-NA-NP	300	2.0	1.12
Trial 2	0.21-100-0.80-YA-NP	> 350	1.7	1.24
	0.21-150-0.80-YA-NP	340	1.4	1.39
	0.21-150-0.80-NA-NP	310	1.4	1.38
	0.21-200-0.80-NA-NP	300	2.0	1.47
Trial 3	0.21-150-0.80-NA-YP	250	2.5	1.38
	0.21-150-0.80-YA-YP	310	2.5	1.39
	0.21-200-0.75-NA-YP	280	1.5	1.47

	0.21-200-0.75-YA-YP	> 350	1.5	1.48
Trial 4	0.21-100-0.80-YA-YP	290	1.8	1.24
	0.21-60-0.80-YA-YP	220	1.9	1.13

Since the considered mixtures presented an almost constant w/p value, variations of D_s as a function of the changes in mixture composition were assessed by referring to the effects of other controlling factors. It was observed that in general terms D_s tended to increase with the increase of cement content (or, equivalently, of V_p/V_g). However, it was noticed that flowability was also affected by the presence of the accelerating additive, the presence of which caused an increase of D_s for each given cement content, probably as a result of an additional lubricating action. Furthermore, when comparing the flowability of mixtures characterized by the same cement dosage, regardless of the presence or absence of the accelerating agent, it was observed that quicklime pretreatment of the sludge led to a reduction of D_s. This can be explained by referring to the hydration precipitates highlighted by means of the SEM analyses described in section 4.2.1, which may have the effect of increasing the internal friction of the mineral powder contained in the mixtures.

The outcomes illustrated above can be clearly recognized by plotting the data of Table 4.4 as shown in Figure 4.9, where D_s is displayed as a function of cement content. In such a plot available data have been grouped into four different series corresponding to the absence or presence of the hardening accelerator (codes NA or YA) and of the quicklime pretreatment (codes NP or YP). In the case of the mixtures which differed only in terms of their distribution modulus (equal to 0.21 or to 0.23), average values have been considered. For those mixtures which exhibited D_s values greater than 350 mm, such a value was considered in the plots.

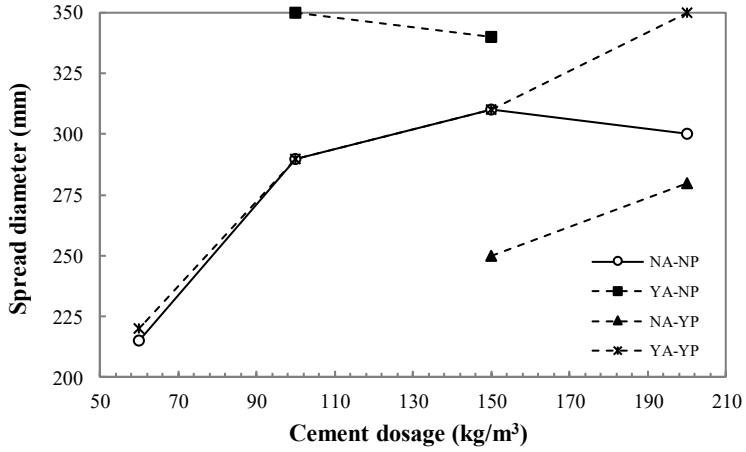

Figure 4.9 Flowability of SC-CBMs laid in field trials.

By analyzing Figure 4.9, it is interesting to note that the combined effects of the use of the accelerator and of quicklime pretreatment evened out, leading to D_s values which up to a cement dosage of 150 kg/m^3 were almost identical to those of the mixtures prepared with no accelerator and with untreated sludge. The consistency of experimental data with the interpretation provided above is remarkable, especially if it is considered that flowability tests are quite empirical and are characterized by an inherent non-negligible variability.

4.3.2 Laboratory tests on hardened mixtures

Compressive strength

Results of compressive strength tests carried out on the SC-CBMs are given in Table 4.5. As expected, in all cases compressive strength progressively increased with curing time. However, since the composition of the considered mixtures varied considerably, obtained values were dispersed in very broad ranges (equal to 0.10-2.51 MPa after 1 day of curing, 0.19-4.60 MPa after 3 days of curing, 0.23-5.65 MPa after 7 days of curing, 0.28-7.38 MPa after 28 days of curing).

Although the SC-CBMs considered in the investigation were different from CLSMs in terms of their composition, they were expected to possess similar properties in terms of strength. Thus, for the critical analysis of obtained results, reference was made to the requirements provided in literature for CLSMs, which are expressed in the form of maximum allowable values of compressive strength after 28 days of curing. According to the guidelines proposed by [48], such a limiting value can be set at 8.3 MPa for all CLSMs, whereas various authors have recommended a maximum limit of 2.1 MPa for those applications in which the CLSMs are required to be easily excavatable [137, 138]. While the first requirement was met by all mixtures laid in the field trials, the second one was satisfied only when the cement dosage was equal to 60 kg/m^3 or 100 kg/m^3. With respect to short-term compressive strength (corresponding to curing times of up to 7 days), minimum required values are not specified for CLSMs since they are usually employed for filling applications with no structural function. Thus, as discussed in detail in section, short-term acceptance thresholds for the self-compacting mixtures subjected to investigation originated from the results obtained from bearing capacity field tests.

Experimental results listed in Table 4.5 are plotted as a function of curing time in Figure 4.10 (lower cement dosages) and Figure 4.11 (higher cement dosages), grouping available data into the same four series defined for the analysis of flowability results (Figure 4.9).

Table 4.5 Compressive strength of SC-CBMs laid in field trials.

	Identification code	Compressive strength (MPa)			
		1 day	3 day	7 day	28 days
Trial 1	0.21-60-0.80-NA-NP	0.12	0.19	0.23	0.28
	0.23-60-0.80-NA-NP	0.11	0.25	0.26	0.28
	0.21-100-0.80-NA-NP	0.23	0.40	0.53	0.67
	0.23-100-0.80-NA-NP	0.10	0.19	0.27	0.34
Trial 2	0.21-100-0.80-YA-NP	0.15	0.23	0.46	0.58
	0.21-150-0.80-YA-NP	0.35	0.98	1.98	2.47
	0.21-150-0.80-NA-NP	0.32	0.99	1.93	2.16
	0.21-200-0.80-NA-NP	0.39	1.80	3.00	3.77
Trial 3	0.21-150-0.80-NA-YP	1.17	2.27	2.52	3.66
	0.21-150-0.80-YA-YP	1.13	2.26	2.71	3.72
	0.21-200-0.75-NA-YP	2.51	4.05	5.41	6.92
	0.21-200-0.75-YA-YP	2.43	4.60	5.65	7.38
Trial 4	0.21-100-0.80-YA-YP	0.31	0.84	1.26	1.67
	0.21-60-0.80-YA-YP	0.43	0.54	0.79	0.90

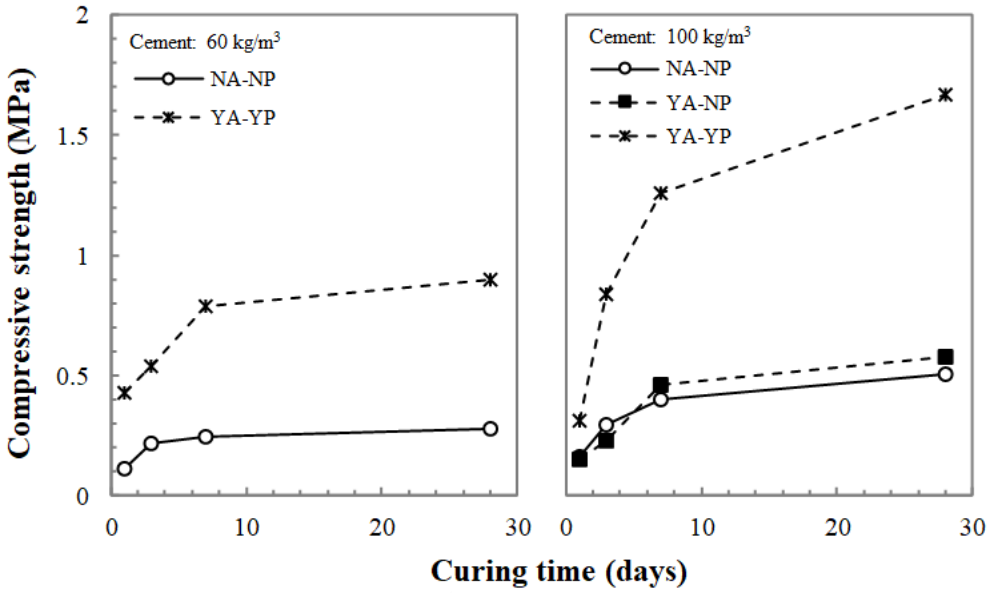

Figure 4.10 Compressive strength of SC-CBMs laid in field trials as a function of curing time (lower cement dosages: 60 kg/m^3 and 100 kg/m^3).

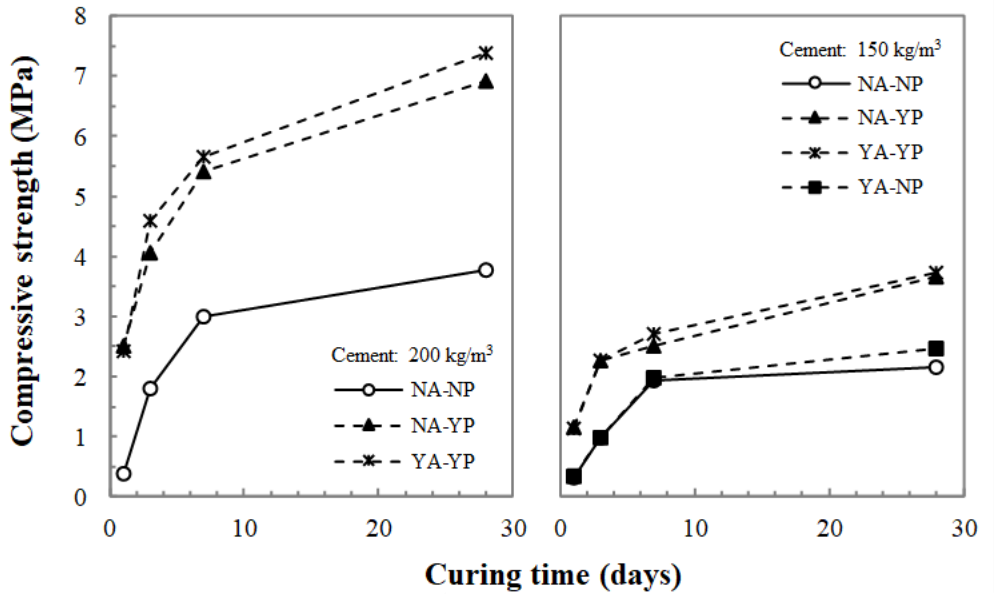

Figure 4.11 Compressive strength of SC-CBMs laid in field trials as a function of curing time (higher cement dosages: 150 kg/m^3 and 200 kg/m^3).

The mixtures which were produced during the first field trial (and 2 further mixtures prepared for field trial 2) contained mineral sludge which had not been subjected to any pretreatment and did not benefit from the use of any hardening accelerator. For these mixtures, indicated with code NA-NP, it was found that after 28 day of curing, achieved strength was extremely low in the case of low cement dosages (60 kg/m^3 and 100 kg/m^3), while it exceeded the 2.1 MPa excavatability limit for higher cement dosages (150 kg/m^3 and 200 kg/m^3). Furthermore, in the short term all these mixtures exhibited a relatively low strength (less than 0.40 MPa after 1 day of curing, less than 2.0 MPa after 3 days) and a very low rate of strength development (from production up to 7 days of curing). In absolute terms these outcomes could not be evaluated with respect to the need of the corresponding foundations to be adequately resistant to construction traffic in the early phases of curing. As previously mentioned, such an analysis required the combined evaluation of the results obtained from full-scale load simulation tests (see section 4.3.3).

In order to modify the strength characteristics of the initially laid mixtures, use was made of the previously mentioned accelerating additive. Experimental data that could be directly compared to those illustrated above were obtained in field trial 2, in which SC-CBMs containing the hardening accelerator were produced with 100 kg/m^3 and 150 kg/m^3. Obtained results (corresponding to the YA-NP series in Figure 4.10 and in Figure 4.11 showed that the employed additive had very limited effects on the strength characteristics of the mixtures. In particular, variations with respect to the initially produced SC-CBMs were

negligible at all curing times. It should be mentioned that unfortunately, as a result of constraints in logistics, the cubical specimens casted on site were stored overnight in the field and were consequently exposed to subzero temperatures before being transported to the laboratory. Thus, it was postulated that such an occurrence may have negatively influenced the effectiveness of the accelerating additive thereby hindering strength development [195].

As illustrated in section 4.2.1, starting from trial 3, the sludge employed for the production of the SC-CBMs was pretreated with quicklime in order to achieve a better control of mixture water content. Experimental results indicated that, as in the case of flowability (see section 4.3.1), compressive strength was significantly affected by sludge pretreatment. This can be appreciated by considering the data of the NA-YP and YA-YP series plotted in Figure 4.10 and Figure 4.11, which indicate that sludge pretreatment led to a significant increase of compressive strength for all cement dosages and at all curing times.

When comparing the NA-YP and YA-YP series, it was confirmed that the hardening accelerator has a limited effect on strength values, with absolute changes that in most cases were smaller than 0.2 MPa. It can be noticed that after 28 days of curing the mixtures containing pretreated sludge achieved strength values which were acceptable from the viewpoint of exacavatability (i.e. smaller than 2.1 MPa) only for low cement dosages (60 kg/m^3 and 100 kg/m^3). Furthermore, these mixtures exhibited short-term strength values (after 1, 3 and 7 days of curing) which were definitely higher than those found for the corresponding mixtures containing untreated sludge.

Resilient modulus

Results obtained from resilient modulus tests carried out after 28 days of curing on the various SC-CBMs are provided in Table 4.6 where they are expressed in terms of the minimum and maximum values achieved in the investigated range of stress conditions. These are indicated in terms of the first stress invariant (θ), also known and bulk stress, which during the tests varied between 0.08 MPa and 0.66 MPa. Experimental results are also displayed in Figure 4.12 (lower cement dosages) and Figure 4.13 (higher cement dosages), where the logarithm of resilient modulus (M_r, expressed in MPa) is plotted as a function of the logarithm of θ (also expressed in MPa). Data have been grouped into the same 4 series utilized for the discussion of flowability and compressive strength results.

Table 4.6 Resilient modulus of SC-CBMs laid in field trials.

	Identification code	Mr (MPa)	
		Minimum	Maximum
Trial 1	0.21-60-0.80-NA-NP	99	302
	0.23-60-0.80-NA-NP	119	303
	0.21-100-0.80-NA-NP	115	584
	0.23-100-0.80-NA-NP	107	454
Trial 2	0.21-100-0.80-YA-NP	250	504
	0.21-150-0.80-YA-NP	304	601
	0.21-150-0.80-NA-NP	310	559
	0.21-200-0.80-NA-NP	403	658
Trial 3	0.21-150-0.80-NA-YP	365	710
	0.21-150-0.80-YA-YP	358	681
	0.21-200-0.75-NA-YP	420	819
	0.21-200-0.75-YA-YP	386	874
Trial 4	0.21-100-0.80-YA-YP	352	778
	0.21-60-0.80-YA-YP	178	474

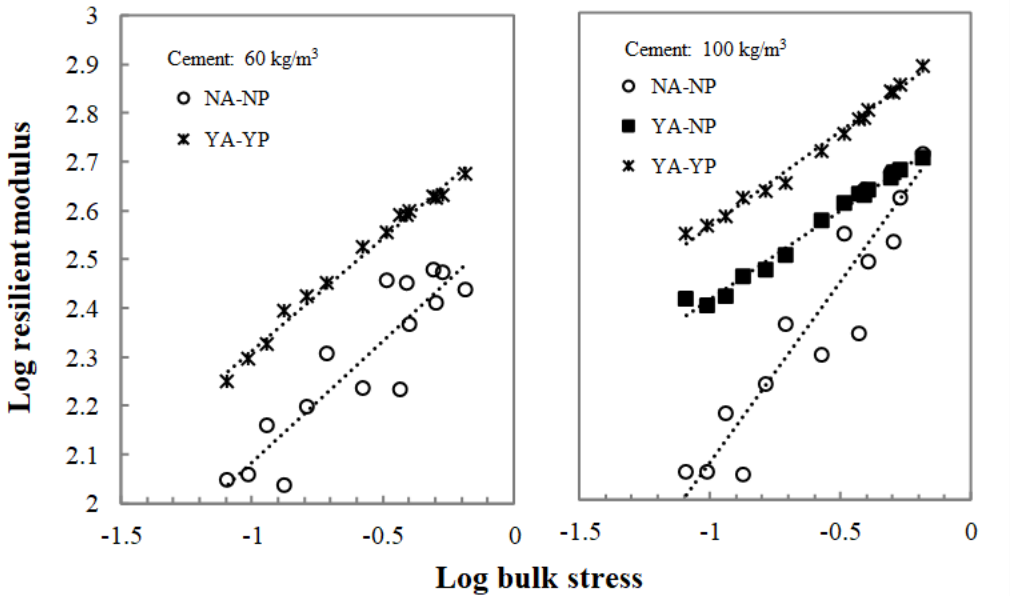

Figure 4.12 Resilient modulus of SC-CBMs laid in field trials as a function of stress state (lower cement dosages: 60 kg/m³ and 100 kg/m³).

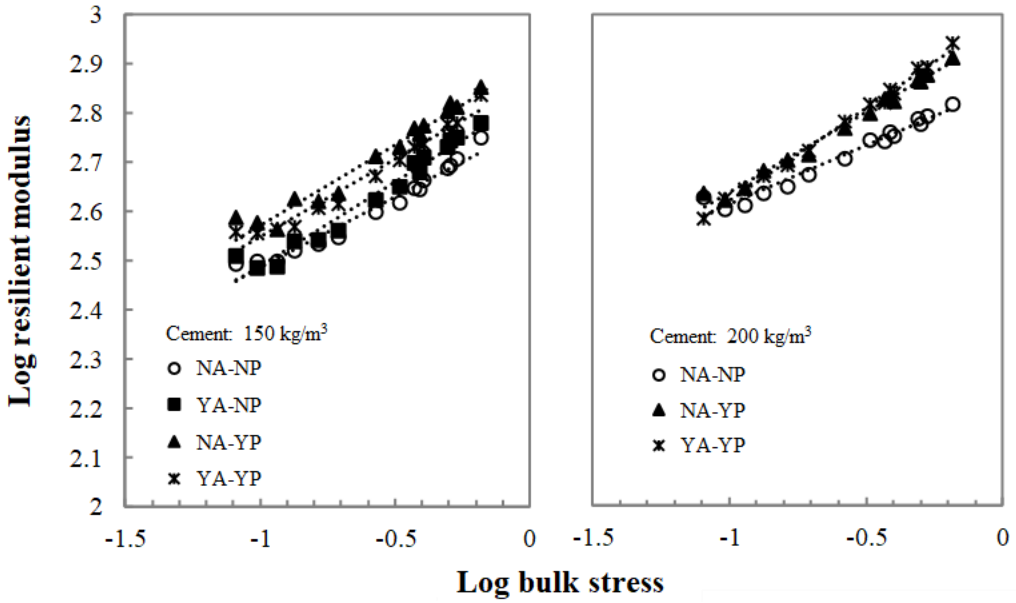

Figure 4.13 Resilient modulus of SC-CBMs laid in field trials as a function of stress state (higher cement dosages: 150 kg/m^3 and 200 kg/m^3)

As expected, resilient modulus was extremely sensitive to variations of cement dosage, with progressively higher values recorded in all stress conditions when passing from 60 kg/m^3 to 200 kg/m^3. By considering increasing cement dosage (60, 100, 150 and 200 kg/m^3), recorded variation ranges were equal to 99-474 MPa, 107-778 MPa, 304-710 MPa and 386-874 MPa. As indicated in Figure 4.12 and Figure 4.13, all mixtures exhibited a non-negligible non-linearity which was observed to be of the stress-hardening type. Such a sensitivity, which can be appreciated by considering the slope of the regression lines fitted to the experimental data points, in general terms was found to decrease with the increase of cement dosage. Such an observation is in line with previous findings [98, 196] and is due to the fact that as the volume of hardened paste increases in a granular composite, its highly linear response has a greater effect on the overall mechanical response, thereby reducing non-linearity.

Acceptance limits for the resilient modulus cannot be defined in absolute terms since stiffness requirements for pavement foundations should be identified as a function of pavement cross section, environmental conditions and design traffic [44]. However, it was encouraging to observe that values recorded during the investigation were comparable to those of high-quality sub-base materials [197, 198, 143]. As in the case of compressive strength, it was found that use of the hardening accelerator and of sludge pretreatment led to an increase of M_r. However, recorded effects were more evident for mixtures prepared with lower cement dosages (60 kg/m^3 and 100 kg/m^3).

In order to capture in more detail the influence on M_r of the various compositional variables, experimental data were fitted to the following model proposed by [103]:

$$M_r = k_1 \cdot p_a \cdot \left(\frac{\sigma_3}{p_a}\right)^{k_2} \cdot \left(\frac{\sigma_d}{p_a}\right)^{k_3} \quad 4.6$$

where p_a is atmospheric pressure (equal to 0.10133 MPa), σ_3 is confining stress (in MPa), σ_d is deviatoric stress (in MPa), k_1, k_2 and k_3 are material-dependent constants.

Results obtained from model fitting are shown in Table 4.7, which contains the values of the material-dependent constants and associated coefficients of determination (R^2). By analysing the data provided in Table 4.7, it was confirmed that the model given in Equation (4.6) is suitable for the description of the resilient response of cement-bound mixtures, with R^2 values which in most cases were greater than 0.97. Few exceptions were found when considering mixtures containing untreated sludge (with cement dosages equal to 60 kg/m^3 and 150 kg/m^3).

Table 4.7 Fitting parameters derived from resilient modulus modelling of SC-CBMs laid in field trials.

	Identification code	k1	k2	k3	R^2
Trial 1	0.21-60-0.80-NA-NP	2262	0.13	0.38	0.830
	0.23-60-0.80-NA-NP	2374	0.17	0.30	0.899
	0.21-100-0.80-NA-NP	3308	0.22	0.64	0.968
	0.23-100-0.80-NA-NP	3019	0.25	0.47	0.965
Trial 2	0.21-100-0.80-YA-NP	4298	0.27	0.08	0.992
	0.21-150-0.80-YA-NP	5021	0.29	0.06	0.983
	0.21-150-0.80-NA-NP	4570	0.22	0.08	0.972
	0.21-200-0.80-NA-NP	5702	0.17	0.08	0.976
Trial 3	0.21-150-0.80-NA-YP	5943	0.27	0.06	0.983
	0.21-150-0.80-YA-YP	5458	0.22	0.11	0.975
	0.21-200-0.75-NA-YP	6809	0.23	0.09	0.989
	0.21-200-0.75-YA-YP	6981	0.24	0.14	0.998
Trial 4	0.21-100-0.80-YA-YP	6289	0.29	0.11	0.994
	0.21-60-0.80-YA-YP	3889	0.31	0.12	0.989

The limiting values of the resilient modulus, expressed by parameter k_1, varied as previously indicated, increasing with cement dosage and revealing the stiffening influence of the hardening accelerator and of sludge pretreatment. Due to the presence of the hardened cement paste, most of the mixtures exhibited a

response under loading which was only marginally affected by shear stresses, thereby showing a low susceptibility to variations of the deviatoric stress σ_d. This led to low values of parameter k_3, which for the majority of the tested SC-CBMs varied in a very narrow range (comprised between 0.06 and 014). The only exceptions came from two of the mixtures produced with untreated sludge and with the lowest cement dosages, equal to 60 kg/m^3 and 100 kg/m^3, which yielded k_3 values respectively equal to 0.34 and 0.55. Such an outcome is consistent with expectations since these mixtures were those with the lowest overall stiffness and were possibly characterized by a less efficient bonding of the cement paste. When considering all the SC-CBMs subjected to testing, greater variations were observed for parameter k_2, which varied between 0.15 and 0.31. This indicates that the mixtures were more sensitive to variations of confining pressure σ_3 which, as extensively shown in literature, can cause non-negligible volumetric effects [37]. No specific relationships could be identified between mixture composition and parameter k_2.

4.3.3 Field tests on constructed slabs

Results of plate loading tests performed on the slabs constructed during field trials are given in Table 4.8, where they are expressed in terms of the strain moduli E_{v1} and E_{v2} measured at the first and second loading cycle, respectively. For the SC-CBMs laid in field trials 1 and 2, tests after 1 day of curing were not carried out. In the first case this was due to the fact that the slabs did not seem to be hardened enough and that on their surface there was still an excess of water. In the second case, there were concerns on the effectiveness of curing since the slabs were exposed overnight to subzero temperatures. Slabs constructed as part of trial 3 were subjected to testing only after 1 day of curing since there were constraints in terms of logistics to carry out further tests in the tunnel. Plate loading tests on the SC-CBMs laid in field trial 4 were discontinued after 7 days of curing due to the fact that they were thereafter overlaid with asphalt layers for the construction of a full pavement cross section [44]. Early curing traffic simulation tests carried out with a heavy vehicle as described in section 4.3.2, on the same day of the earliest plate loading test (see Table 4.8), with the only exception of the mixtures laid in field trial 4, which were not subjected to such tests because of safety concerns related to the high elevation of the slab surface. In all cases obtained results were positive, the fully loaded truck being capable of slowly moving on top of the slabs with no true damage to the laid SC-CBMs. In the case of the mixtures characterized by lower cement dosages (60 kg/m^3 and 100 kg/m^3), the truck created visible surface imprints which had a depth approximately corresponding to tire tread; for the mixtures with a higher cement dosage (150 kg/m^3 and 200 kg/m^3), the surface remained perfectly smooth even after loading. Some photos taken during the field tests are shown in Figure 4.14.

Figure 4.14 Photos of field tests on slabs (Field trial 1).

When considering the results obtained from the first loading cycle applied during plate loading tests, several observations were made. As discussed in the following, they are related to the shape of the stress-settlement curves and to the nature of recorded displacements. In the case of the 4 mixtures laid in field trial 1, which were characterized by relatively low values of compressive strength and resilient modulus, significant settlements occurred after 3 and 7 days of curing under the first loading increment (up to 0.01 MPa). As shown in Figure 4.15, such an anomaly ceased to occur when reaching 28 days of curing. These outcomes can be explained by hypothesizing that in the very early phase of curing these mixtures exhibited an initial settlement due to the excess of water at the slab surface. Additional effects may be due to the slow hardening of the slabs, which is consistent with the very low rate of strength development highlighted when discussing compressive strength results.

Table 4.8 Strain moduli of SC-CBMs laid in field trials.

	Identification code	E_{v1} (MPa)				E_{v2} (MPa)			
		1 day	3 days	7 days	28 days	1 day	3 days	7 days	28 days
Trial 1	0.21-60-0.80-NA-NP	-	15.2	27.5	30.8	-	74.5	237.4	258.1
	0.23-60-0.80-NA-NP	-	11.0	16.5	28.8	-	330.4	168.7	414.3
	0.21-100-0.80-NA-NP	-	20.3	44.9	47.5	-	251.9	384.8	216.9
	0.23-100-0.80-NA-NP	-	17.6	55.2	57.7	-	395.2	329.2	413.7
Trial 2	0.21-100-0.80-YA-NP	-	18.1	38.1	82.1		145.2	409.2	343.6
	0.21-150-0.80-YA-NP	-	152.8	179.4	468.9	-	428.3	650.7	713.0
	0.21-150-0.80-NA-NP	-	161.2	372.5	715.9	-	444.2	517.2	1260.6
	0.21-200-0.80-NA-NP	-	238.8	392.6	809.2	-	486.1	805.7	3042.9
Trial 3	0.21-150-0.80-NA-YP	176.0	-	-	-	411.6	-	-	-
	0.21-150-0.80-YA-YP	255.9	-	-	-	887.1	-	-	-
	0.21-200-0.75-NA-YP	327.2	-	-	-	1102.1	-	-	-
	0.21-200-0.75-YA-YP	578.7	-	-	-	733. 7	-	-	-
Trial 4	0.21-100-0.80-YA-YP	22.5	167.2	92.1	-	59.3	585.9	399.0	-
	0.21-60-0.80-YA-YP	15.6	33.4	50.3	-	142.1	255.8	320.8	-

In general terms it was noticed that the stress-settlement curves obtained from experimental measurements were of three possible types. In the case of the SC-CBMs laid in field trial 1, characterized by a low cement dosage (60 kg/m^3 and 100 kg/m^3) with no hardening accelerator and containing untreated sludge, the stress-settlement relationships were found to be non-linear with a clear stress-softening character. For the mixtures with higher cement contents (150 kg/m^3 and 200 kg/m^3) produced for field trial 2, with and without hardening accelerator, recorded curves were clearly linear in the early stage of curing (i.e. up to 7 days), while at longer curing time (after 28 days) there were characterized by a non-negligible stress-stiffening. Results of plate loading tests carried out on the slabs of field trial 3, which were prepared with SC-CBMs characterized by high cement

dosages (150 kg/m^3 and 200 kg/m^3), yielded stress-settlement curves of the stress-stiffening type even after 1 day of curing. However, it should be considered that the mixtures contained sludge pretreated with quicklime and that the slabs were cured inside a tunnel at a relatively high temperature (of the order of 25°C). It is very interesting to note that the mixture with a cement dosage of 100 kg/m^3 laid in field trial 4 exhibited the three types of responses as a function of curing time, changing from stress-softening (after 1 day of curing) to linear (after 3 days of curing) and then to stress-stiffening (after 7 days of curing). In such a context it should be underlined that hardening progression benefited from the presence of both the accelerating additive and of the quicklime pretreatment. Figure 4.16 shows examples of the three types of stress-settlement curves recorded during the investigation.

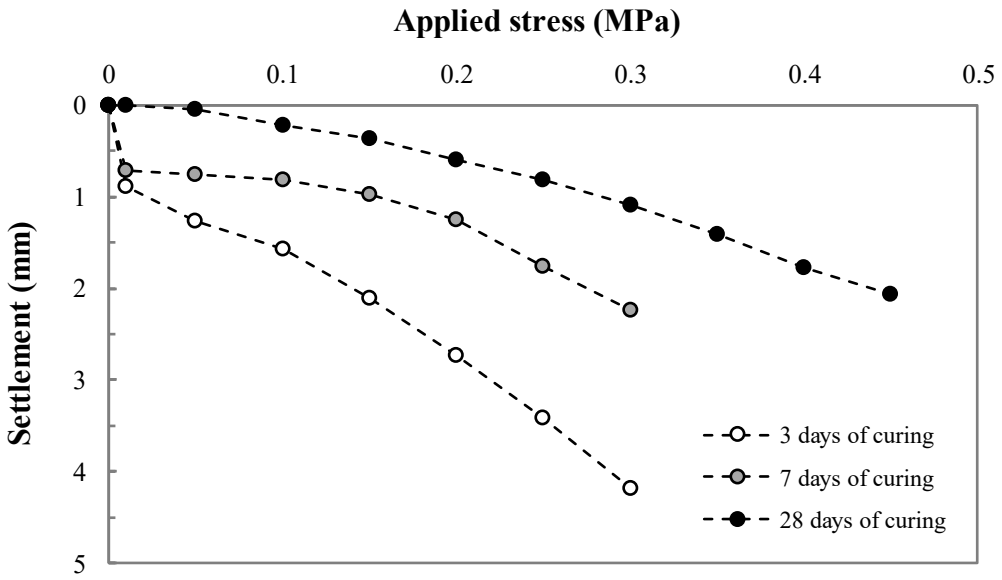

Figure 4.15 Typical stress-settlement curves obtained from plate loading tests carried out on SC-CBMs with a low cement dosage (100 kg/m^3).

For a more detailed discussion of experimental results, analysis of the stress-settlement curves obtained from the first loading cycle in plate loading tests was supplemented by the evaluation of the nature of recorded displacements, which can combine reversible and permanent components [199]. Such an assessment was carried out by considering the response obtained during unloading and in particular by comparing the residual settlement after complete stress removal ($s_{0,u}$) to the maximum value recorded under the maximum applied stress ($s_{max,1}$). In quantitative terms, this was done by calculating the percentage of permanent settlement (s_p), defined as indicated in the following expression:

$$s_p = \frac{s_{0,u}}{s_{max,1}} \cdot 100 \qquad 4.7$$

Values of the s_p parameter are listed in Table 4.9 for all slabs subjected to testing. The data clearly indicate that permanent deformations occurring under the first loading cycle of plate loading tests was significant at all curing times for the mixtures considered in the investigation. In general terms it was observed that these non-reversible settlement components decreased in time with the progress of hardening and were affected by cement dosage, use of the hardening accelerator and sludge pretreatment. These factors had the same type of effects which were observed for compressive strength and resilient modulus test results (see section 4.3.2).

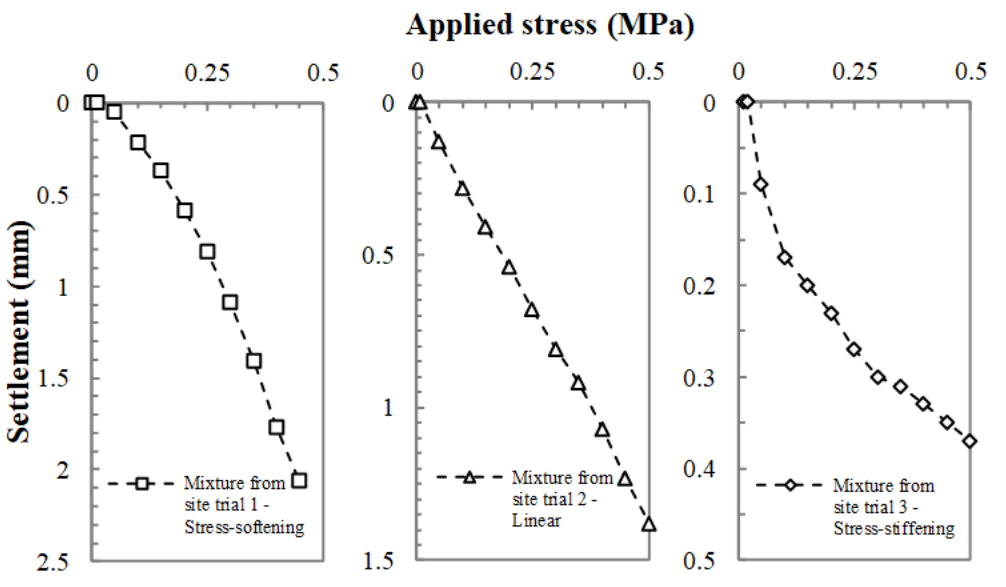

Figure 4.16 Different types of stress-settlement curves obtained from plate loading tests carried out on SC-CBMs laid in field trials.

It should be underlined that permanent settlements occurring in the foundation as a result of the first loading cycle imposed during plate loading tests are not representative of those which are expected in service under the action of regular traffic. This is due to the fact that in all cases the foundation is bound to be subjected to loading of construction equipment during the laying and compaction of the upper layers of the pavement. Thus, most of the permanent settlements are expected to take place in such phases. Furthermore, it should also be considered that in service the pressure applied to the top of the foundation is significantly reduced by the load distribution effect due to the upper pavement layers, with a consequent further reduction of potential permanent settlements.

As mentioned in the previous sections, measurement of strain modulus E_{v1} was considered of interest for the assessment of the possibility of subjecting the SC-CBMs to the action of construction traffic in the early phases of curing with no damage. In such a context, the identification of a minimum threshold value to be adopted as an acceptance criterion stemmed from the combined analysis of recorded E_{v1} values and of the outcomes of the simulation tests carried out by means of the fully loaded truck. Thus, by considering obtained results, it can be stated that trafficability conditions were reached by the constructed slabs when achieving a E_{v1} value not smaller than 10 MPa. Such a limit was barely met by the slab prepared in field trial 1 with a cement dosage of 60 kg/m^3 and with a distribution modulus of 0.23. Nevertheless, even in this case after the passage of the heavy vehicle no significant damage occurred in the constructed slabs.

Table 4.9 Percentages of permanent settlement after the first loading cycle of plate loading tests carried out on SC-CBMs laid in field trials

	Identification code	s_p (%)			
		1 day	3 days	7 days	28 days
Trial 1	0.21-60-0.80-NA-NP	-	100	94.6	91.4
	0.23-60-0.80-NA-NP	-	99.5	96.1	93.3
	0.21-100-0.80-NA-NP	-	97.6	94.8	86.9
	0.23-100-0.80-NA-NP	-	98.5	91.3	91.1
Trial 2	0.21-100-0.80-YA-NP	-	73.8	100	71.0
	0.21-150-0.80-YA-NP	-	80.3	50.0	45.8
	0.21-150-0.80-NA-NP	-	74.6	33.3	56.3
	0.21-200-0.80-NA-NP	-	75.5	43.3	78.6
Trial 3	0.21-150-0.80-NA-YP	69.7	-	-	-
	0.21-150-0.80-YA-YP	55.6	-	-	-
	0.21-200-0.75-NA-YP	59.5	-	-	-
	0.21-200-0.75-YA-YP	21.1	-	-	-
Trial 4	0.21-100-0.80-YA-YP	82.4	85.1	84.3	-
	0.21-60-0.80-YA-YP	90.7	87.7	87.9	-

It can be noticed that trafficability conditions were reached at curing times which correspond to compressive strength values not smaller than 0.19 MPa (see Table 4.5). For the specific type of SC-CBMs considered in the investigation, such a value can therefore be used as an acceptance limit which when satisfied identifies the curing time needed before allowing construction traffic to move on top of the pavement foundation.

In the context of the investigation, evaluation of strain modulus E_{v2} was carried out with the main purpose of identifying the bearing capacity of the pavement foundation in service [200]. Consequently, analysis of obtained results mainly focused on data obtained in fully cured conditions, which were hypothesized to be reached 28 days after placement. As indicated in Table 4.8, these tests were carried out only on the slabs constructed as part of field trials 1 and 2. Obtained results showed that for lower cement dosages (60 kg/m^3 and 100 kg/m^3) E_{v2} was of the order of 200-400 MPa, whereas it reached significantly higher values, greater than 1,000 MPa, in the case of higher cement dosages (150 kg/m^3 and 200 kg/m^3). It was also observed that the evolution of E_{v2} as a function of curing time was highly dependent upon mixture composition, but no clear trends could be identified. For those mixtures which were subjected to testing at curing times less than 28 days, recorded values were of the same order of magnitude of those of the other mixtures.

The data listed in Table 4.8 indicate that recorded E_{v2} values were significantly higher than the classical threshold limit adopted for embankments covered by a capping layer, equal to 120 MPa. Thus, from a quality assurance viewpoint, all SC-CBMs are fit for purpose in terms of their long-term bearing capacity.

4.3.4 Recommended acceptance criteria

Results collected during the experimental investigation can be used for the identification of performance-related acceptance criteria, outlined in the following, which may be adopted in future construction works in road tunnels.

Flowability**,** which may be considered as a prerequisite for the acceptance of any SC-CBM, should be continuously checked during production and at the laying site. In such a context, it seems appropriate to assume a minimum allowable value of the spread diameter equal to 200 mm.

In order to ensure that the SC-CBMs laid for the formation of the pavement foundation can be subjected to the loading of construction equipment in the early phases of curing with no significant damage, it is recommended to refer to two different acceptance thresholds. When considering the properties of the mixture, either in the design phase or during quality assurance operations, the curing time needed to reach a value of compressive strength equal to 0.19 MPa (determined as per EN 12390-2/3) needs to be evaluated. As discussed before, such a curing time can be considered as the minimum time which is needed before allowing the foundation to be subjected to heavy loads. As a supplement to such an evaluation, plate loading tests can be carried out in the field in accordance to DIN 18134. It is suggested that construction equipment should be allowed to transit on the foundation only after recording a value of the strain modulus E_{v1} greater than 10 MPa. This limiting value may be prudentially increased to 20 MPa, which is

sometimes used for the quality assurance of standard earthworks, in order to account for variability of SC-CBM production. For the SC-CBMs laid in the field trials were characterized by a low cement dosage (60 kg/m^3 and 100 kg/m^3), it was observed that trafficability conditions were always reached after 3 days of curing.

Other acceptance criteria which may be considered in construction works include the verification of the long-term stiffness and bearing capacity of the foundation. These properties may be assessed after the achievement of full curing (i.e. after 28 days) by performing resilient modulus tests (in the laboratory, as per AASHTO T 307-99) and plate loading tests (in the field). Resilient modulus values should be employed as part of pavement design analyses, whereas the strain modulus E_{v2} derived from plate loading tests may be compared to the classical 120 MPa threshold assumed for general road construction activities. Too high values of the resilient and strain moduli may be suspect in terms of the potential brittleness of the materials, with the consequent risk of undesired reflective cracking phenomena in the completed pavement.

It is anticipated that the acceptance criteria illustrated above may need to be adjusted and fine-tuned when considering the results coming from a broader range of SC-CBMs. Nevertheless, they can be regarded as a useful reference for future applications. Field trials of SC-CBMs proved their feasibility for using in real paving applications. It is necessary to evaluate the performance of these materials when used in pavement designs. Pavements with cement-stabilized layers in the foundation layers behaves different than the pavements with unbound granular layers in the foundation. This affect the load transfer mechanism and service life of the pavement. In the next stage, a pavement design exercise was conducted to assess the performance of conventional pavement solutions and innovative section with self-compacting cement-bound mixtures in the pavement foundation. A summary of the recommended acceptance criteria is listed in Table 4.10.

Table 4.10 Acceptance criteria for field application

Properties	**Recommended acceptance criteria**
Required diameter of flow spread	≥ 200 mm
Required time for allowing construction loading	
• Achievement of strain modulus value (E_{v1})	≥ 20 MPa
• Achievement of compressive strength	≥ 0.19 MPa
Required long term stiffness and bearing capacity	
• Resilient modulus	As required by the pavement designers
• Strain modulus value (E_{v2})	≥ 120 MPa

5. Self-compacting cement-bound mixtures in pavement design

While the previous chapters of the thesis discussed the mix design and performance assessment of SC-CBMs, this chapter is dedicated to a case study, dealing with the incorporation of SC-CBMs into pavement design. A full-scale field trial of a pavement section and subsequent evaluation of materials properties was conducted as a part of this study. A pavement design exercise based on the real traffic and environmental data collected from the Frejus road tunnel, which connects Italy and France, was performed with SC-CBMs in the foundation layers.

5.1 Pavement design

The purpose of pavement design is to find a match between the estimated design traffic and a pavement cross section of adequate thickness, which could provide satisfactory performance during the service life. The design of flexible or rigid pavement in a tunnel is not different from that of pavement in an open area [14]. Pavement design methodologies are continuously evolving and Mechanistic-Empirical (ME) pavement design methodologies are widely used across the world for designing flexible pavements. ME approach uses a combination of mechanistic analysis and empirical equations to arrive at the final pavement cross section. The mechanistic analysis involves the calculation of pavement responses in terms of stresses and strain on the different layers of the pavement with the application of wheel loading using a multi-layer elastic approach. This multi-layer elastic approach works with the basic assumptions that each layer is homogenous, isotropic and linearly elastic with a characteristic Young's modulus of elasticity and Poisson's ratio. Moreover, it is assumed that the layers are horizontally infinite, weightless and continuity conditions are met at the interfaces. The thickness of each layer is finite whereas the subgrade is infinite. The load is applied uniformly on the surface over a circular area [132]. Empirical equations are used to convert such pavement responses to relevant pavement damage. Such equations connecting pavement response to damage are often developed based on the large data collected from similar pavements. Several countries proposed their empirical equations which suit to local conditions. AASHTO, SAPEM and Austroads are three such guidelines proposed in the United States of America, South-Africa and Australia, respectively. Different pavement methodologies

differ in terms of the underlying assumptions and transfer functions they use for the calculation of pavement damage.

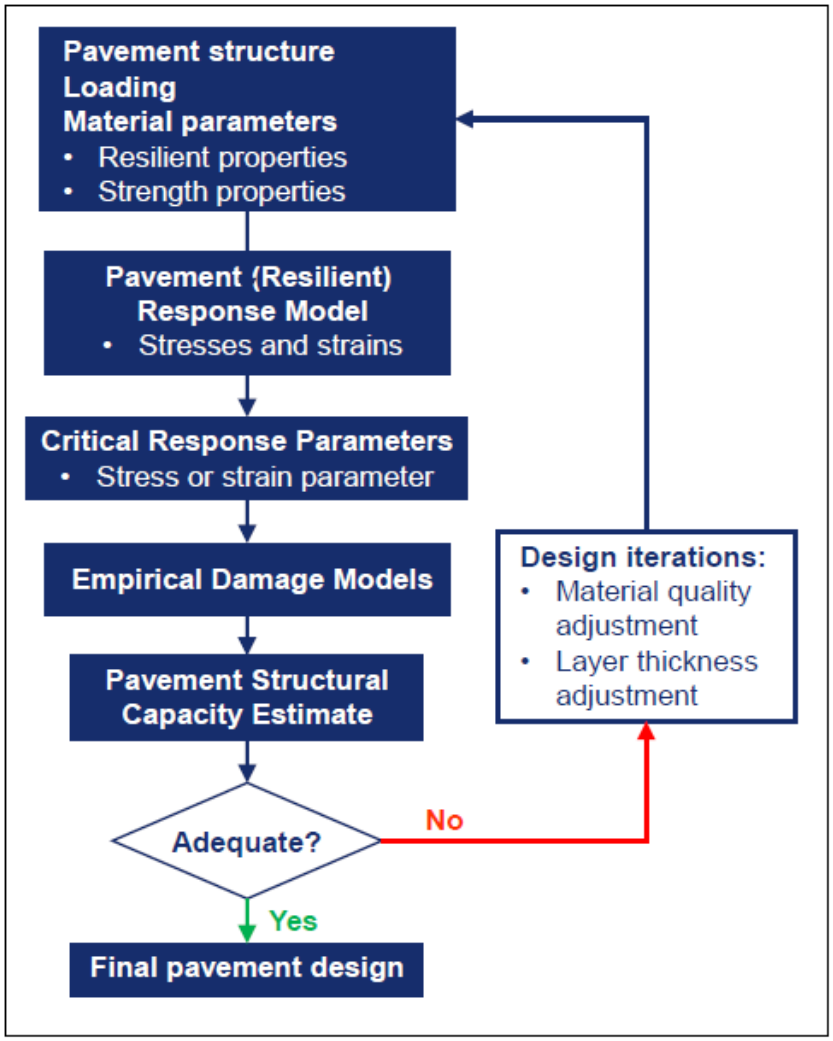

Figure 5.1 Schematic diagram of a mechanistic-empirical procedure [36] [201]

In the mechanistic-empirical approach of pavement design (Figure 5.1), a trial pavement section is checked for the pavement bearing capacity by evaluating the critical response of the layers at several chosen locations (Figure 5.2). These responses are used in the empirical damage models to evaluate the structural capacity. Finally, an iterative approach is adopted to find out the pavement cross section which is adequate for the design traffic. Some countries like Austria have a specific standard which deals with the pavement design in tunnels. The Austrian standard RVS 09.01.23 prescribe the thickness of the asphalt layer in tunnels as shown in Figure 5.3 [202, 203].

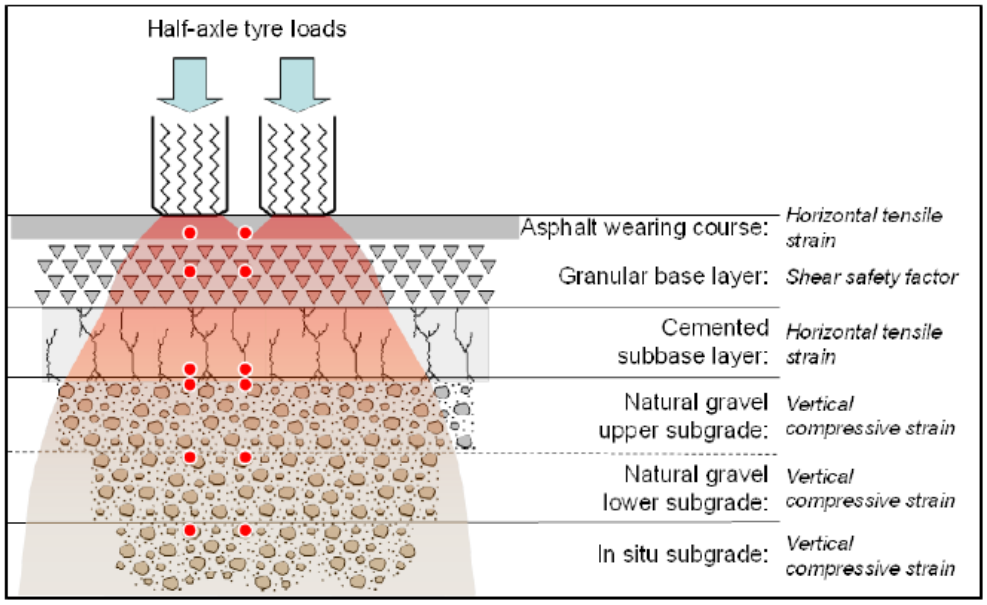

Figure 5.2 Critical locations considered in the South-African design method [36]

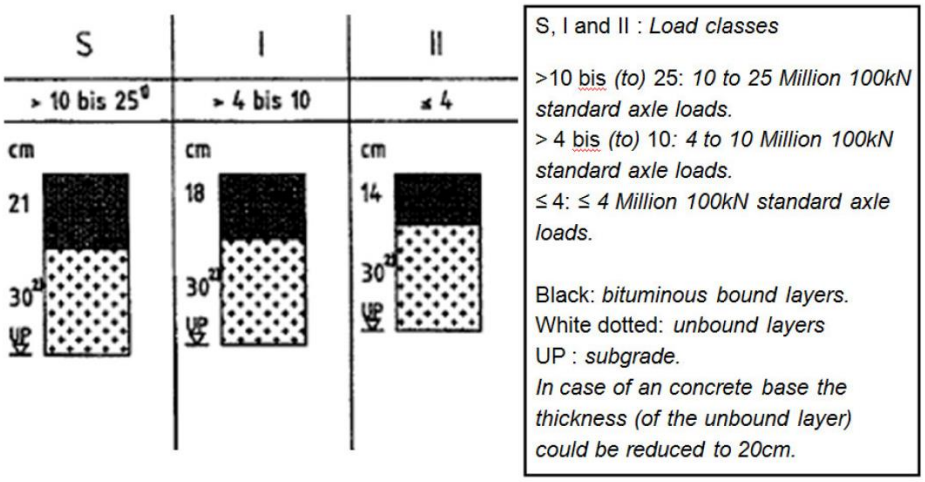

Figure 5.3 Austrian catalogue for flexible pavement design in tunnels [202] [16]

5.2 Design of pavements in road tunnels

Selection of a pavement solution for road tunnels depends upon several factors ranging from estimated traffic, safety, cost, availability of materials, presence of buried utility lines, logistics of construction operations, and expertise of involved contractors. Various pavement types can be selected, including flexible, rigid and semi-rigid, but designers may also need to deviate from

standard solutions, identifying innovative materials and technologies which are compatible with site-specific requirements. Safety of pavements in road tunnels are dependent on different factors like geometry, design, traffic management and the behaviour of road user. Pavements in road tunnels are subjected to a temperature regime which is different from that of open roadways. In particular, temperatures tend to be significantly higher and characterized by a lower daily and seasonal variability, thus leading to lower stiffness values of the bitumen-bound upper layers. Hence, in order to reduce deflections and strains under loading, pavements of the semi-rigid type can be selected, in which asphalt concrete layers are placed over a relatively stiff cement-stabilized foundation [41]. Semi-rigid pavements constitute a significant portion of the European road network [39] and have proven to exhibit satisfactory performance in service [40]. Furthermore, they may easily incorporate recycled materials in the foundation and may lead to a reduction of bitumen consumption as a result of the use of thinner asphalt layers [43].

Semi-rigid pavements with hydraulically bound layers are widely used in Europe for pavements that carry a heavy volume of traffic (Figure 5.4). Sand-cement or soil-cement is used as the hydraulically bound material in several countries [204]. The asphalt layer in a semi-rigid pavement takes care of the functional responsibilities, by providing a smooth riding surface with adequate skid resistance and noise levels. It also provides insulation over the hydraulically bound layer to prevent the moisture ingress and movements associated with weathering impacts such as thermal and freeze movements. The thickness of the layer is chosen depends on various factors and the threat of reflective cracking is one of the most influencing factors. The bound base act as a structural layer of the pavement which would have a role in the load distribution and provides support to the upper layers, thereby minimizing the stresses in the base layer [204].

The fire resistance of materials used for the construction of pavements is one of the main factors which controls the safety of pavements in the case of a fire. Due to tunnel geometry, absence of enough oxygen and poor visibility, the fumes of fire with toxic gases worsen the situation leading to more causalities. The cause of tunnels fires in the past was mostly due to accidents of vehicles inside the tunnel which created fire and then spread to other vehicles and the pavement. The liquid fuels used in the vehicles are the primary responsible factors which need to be managed during any fire accident. From the fire propagation point of view, there is not a unanimous opinion that asphalt contributes to the propagation in some way.

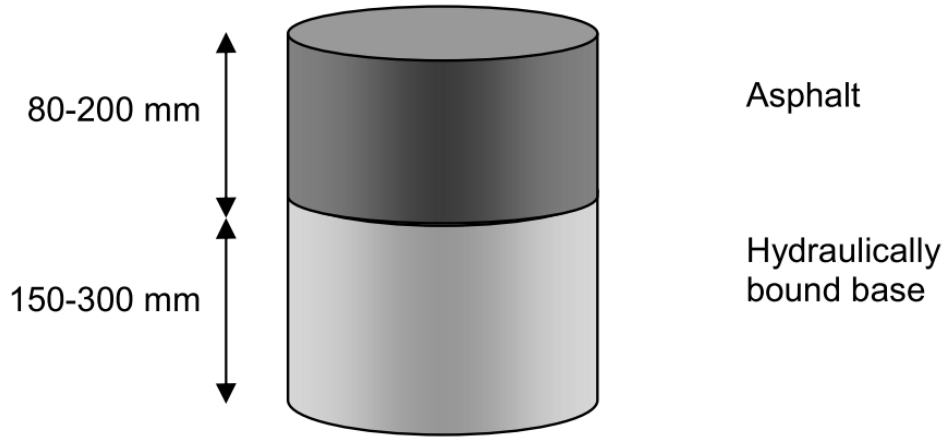

Figure 5.4 Typical cross section of European semi-rigid pavement for heavy traffic [204]

5.2.1 Durability of SC-CBMs

The performance of self-compacting cement-bound mixtures in the pavement foundations of the road tunnels would be influenced by the durability of SC-CBMs. However, pavements in the road tunnels are exposed to a relatively constant climatic and environmental conditions in comparison to the open roadways. Common durability issues in the cement-bound mixtures are their shrinkage and damages related to cyclic freeze-thaw experiences. Hence, SC-CBMs developed in the preceding sections were studied for their response to the shrinkage and freeze-thaw tests. These experiments were conducted in order to have a final check on the durability of SC-CBMs before employing them in the pavement design.

Shrinkage test

There is no specific standard for the shrinkage measurement of SC-CBMs. A prism mould of 25 mm x 25 mm x 285 mm with a dial gauge arrangement for measuring the length change is commonly used for cement paste, mortar and concrete (Figure 5.5). This procedure is adopted from ASTM C 490-17 [205]. The gauge length is identified as 250 mm. periodically change in length was measured with the help of a length comparator. A similar procedure was adopted by different researchers for the shrinkage measurement of CLSMs and alkali-activated materials [206, 207]**.** The selected mixtures that were studied in the Chapter 2 were used in the length change measurements as prescribed in [205].

The results of the length change measurements for all the mixtures are indicated in Table 5.1.

Figure 5.5 Shrinkage measurements

Table 5.1 Length change measurements

Selected mixtures	Δl (%)
q - 0.23-0.8, cement = 60 kg/m^3	0.042
q - 0.21-0.8, cement = 100 kg/m^3	0.040
q - 0.23-0.8, cement = 100 kg/m^3	0.053

The percentage of length change (Δl) was found to be less than 0.06% for all the SC-CBMs when measured at 28 days of age. This also indicated that the durability issues associated with the autogenous shrinkage are not of any concern for SC-CBMs.

Freeze and thaw tests

Freeze and thaw properties of the SC-CBMs were measured according to ASTM D 560-16 [208]. The original standard was proposed for the soil-cement mixtures but there were several instances where this was applied to CLSM mixtures [25, 209]. It was reported that the freeze and thaw test methods used for conventional concrete are too severe for CLSMs [19]. Hence the same standard was followed for evaluation of SC-CBMs.

SC-CBM samples that are cured for 7 days were exposed to a temperature change from −18°C (a freezer) to 23°C (laboratory temperature) in each cycle. Each cycle consists of 24 hours in the freezer and another 24 hours in the laboratory environment. Samples were exposed to 12 cycles unless they suffered

severe damage at an earlier time (Figure 5.6). Mass loss was measured as an indicator of damage. The total mass loss at the end of the cycles is divided by the original mass of the cylinder to find out the mass loss (Δw_{12} (%)).

Figure 5.6 Specimens after 1 cycle (left) and after 12 cycles (right)

Table 5.2 Mass loss after 12 cycles

Selected mixtures	Δw_{12} (%)
q - 0.21-0.8, cement = 60 kg/m^3	4.46
q - 0.21-0.8, cement = 100 kg/m^3	2.00

For soil-cement mixtures, a mass loss of 14% is identified as the maximum allowable limit. For the SC-CBMs the mass loss was less than 5% in both the mixtures. Comparing with the allowable limits prescribed for soil-cement mixtures [209], SC-CBMs are also durable in relation with the freeze and thaw issues.

5.2.2 Case study of pavement design

In the specific case of a newly constructed major motorway tunnel (Figure 5.7) (13 km in length), a standard semi-rigid pavement cross section was chosen in the preliminary design phase, which focused on its load-bearing capacity. Following the development of SC-CBMs as described in Chapters 2-4, A further design exercise was conducted to optimize the pavement section which was deemed necessary in order to fulfill several additional needs. These were related to the potential constraints encountered in the compaction of subgrade and foundation materials, to the presence of underground utilities, including a high-voltage transmission line, and to the desire of reducing the consumption of virgin aggregates. Regarding the utility lines, their placement needs to be considered at the initial design phase itself. Utility cuts would damage the pavements and in an important road tunnel utility cuts would disrupt the traffic flow [210].

To make an efficient use of available space, such utility lines can be housed at the invert space of tunnels which would also acts as the foundation of pavements of the road tunnels. Design and construction of such a multi-purpose foundation which can house all the utility lines in addition to serving as a pavement foundation is an attractive solution to the tunneling industry. Consequently, innovative pavement cross sections were identified, in which the use of self-levelling and self-compacting cement-bound mixtures (SC-CBMs) was considered for the formation of the subgrade and foundation. These mixtures were designed in order to incorporate significant amounts of recycled materials such as Reclaimed Asphalt Pavement (RAP) and mineral sludge retrieved from aggregate washing operations as mentioned in the previous chapters [45, 23, 188].

Figure 5.7 New tunnel under construction at Frejus

In this case, the choice of invert filling and its thickness was affected by the required vertical clearance inside the tunnel. The selected foundation materials has to satisfy both performance requirements of a pavement foundation as well as other expected functional requirements. Space available for the movement of heavy machineries to lay and compact such materials was also limited in tunnels. Poor thermal conductivity of such foundation materials could also lead to the damage of high-voltage cables during their operation. Placement of cables in separate small culverts constructed at the tunnel invert and backfilling remaining area is one common practice which creates additional cost and inconvenience to the construction. Also this creates differential bearing capacity for the foundations. Burial of utility lines after excavating the required area of compacted filling is another approach that is commonly practiced. Both the above methods for the placement of utility lines are not efficient for aforementioned reasons. Moreover, as mentioned before the high voltage cables needs to be surrounded by a high thermally conductive medium in order to ensure their optimum performance. Future excavation of the foundation layers would be also necessary in case of some maintenance needs of the buried utilities.

This chapter summarizes the studies which were carried out as part of pavement optimization using SC-CBMs in the foundation layers. Expected performance of the innovative solutions and of a reference standard cross section were assessed by means of a mechanistic-empirical approach in which predicted traffic and environmental conditions were taken into account. Mechanical properties of materials were mainly derived from the outcomes of field investigations carried out on a full-scale test section and of laboratory tests performed on materials sampled on site.

5.3 Pavement cross sections

The standard semi-rigid pavement cross section considered in the preliminary design phase (indicated as “CS”) included a compacted soil subgrade, a cement-stabilized foundation (thickness 20 cm) and three layers of dense-graded asphalt concrete (total thickness 19 cm).

The innovative pavement solutions included self-levelling and self-compacting cement-bound mixtures (SC-CBMs) for the formation of both the subgrade and foundation (cross section “GG”) or of the subgrade only (cross section “CG”). In the latter case, it was hypothesized that the foundation would be constructed with the same type of standard cement-stabilized mixture (CBM) considered as part of cross section CS. For both pavements, as in the case of cross section CS, the foundation thickness was maintained equal to 20 cm and total thickness of the asphalt layers was fixed at 19 cm since such a value was considered adequate for the prevention of reflective cracking [20]. It was hypothesized that the 19 cm would be constituted by 10 cm base course, 5 cm binder course and 4 cm wearing course.

For all pavement solutions (Figure 5.8) the total thickness of subgrade considered in calculations was equal to 1 m. Such a value results from the geometry of the tunnel invert, which is filled in its lower portion by lean Portland cement concrete that acts as a rigid base. It should be mentioned that after completion of preliminary design, the tunnel administration accepted to allow the installation of a high-voltage transmission line within the pavement subgrade. The corresponding design led to the identification of an appropriate layout of conduits and cables to be buried at a depth below the subgrade surface equal to approximately 80 cm.

Performance evaluation of the considered pavement cross sections was carried out by means of a mechanistic-empirical approach which required the prediction of traffic volumes, environmental conditions and mechanical properties of materials. The motorway tunnel for which the study was carried out is a new infrastructure, recently excavated in parallel to an existing tunnel, open to traffic since 1980. Thus, data available for the existing tunnel were employed for the

identification of traffic and temperature conditions relevant for the design of the new pavement (see sections 5.3.1 and 5.3.2). Mechanical properties of materials constituting the various pavement layers were derived from field and laboratory tests, from available literature, and from technical specifications (see section 5.3.3). Transfer functions employed for the calculation of design lives, briefly discussed in section 5.3.4, were those provided by the SAPEM, South African Pavement Design Manual [84].

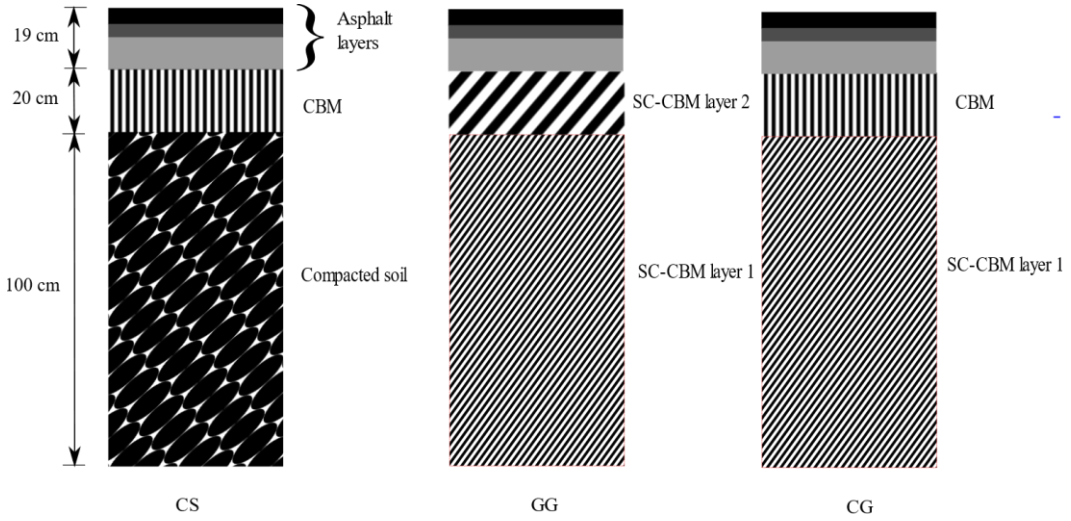

Figure 5.8 Cross sections considered for the analysis

5.3.1 Design traffic

A synthesis of the two-way traffic data collected for the existing tunnel for a period of five years is shown in Table 5.3, in which the number of passes are given for light (motorcycles, cars and vans) and heavy vehicles (buses, trucks and trailers). The percentage of heavy vehicles, of the order of 40%, was approximately constant in time. It was observed that annual traffic growth values were quite variable, ranging between 0.1% and 7.0%. Thus, the average value, equal to 3.0% was assumed for traffic predictions.

In subsequent calculations, light vehicles were neglected, whereas the heavy vehicles were converted into 80 kN equivalent single axle loadings (ESALs) by taking into account the vehicle sub-categories and relative percentages recorded at the tunnel entrance for toll collection. Individual truck factors were derived from the axle loads indicated in the Italian pavement catalogue [211] and by referring to the equivalent axle load factors (EALFs) reported in the 1993 AASHTO Guide for a Structural Number (SN) equal to 5 and a final Present Serviceability Index (PSI) equal to 3.0. The average truck factor obtained by means of such an

approach was found to be equal to 2.0. A lane factor equal to 0.8 was assumed for design purposes.

Table 5.3 Traffic data collected for the existing tunnel

Year	2014	2015	2016	2017	2018
Light vehicles	998,342	1,115,511	1,129,051	1,100,382	1,099,845
Heavy vehicles	701,728	703,653	736,248	766,561	813,233
Total	1,700,070	1,819,164	1,865,299	1,866,943	1,913,078

Monthly traffic distribution was also made available by the tunnel administration and it was found that no significant changes occurred in the considered years (with the only exception of the year 2015, which was treated as an outlier). These data were later used in damage calculations for the considered pavement cross sections (see section 5.4).

It was planned that pavement construction would occur in two stages. In particular, it was envisioned that after laying of the binder course, the tunnel would be accessed for 2 years exclusively for the instalment of all accessory utilities, including ventilation, lighting and safety systems. The pavement would then be completed with the laying of the 4 cm wearing course. Construction traffic anticipated in the 2 years of finishing operations was estimated based on the planned daily activities and was found to correspond to 7,508 passes of three- and four-axle trucks on each lane. For the considered vehicles the average truck factor was equal to 2.14.

Upon request of the tunnel administration, pavement design life, inclusive of the 2 years of tunnel completion, was set equal to 20 years. Based on the data and assumptions illustrated above, corresponding total design traffic expressed in ESALs was found to be equal to 16.2 million.

5.3.2 Design temperatures

Available data consisted in hourly air temperatures recorded for one year along the existing tunnel in 4 fixed stations (Figure 5.9). As expected, lower values were reached near the tunnel entrance. Thus, as part of a conservative approach, average values derived only from the 3 stations closer to the tunnel center were considered in subsequent analyses. Hourly data were converted into average daily and monthly temperatures. As a result, four different periods characterized by a similar average monthly temperature were identified and were then associated to average air temperature values ($T_{air,p}$).

In order to calculate pavement design temperatures, the presence of the buried high-voltage line was considered. Thus, its operating temperature was calculated

by taking into account the requirements fixed by line designers and by making use of the model proposed by Neher and McGrath [176]. In each of the abovementioned periods, air temperature was considered representative of far field conditions, while the resistivity of the materials surrounding the cables and conduits varied from one cross section to the other. In the case of cross section CS, calculations were carried out by considering the presence of a lean concrete duct-bank and of a soil backfill, with thermal resistivity values equal to 1.368 K·m/W and 1.2 K·m/W, respectively. For the GG and CG pavements, no duct-bank was planned to be constructed, so modelling was based on a single resistivity value, equal to 0.860 K·m/W, representative of the SC-CBM intended for use for the formation of the subgrade. Thermal resistivity values indicated above for lean concrete and for the SC-CBM were measured by the Authors by means of the thermal needle probe technique indicated by ASTM D 5334-14 [188], as in Chapter 3. In the case of the backfill soil, the considered value was retrieved from literature.

In order to derive pavement temperature profiles, surface temperature was considered equal to air temperature, whereas at 120 cm below the surface, temperature was assumed to be equal to the average of the temperatures reached inside the conduits of the 4 cables constituting the high-voltage line. Temperature gradients within the pavement layers and subgrade were assumed to be inversely proportional to the corresponding thermal resistivity values. Representative pavement design temperatures ($T_{pav,p}$) were thereafter calculated for each period at a depth from the surface equal to one-third of the total thickness of the asphalt layers.

The laying arrangement of high-voltage cables, were different according to the chosen materials for the construction of foundation layers of the pavement. For the cross section CS, which would have the high-voltage cables buried in a lean cement concrete duct bank placed in compacted soil backfill foundation whereas cross-sections GG and CG wouldn't need any cement concrete duct bank as there was innovative self-leveling and self-compacting thermal backfills with adequate thermal conductivity and strength as the pavement foundation.

The base layer below the asphalt concrete was a cement stabilized layer for CS and CG whereas a self-compacting layer with 60 kg/m^3 of cement in the case of cross section GG. Pavement temperatures of the considered cross section would change depends on the materials used for the construction of its layers. Initially, the average monthly air temperatures measured inside the tunnel close to its center was calculated from the hourly data provide by the tunnel administration. Due to the presence of high-voltage cables below the carriage way, pavement temperature was calculated using the relationship connecting the current carrying capacity of the buried high-voltage cables and heat dissipation around the cables. Thus using measured air temperature as the input data, resultant temperature due

to the operation of the high-voltage cables at their axis was calculated from the standard procedure to calculate the current carrying capacity of high-voltage cables. Laboratory measured thermal resistivity of soil, self-compacting layer 1 (with 100 kg/m^3) and self-compacting layer 2 (with 60 kg/m^3) of 1.2, 0.86 and 1.22 K.m/W respectively were used in these calculations in line with the thermal conductivity studies performed on the mixtures.

Once temperature close to the axis of the high-voltage cables was calculated, it was used in deriving the temperate at the 1/3rd depth of the asphalt layer using the thermal resistivities of asphalt concrete layer and base layer which is a cement stabilized layer for CS and CG whereas a self-compacting layer with 60 kg/m^3 in case of GG. The thermal resistivity of asphalt and cement stabilized layers were 1 and 0.952 K.m/W respectively. Results obtained by means of the modelling approach synthesized above are provided in Table 5.4.

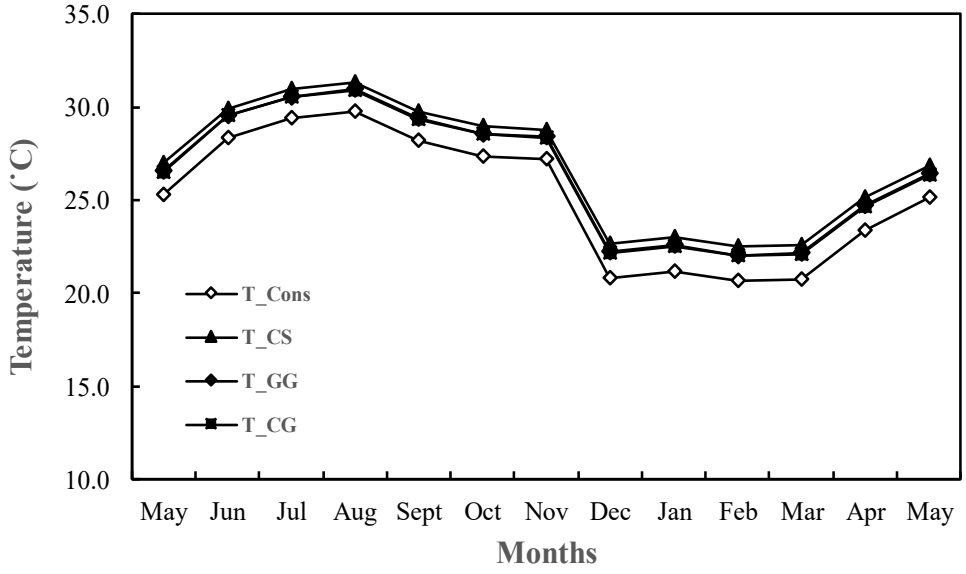

Figure 5.9 Estimated variation in temperature with seasons

5.3.3 Mechanical properties of materials

Assessment of the mechanical properties of materials constituting the various pavement layers was carried out by focusing on elastic moduli. Values of Poisson's ratio were derived from relevant literature. A full-scale pavement section was constructed by replicating cross section GG with a reduced asphalt thickness of 15 cm (10 cm binder course, 5 cm wearing course). The test section had a length of 14 m and width of 4 m (Figure 5.10). The SC-CBM subgrade and foundation had a thickness of 100 cm and 20 cm, respectively. Both asphalt mixtures, which were intended for use in the final construction of the pavement in

the tunnel, contained polymeric additives for the improvement of rutting and fatigue resistance.

Table 5.4 Air and pavement design temperatures

Period	Months	$T_{air,p}$ (°C)	$T_{pav,p}$ (°C)			
			Final phase of construction	Service life		
			CS-GG-CG	CS	GG	CG
1	January-March	20.8	20.8	22.7	22.2	22.2
2	April-May	24.6	24.6	26.3	25.9	25.9
3	June-November	28.4	28.4	30.0	29.6	29.5
4	December	20.8	20.8	22.7	22.2	22.2

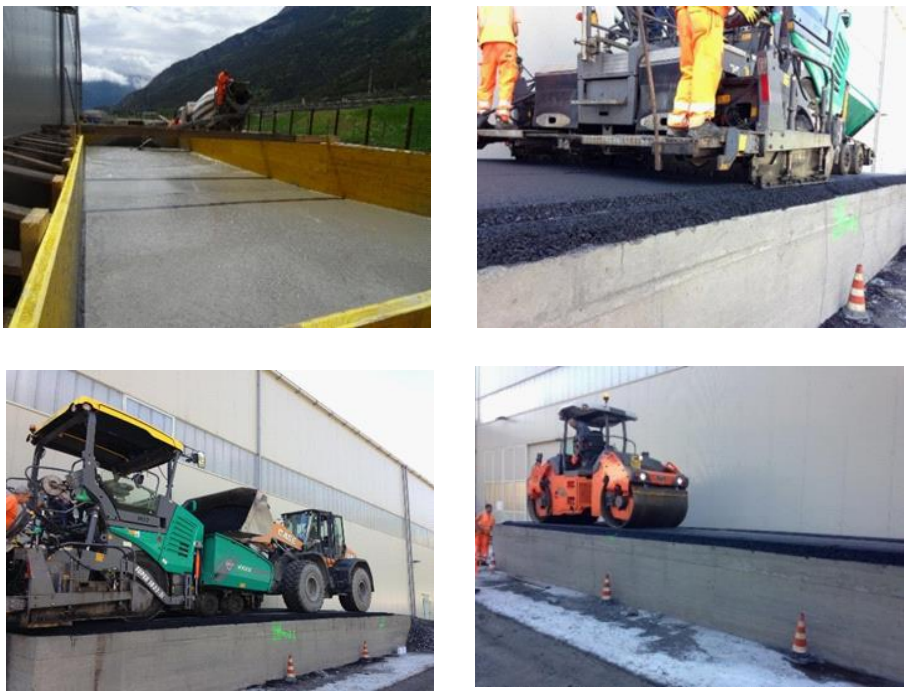

Figure 5.10 Construction of full scale section at the site

Following previous investigations, the SC-CBMs were designed to achieve a satisfactory flowability, while guaranteeing adequate short-term and long-term mechanical properties. In particular, a 170-300 mm acceptance range was fixed for spread diameter [123] and threshold values were identified for compressive strength [193], which was required to be greater than 0.5 MPa at 3 days of curing and less than 2.0 MPa at 28 days of curing.

The SC-CBMs employed in the test section and proposed for use in the tunnel contained 20% gravel, 36% fine sand, 20% RAP and 24% mineral sludge (percentages by weight). Cement content was set equal to 100 kg/m^3 and 60 kg/m^3 in the subgrade and foundation, respectively. Water content was that corresponding to a water-to-powder ratio equal to 0.8 ("powder" being the sum of cement and mineral sludge).

During the construction of the test section, samples of the two SC-CBMs were taken for the immediate assessment of spread diameter which in both cases was found to be of the order of 250 mm. Specimens were also prepared for the laboratory evaluation of compressive strength. Corresponding results obtained after 3 and 28 days of curing, respectively equal to 0.84 MPa and 1.67 MPa for the mixture with 100 kg/m^3 cement dosage and to 0.50 MPa and 0.9 MPa for the mixture with 60 kg/m^3 cement dosage, satisfied the previously mentioned acceptance requirements.

Falling Weight Deflectometer (FWD)

Falling Weight Deflectometer (FWD) stimulates in-service wheel loading and measure the instantaneous deflections which is later used to backcalculate the modulus of the different layers. The deflections are measured at number of points in order to create a deflection bowl. To understand the condition of the pavement, further anlyses were perfromed on the deflection data and in-situ stiffness of the different layers were evaluated. As the first step, reasonable assumptions of the elastic modulus were made and corresponding deflection bowls were calculated, these obtained deflection bowls are compared with the calculated deflection bowl is compared with the measured deflection at the field and adjustments in the initial stiffness modulus are made to match these deflection bowls. This way structural assessment of the pavement layers as well as can be performed. Such stiffness values can also be made use in the pavement design.

FWD tests were performed over the finished pavement surface at three different loading levels (47, 63 and 83 kN). The diameter of the plate used for loading was 300 mm. The position of geophones from the center of the loading plate was at measured to be at distance of 0, 200, 300, 450, 600, 900, 1200, 1500 and 1800 mm. At the time of testing, a temperature of 16°C was recorded at mid-depth in the asphalt layers (Figure 5.11). Back-calculation was carried out with an iterative procedure by employing the BISAR software [212] and by hypothesizing full slip between the bottom asphalt course and the extremely smooth underlying foundation. Computed elastic modulus values were equal to 3,500 MPa, 350 MPa and 1,000 MPa for the asphalt layers, foundation and subgrade, respectively. For the subgrade soil and for the CBM foundation included in cross section CS, values of 200 MPa and 800 MPa, respectively, were assumed consistently with preliminary design hypotheses. In the case of the asphalt layers, cores were taken

in order to assess their volumetric characteristics. Unfortunately, due to the physical constraints imposed by the test section, which was quite narrow and with a working surface located 1 m above the ground, achieved compaction level was lower than expected. In particular, measured air void content, equal to 9.7%, was definitely higher than the target value of 7.0%, compatible with mix design studies and technical specifications.

Figure 5.11 FWD testing over the full scale trial section

For the purpose of pavement evaluation, the elastic modulus of the asphalt layers was adjusted for temperature using Eq. 5.1 [213]. Moreover, it was assumed that during construction operations in the tunnel, target void content would be reached. Thus, the modulus was adjusted further by making use of the same functional dependency proposed by Bonnaure et al. [214] for stiffness values measured in the bending mode.

$$E = 10^{a\left(T^2{}_{ref} - T^2\right)} . E_{ref} \qquad 5.1$$

where E is the modulus of elasticity at the temperature of acquisition, E_{ref} is the modulus of elasticity at the reference temperature, T is the temperature of the pavement during the data acquisition (ºF), T_{ref} is the reference temperature of the pavement (ºF), and a is a constant, for which the value is assigned as 0.000147362

Results obtained by means of the procedure outlined above are given in Table 5.5, where they are presented for each temperature period, pavement cross section and phase.

Table 5.5 Elastic modulus of asphalt layers

Period	Months	Elastic modulus (MPa)			
		Final phase of construction	Service life		
		CS-GG-CG	CS	GG	CG
1	January-March	3,185	2,742	2,845	2,855
2	April-May	2,334	2,007	2,083	2,090
3	June-November	1,660	1,428	1,481	1,486
4	December	3,185	2,742	2,845	2,855

5.3.4 Transfer functions

The objective of a pavement design is to have enough structural capacity of the pavement to meet traffic demands under the given environmental conditions. South-African pavement design methodology (SAPEM) has been widely used to design pavements built over cement-stabilized foundations [36]. The SC-CBMs, intended to use for this case study, had their mechanical properties similar to the properties of cement-stabilized layers included in SAPEM. Hence, transfer functions used for performance evaluation were drawn from the SAPEM [36]. Minor adjustments were needed in order to take into account the specific properties of the employed materials.

In the case of the asphalt layers, analyses focused exclusively on fatigue cracking, the transfer function of which depends upon elastic modulus and thickness. However, an additional shift factor of 1.10 was introduced in calculations in order to account for the performance-related benefits deriving from the use of polymeric additives.

Performance of the CBM and SC-CBM foundation layers was analyzed in two phases (Figure 5.12). In phase 1, the layers were assumed to be intact and were consequently modelled in terms of their fatigue resistance under bending. The corresponding transfer functions were selected by fitting the considered materials into the categories indicated by the SAPEM (C3 for the CBM, C4 for the SC-CBM). In phase 2, reached as a result of cracking, they were considered as unbound granular materials with a reduced modulus (of classes EG4 and EG5, respectively, for the CBM and for the SC-CBM). In such a state, their performance was assessed in terms of their resistance to shear failure.

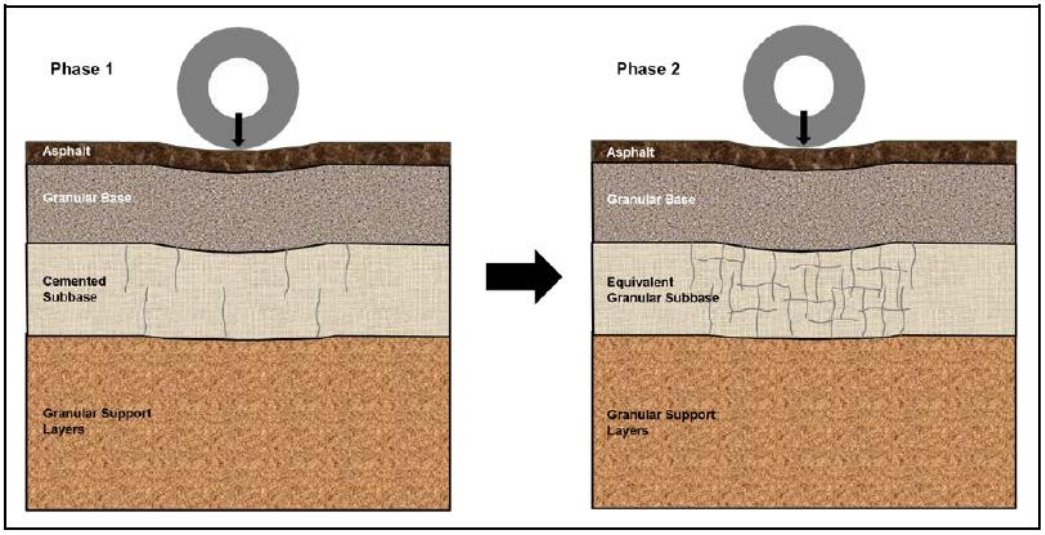

Figure 5.12 Change of a cemented in layer to equivalent granular layer [36]

For all pavement cross sections, the same transfer function was employed for the performance assessment of the subgrade. In particular, a reliability of 95% was selected, which corresponds to a terminal rut depth of 10 mm.

Design calculations were performed by combining the results obtained in the various temperature periods and by introducing the concept of cumulated damage. The response under loading of the pavement cross sections in each period was assessed by means of the BISAR software by assuming full adhesion between the layers and by considering an equivalent single axle loading of 80 kN with a contact pressure of 577.4 kPa.

The ultimate life of a pavement in SAPEM is computed in 2 phases (see Figure 5.13). The cemented layer serves as an intact bound layer in phase 1 and as an equivalent granular layer in phase 2 within its service life (Figure 5.12). The stresses and strains obtained by modeling phase 1 with an intact cemented sub-base are used in the corresponding transfer functions to predict the life of the layers in this phase. Bounded cemented layer has lower fatigue life compared to an asphalt layer. Hence, the difference between the life of an asphalt layer and cemented layer is computed as the residual life of the asphalt layer.

Following the fatigue failure of a cemented layer, an equivalent granular layer is formed which behaves like an unbound granular layer with lower stiffness and leads to higher stresses and strains in other layers. This reduces the residual life of other pavement layers compared to their predicted life in phase 1. Hence, predicted life of all the layers are calculated again for the phase 2 based on the stresses and strains computed for this scenario. For all the layers, this rate of reduction is assumed to be equal to the ratio of life of the layer in phase 1 and 2.

Residual life of asphalt layer in phase 1 is divided by the rate of reduction to obtain the adjusted residual life.

Finally, for the calculation of ultimate life of the pavement, predicted life of the layers in phase 1 is added to their adjusted residual life, as shown in Figure 5.13. However, cement treated layers are an exception as they are in a different state in both the phases and a direct summation of their life in the two phases gives its ultimate life. The minimum of the two is the ultimate design life of the pavement and the layer with the minimum ultimate life is identified as the critical layer for that pavement.

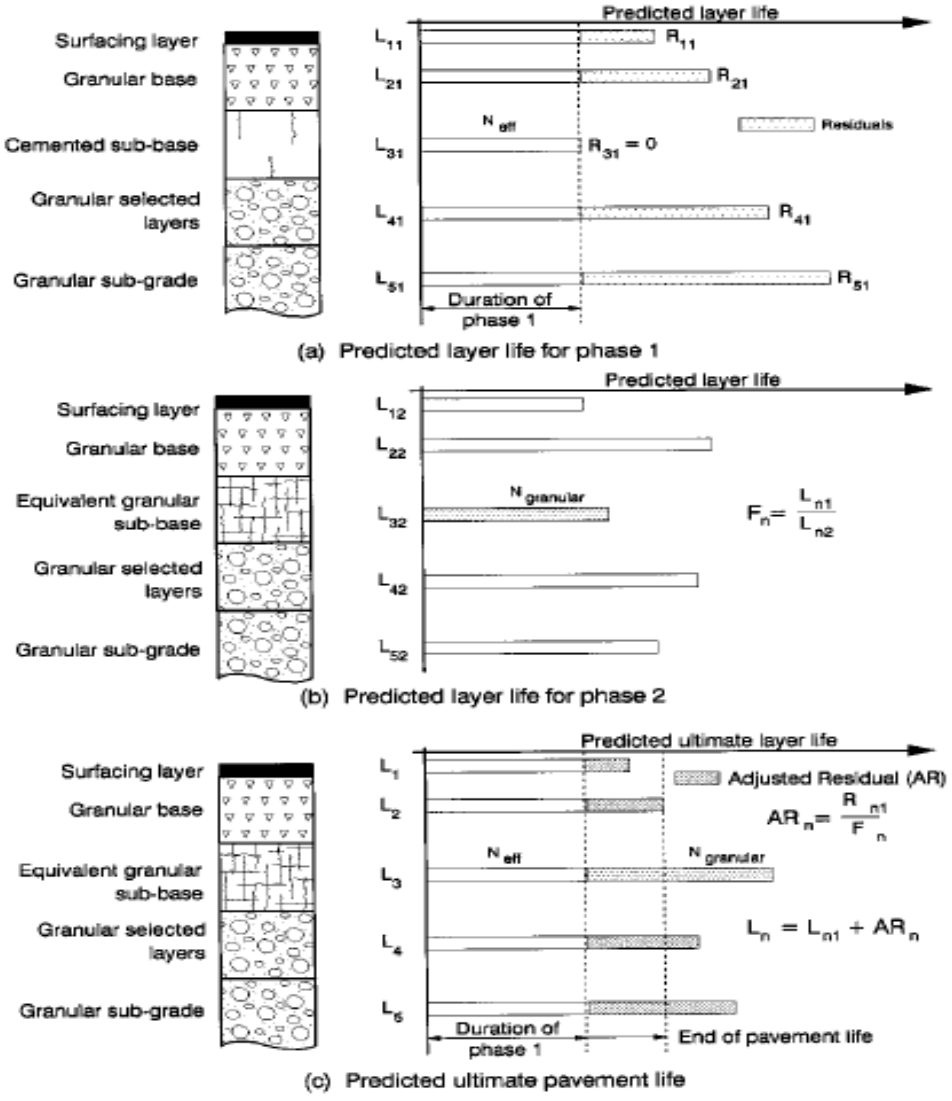

Figure 5.13 Computation of ultimate pavement life as per SAPEM [36]

5.4 Design life

The design life of each pavement solution, expressed in terms of allowable ESALs and corresponding years of traffic, was computed as the sum of three terms associated to the final stage of construction and to the previously mentioned phases 1 and 2.

Obtained results are synthesized in Table 5.6. In all cases final conditions were reached as a result of fatigue cracking in the asphalt layers, thus indicating that their performance potential was fully exploited. Furthermore, accumulation of permanent deformation in the subgrade was not of concern for any of the considered solutions.

Table 5.6 Design life of considered pavement solutions

	ESALs			**Years**		
	CS	**GG**	**CG**	**CS**	**GG**	**CG**
Construction + Phase 1	9.19E+06	9.83E+06	9.71E+06	13.3	14.0	13.8
Phase 2	7.25E+06	1.78E+06	1.42E+07	6.9	1.8	12.2
Total	1.64E+07	1.16E+07	2.39E+07	20.2	15.8	26.0

From the data listed in Table 5.6 it can be observed that the CG pavement cross section provided the highest design life, equal to 26 years, followed in ranking by solutions CS and GG. Both cross sections with a CBM foundation satisfied the requirement of 20 years design life. On the contrary, the cross section with the two-layer SC-CBM supporting system was found to have a shorter design life, close to 16 years, which in any case corresponds to a remarkably high traffic (equal to 11.6 million ESALs).

It can be observed that the three solutions exhibited a similar design life associated to the sum of the construction completion phase and of the phase 1 pre-cracking stage. However, the highest number of allowable loadings were found in the case of cross section GG, followed in ranking by CG and CS. This is due to the fact that phase 1 transfer functions employed for calculations yield numbers of loadings to cracking of the cement-stabilized layers which depend not only upon load-induced tensile strains but also on the ductility of the mixtures (expressed in terms of the so-called strain-at-break). Thus, less stiff materials such as the SC-CBMs (associated to category C4), may yield higher fatigue lives in comparison to stiffer materials such as the C3-type CBMs.

Despite their similar early behavior, the three cross sections showed a totally different response in phase 2, the highest and lowest lives being associated to

solutions CG and GG, respectively. As highlighted in Figure 5.14, this is essentially due to the fact that asphalt damage in both phases progressed with completely different rates, which were affected by the stiffness of both the foundation and the subgrade. Figure 5.14 also shows that a similar dependency upon stiffness support was exhibited by the cement-stabilized foundations in phase 2, the lowest damage rates being associated to the cross sections containing the stiffer SC-CBM subgrade (GG and CG).

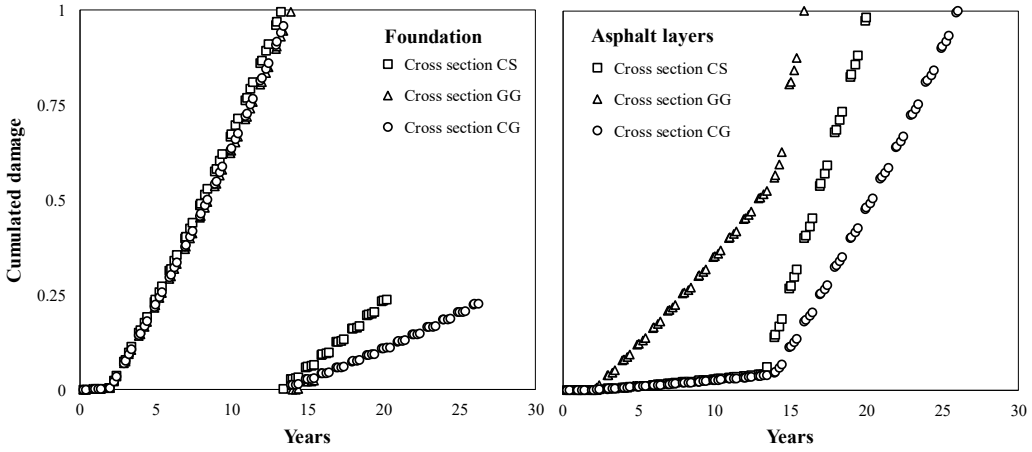

Figure 5.14 Cumulated damage of considered pavement solutions

6. Conclusions

The main objective of this research was to develop self-compacting cement-bound mixtures for constructing pavement foundations in road tunnels. The proposed objective was achieved by adopting a systematic approach. Each part of this thesis addresses a specific topic of interest within this objective. The first two parts of the thesis deal with the mix design procedure of self-compacting cement-bound mixtures and their thermal properties. Studies performed in the first part resulted in the development of a mix design methodology. The second part of the thesis demonstrated the suitability of SC-CBMs for using in pavement foundations containing buried high-voltage cables as well as in fluidized thermal backfills. The third part of the thesis was dedicated to the field trials of SC-CBMs and to the use of such mixtures in pavement design. Field trials resulted in further optimization of the performance of these mixtures and acceptance criteria for quality control were formulated in Chapter 4. Different cross sections were designed with conventional foundation materials and SC-CBMs in Chapter 5, and a relative ranking of the cross sections was made depending on the anticipated design life. Savings in the consumption of natural aggregates was also highlighted with the use of innovative SC-CBMs.

6.1 Mix design of self-compacting cement-bound mixtures

A rational mix design methodology for the design of self-compacting cement-bound mixtures was presented in the first part. It was shown that the composition of the SC-CBMs can be defined by optimizing the characteristics of the cementitious paste and of the aggregate skeleton. Key factors which should be considered in such a context are combined particle size distribution of granular components, content of fines and water-to-powder ratio. It was also postulated that the dosage and type of employed cement and superplasticizing additive may have a relevant role in controlling the main performance-related properties. These include flowability in the fresh state, and stiffness and strength in the hardened, fully cured state achieved in the long-term.

When referring to SC-CBMs possessing a gradation sufficiently close to the reference one assumed for design purposes, it was shown that flowability is especially sensitive to variations of the water-to-powder ratio which affects the consistency of the cementitious paste. Likewise, for SC-CBMs possessing such an optimized bulk structure, the water-to-powder ratio was found to be the main

controlling factor of mechanical properties achieved in the hardened state since it dictates the stiffness and porosity of the binding cementitious paste.

Based on the experimental results obtained in the entire investigation, a mix design procedure was proposed. One of its distinctive features is that it leads to the definition of the design composition of an SC-CBM with a limited number of experimental tests, thus minimizing required time and involved costs. It is also structured in such a way to be expanded to provide a more detailed analysis of materials and to be easily adapted to other applications by amending the set of considered properties and by conveniently adjusting target values. Feasibility of following the mix design procedure was demonstrated by referring to the obtained experimental results and by identifying the optimal SC-CBM formulation.

6.2 Thermal properties of self-compacting cement-bound mixtures

Thermal properties of these mixtures were also evaluated to understand their feasibility for backfilling high-voltage cables that need to be buried in the pavement foundation of road tunnels. Results of the experimental investigation showed that SC-CBMs possess adequate thermal conductivity and thermal stability required for using in pavement foundations which contain buried high-voltage cables and as Fluidized Thermal Backfills (FTBs). Thermal conductivity of the SC-CBMs were mainly affected by the cement content of the mixtures. Age of the samples and water to powder ratio showed a lesser influence on the thermal conductivity. Homogeneity of the mixtures are important for their thermal properties. Segregation and bleeding negatively affects thermal conductivity. SC-CBMs containing significant quantities of recycled materials can be successfully designed by ensuring satisfactory flowability and thermal conductivity properties for application in thermal backfills.

6.3 Field trials, Optimization and Pavement design

Four full-scale field trials were conducted with the objective of performance assessment of SC-CBMs. The production, laying and evaluation of 14 different SC-CBMs, in this series of field trials concluded that the considered mixtures are suitable for their intended use. In particular, it was found that SC-CBMs prepared with a cement dosage of up to 100 kg/m^3 possess the required properties of flowability, strength and stiffness. On the contrary, mixtures with higher cement dosages (150 kg/m^3 and 200 kg/m^3) fail to meet all the performance-related requirements as a result of their high long-term strength which jeopardizes excavatability. Furthermore, they may be more prone to long-term cracking and

may consequently promote the occurrence of reflection cracks in the overlying pavement layers.

This stage further confirmed that the adopted mix design procedure, based on the use of a reference particle size distribution and on the optimization of the composition of cement paste, leads to SC-CBMs which are characterized by an adequate flowability, with a spread diameter (determined as per ASTM D6103) greater than 200 mm, and by a satisfactory stability, with no occurrence of bleeding or segregation. The short-term and long-term mechanical properties of the SC-CBMs can then be tuned by selecting the appropriate cement dosage and by considering the additional effects which are due to other components. Moreover, it was found that use of a hardening accelerator was not very effective, whereas a significant increase of strength and stiffness was observed when employing mineral sludge pretreated with quicklime. This is a very useful insight for the reuse of similar wet-sludges in cement-bound mixtures.

Results collected during the experimental investigation were used for the identification of recommended performance-related acceptance criteria which may be adopted in future construction works in road tunnels and possibly improved when considering the results coming from a broader range.

As a case study, three different pavement cross-sections were studied for their suitability of using in road tunnels. Based on the results obtained in the optimization activities, it is recommended to adopt the innovative CG pavement cross section as the final construction solution when there is high traffic. In fact, it was shown that such a choice leads to a non-negligible improvement of design life with respect to the CS cross section initially proposed in the preliminary design phase, thereby accommodating for unexpected variabilities occurring during construction and in service. Furthermore, it yields supplementary advantages which are related to the ease of construction (i.e. no need for subgrade compaction), to the better thermal conductivity (relevant due to the presence of a high-voltage buried line) and to the possibility of employing significant amounts of recycled materials. In such a context, it should be underlined that the laying of the SC-CBM subgrade for a length of 1 km in the tunnel implies the use of 1,700 tons and 2,000 tons of RAP and mineral sludge, respectively. This leads to a significant reduction of the consumption of virgin materials and of waste landfilling, thereby increasing the sustainability of construction operations.

The pavement cross section including two SC-CBM layers (solution GG) proved to be inferior to other two solutions in terms of design life. Nevertheless, it should be considered for other future applications characterized by a design traffic corresponding to the calculated ESALs (equal to 11.6 million). Moreover, further improvements may be sought by employing high-performance asphalt mixtures which may allow designers to fully exploit the low damage rate exhibited by the SC-CBM foundation. Finally, it should be emphasized that such a pavement

solution may provide further advantages with respect to the use of recycled materials, with a further increase of the quantities of employed RAP and mineral sludge of the order of 25%.

Overall, this thesis demonstrated the suitability of self-compacting cement-bound mixtures in pavement foundations of road tunnels. In the future, the proposed mix design approach can be used for the development of self-compacting cement-bound mixtures with other recycled components, whereas the experimental investigation adopted for the field trial activities can be adopted for preparing the relevant performance-related specifications. An integrated approach considering the overall performance of available pavement solutions can be adopted for the selection of the most suitable pavement cross section that satisfies the given requirements. The findings illustrated in this thesis are extremely relevant in the context of pavement engineering as well as for solid waste management. SC-CBMs can be used in various other applications like in trench backfilling, construction of embankments and in flowable thermal backfills. Waste materials including construction and demolition wastes can be valorized following a similar approach contributing to effective solid waste management efforts.

6.4 Recommendations for future research

Further research can be carried out in different directions, some of which are listed below.

[1] It is recommended that future studies related to the proposed mix design procedure of SC-CBMs should include a more thorough evaluation of the role played by other recycled components (e.g. construction and demolition waste and industrial by-products)

[2] The studies could also be extended to base the comparative analysis of cement pastes on the measurement of rheological characteristics which may supplement the visual observations performed as per the current version of the design method. Deriving correlations between rheology of the pastes and SC-CBMs can also be an interesting task to pursue further.

[3] Improvements to the mix design method may be also sought by including in the selection process the assessment of the short-term mechanical properties of SC-CBMs. Such an evaluation may be relevant from a practical point of view since it may be necessary to allow construction traffic to move on top of the pavement foundation in its early stages of curing, with the occurrence of no significant

damage in the mixture. Thus, minimum acceptance limits for stiffness and strength may be introduced into to design procedure.

[4] Thermal properties of the SC-CBMs can be further modified by changing the composition. Other fillers could be considered in the composition in development of further studies. As needle probe is a suitable devise for the measurement of thermal conductivity, the role of contact resistance between the probe and hole made on the samples on thermal conductivity can be further studied. The observed effects of composition variables should be taken into account in the development of further studies.

[5] Specific studies which can address the fatigue and rutting properties of the SC-CBMs can be conducted in order to derive specific transfer functions for the pavement design.

[6] Detailed life-cycle analyses which take into account economic-environmental impacts by means of Life Cycle Cost Analysis (LCCA) and Life Cycle Analysis (LCA) can be conducted.

7. References

[1] PIARC, “Road tunnels: complex underground networks,” World Road Association, Paris, France, 2016.

[2] PIARC, “Road tunnel operations: first steps towards a sustainable approach,” World Road Association, Paris, France,, 2017.

[3] C. Jofre, J. Romero and R. Rueda, “Contribution of concrete pavements to the safety of tunnels in case of fire,” European Concrete Paving Association, 2010.

[4] E. Puente, D. Lázaro and D. Alvear, “Study of tunnel pavements behaviour in fire by using coupled cone calorimeter – FTIR analysis,” *Fire Safety Journal,* vol. 81, pp. 1-7, 1 4 2016.

[5] A. Leitner, “The fire catastrophe in the Tauern Tunnel: experience and conclusions for the Austrian guidelines,” *Tunnelling and Underground Space Technology,* vol. 16, p. 217223, 2001.

[6] F. Pedrazo Majarrez, “Semi-rigid pavement performance and construction techniques for semiarid areas,” *Road Materials and Pavement Design,* vol. 14, no. 3, pp. 615-637, 2013.

[7] EAPA, “Asphalt in Figures 2016, European Asphalt Pavement Association,” 2016.

[8] Z. Guo, Q. Yang and B. Liu, “Mixture design of pavement surface course considering the performance of skid resistance and disaster proof in road tunnels,” *Jounral of Materials in Civil Engineering,* vol. 21, no. 4, pp. 186-190, 2009.

[9] A. Bendelius, “Tunnel fire and life safety within the world road association (PIARC),” *Tunnelling and Underground Space Technology,* vol. 17, no. 2, pp. 159-161, 1 4 2002.

[10] European Commission, “Directive 2004/54/EC of the European Parliament and of the Council of 29 April 2004 on minimum safety requirements for tunnels in the Trans-European Road Network,” European Commission, Brussels, 2004.

[11] PIARC, “Integrated approach to road tunnel safety,” World Road Association (PIARC), France, 2007.

[12] PIARC, “Risk Analysis for Road Tunnels,” World Road Association (PIARC), France, 2008.

[13] PIARC, “Human factors and road tunnel safety regarding users,” World Road Association (PIARC), France, 2008.

[14] Austroads, “Guide to road tunnels part 2: planning, design and commissioning,” Austroads, Sydney, Australia, 2019.

[15] J. Qiu, T. Yang, X. Wang, L. Wang and G. Zhang, “Review of the flame retardancy on highway tunnel asphalt pavement,” *Construction and Building Materials,* vol. 195, pp. 468-482, 20 1 2019.

[16] EAPA, “Asphalt pavements in tunnels,” European Asphalt Pavement Association, Brussels, 2008.

[17] L. Moretti, G. Cantisani and P. Di Mascio, “Management of road tunnels: Construction, maintenance and lighting costs,” *Tunnelling and Underground Space Technology,* vol. 51, pp. 84-89, 1 1 2016.

[18] L. Huang, R. André Bohne, A. Bruland, P. Drevland Jakobsen and J. Lohne, “Life cycle assessment of Norwegian road tunnel,” *The International Journal of Life cycle Assessment,* vol. 20, no. 2, pp. 174-184, 2015.

[19] Sitaf SpA, “Frejus tunnel - design documents,” Italy, 2012.

[20] Austroads, “Guide to pavement technology part 2: Pavement structural design, AGPT02-17,” Austroads Ltd, Sydney, Australia., 2017.

[21] M. Frost, The performance of pavement foundations during construction, Loughborough University: Doctoral dissertation, 2000.

[22] S. Nazarian, M. Mazari, I. Abdallah, A. J. Puppala, L. N. Mohammad and M. Y. Abu-Farsakh, “Modulus-based construction specification for compaction of earthwork and unbound aggregate,” Transportation Research Board, Washington, DC, 2015.

[23] E. Choorackal, P. Riviera, D. Dalmazzo, E. Santagata, L. Zichella and P. Marini, “Performance-related characterization of fluidized thermal backfills containing recycled components.,” *Waste and Biomass Valorization,* 2019.

[24] Y. Shen, H. Niu, Y. You, X. Zhuang and T. Xu, “Promoting cable ampacity by filling low thermal resistivity medium in ducts,” in *2013 IEEE PES Asia-Pacific Power and Energy Engineering Conference (APPEEC)*, 2013.

[25] K. J. Folliard, L. Du, D. Trejo, C. Halmen, S. Sabol and D. Leshchinsky, “NCHRP Report 597- Development of a recommended practice for use of controlled low-strength material in highway construction,” Transportation Research Board of the National Academies, Washington, DC, 2008.

[26] Y. Zhang, A. E. Johnson and D. J. White, “Laboratory freeze–thaw assessment of cement, fly ash, and fiber stabilized pavement foundation materials,” *Cold Regions Science and Technology,* vol. 122, pp. 50-57, 2016.

[27] T. Bennert, W. J. Papp, A. Maher and N. Gucunski, “Utilization of construction and demolition debris under traffic-type loading in base and subbase applications,” *Transportation Research Record: Journal of the Transportation Research Board,* vol. 1714, no. 1, pp. 33-39, 1 1 2000.

[28] F. Maghool, A. Arulrajah, S. Horpibulsuk and Y.-J. Du, “Laboratory evaluation of ladle furnace slag in unbound pavement-base/subbase

applications," *Journal of Materials in Civil Engineering,* vol. 29, no. 2, p. 04016197, 2017.

[29] S. H. Chen, D. F. Lin, H. L. Luo and Z. Y. Lin, "Application of reclaimed basic oxygen furnace slag asphalt pavement in road base aggregate," *Construction and Building Materials,* vol. 157, pp. 647-653, 30 12 2017.

[30] U.-M. Mroueh, P. Eskola and J. Laine-Ylijoki, "Life-cycle impacts of the use of industrial by-products in road and earth construction," *Waste Management,* vol. 21, pp. 271-277, 2001.

[31] D.-H. Chen, F. Hong and F. Zhou, "Premature cracking from cement-treated base and treatment to mitigate its effect," *Journal of Performance of Constructed Facilities,* vol. 25, no. 2, pp. 113-120, 4 2011.

[32] K. Sobhan and M. Mashnad, "Fatigue behavior of a pavement foundation with recycled aggregate and waste HDPE strips," *Journal of Geotechnical and Geoenvironmental Engineering,* vol. 129, no. 7, pp. 630-638, 7 2003.

[33] P. Pérez, F. Agrela, R. Herrador and J. Ordoñez, "Application of cement-treated recycled materials in the construction of a section of road in Malaga, Spain," *Construction and Building Materials,* vol. 44, pp. 593-599, 1 7 2013.

[34] T. Scullion and P. Harris, "Forensic evaluation of three failed cement-treated base pavements," *Transportation Research Record: Journal of the Transportation Research Board,* vol. 1611, no. 1, pp. 10-18, 1 1 1998.

[35] H. L. Theyse, M. De Beer and F. C. Rust, "Overview of South African mechanistic pavement design method," *Transportation Research Record: Journal of the Transportation Research Board,* vol. 1539, no. 1, pp. 6-17, 1 1 1996.

[36] SANRA, "South African Pavement Engineering Manual (SAPEM)," South African National Roads Agency, Pretoria, South Africa., 2014.

[37] A. Arulrajah, J. Piratheepan, M. M. Disfani and M. W. Bo, "Resilient moduli response of recycled construction and demolition materials in pavement subbase applications," *Journal of Materials in Civil Engineering,* vol. 25, no. 12, pp. 1920-1928, 12 2013.

[38] K. P George, "Characterization and structural design of cement-treated base," *Transportation Research Record,* vol. 1288, pp. 78-87., 1990.

[39] B. Ferne, "Long-life pavements - A European study by ELLPAG," *International Journal of Pavement Engineering,* vol. 7, no. 2, pp. 91-100, 2006.

[40] D. Merrill, A. Van Dommelen and L. Gaspar, "A review of practical experience throughout europe on deterioration in fully-flexible and semi-rigid long-life pavements," *International Jornal of Pavement Engineering,* vol. 7, no. 2, pp. 101-109, 2006.

[41] P. Solanki and M. Zaman, "Design of semi-rigid type of flexible pavements," *International Journal of Pavement Research and Technology,* vol. 10, no. 2, pp. 99-111, 1 3 2017.

[42] M. Nunn, "Development of a more versatile approach to flexible and flexible composite design, TRL Report 615," TRL Limited,, Wokingham,

U.K., 2004.

[43] J. Zheng, "Design guide for semirigid pavements in China based on critical state of asphalt mixture," *Journal of Materials in Civil Engineering,* vol. 25, no. 7, pp. 899-906, 7 2013.

[44] P. P. Riviera, E. Choorackal and E. Santagata, "Performance evaluation of innovative and sustainable pavement solutions for road tunnels," in *5th International symposium on asphalt pavements and environment (APE)*, Padua, Italy, 2019.

[45] P. P. Riviera, G. Bertagnoli, E. Choorackal and E. Santagata, "Controlled low-strength materials for pavement foundations in road tunnels: feasibility study and recommendations," *Materials and Structures,* vol. 52, no. 4, p. 72, 25 8 2019.

[46] K. Malmedal, C. Bates and D. Cain, "The effect of underground cable diameter on soil drying, soil thermal resistivity and thermal stability," in *IEEE Green Technologies Conference*, 2016.

[47] H. Okamura, K. Ozawa and M. Ouchi, "Self-compacting concrete," *Structural Concrete,* vol. 1, no. 1, pp. 3-17, 2000.

[48] ACI 229R-13, "Controlled low-strength materials,," ACI Committee 229, Farmington Hills, MI, 2013.

[49] T.-C. Ling, S. K. Kaliyavaradhan and C. S. Poon, "Global perspective on application of controlled low-strength material (CLSM) for trench backfilling – An overview," *Construction and Building Materials,* vol. 158, pp. 535-548, 2018.

[50] M. C. Nataraja, T. S. Nagaraj, S. Bhavanishankar and B. M. Ramalinga Reddy, "Proportioning cement based composites with burnt coal cinder," *Materials and Structures,* vol. 40, no. 6, pp. 543-552, 20 2 2007.

[51] E. Gennesseaux, T. Sedran, J. M. Torrenti and M. Hardy, "Formulation of optimized excavatable cement treated materials using a new punching test apparatus," *Materials and Structures,* vol. 51, no. 3, 2018.

[52] J. Qian, Y. Hu, J. Zhang, W. Xiao and J. Ling, "Evaluation the performance of controlled low-strength material made of excess excavated soil," *Journal of Cleaner Production,* vol. 214, pp. 79-88, 20 3 2019.

[53] R. Janardhanatn, F. Burns and R. D. Peindl, "Mix design for flowable fly ash backfill material," *Journal of Materials in Civil Engineering,* vol. 4, no. 3, pp. 252-263, 8 1992.

[54] S. Bhat and C. Lovell, "Design of Flowable Fill: Waste Foundry Sand as a Fine Aggregate," *Transportation Research Record,* vol. 1546, no. 1, pp. 70-78, 1996.

[55] S. Bouzalakos, A. W. L. Dudeney and B. K. C. Chan, "Formulating and optimising the compressive strength of controlled low-strength materials containing mine tailings by mixture design and response surface methods," *Minerals Engineering,* vol. 53, pp. 48-56, 2013.

[56] V. Alizadeh, "New approach for proportioning of controlled low strength materials," *Construction and Building Materials,* vol. 201, pp. 871-878, 20 3 2019.

[57] C. Shi, Z. Wu, K. Lv and L. Wu, *A review on mixture design methods for self-compacting concrete,* vol. 84, pp. 387-398, 2015.

[58] H. J. H Brouwers and H. J. Radix, "Self-compacting concrete: the role of the particle size distribution," in *First International Symposium on Design, Performance and Use of Self-Consolidating Concrete*, 2005.

[59] H. J. H. Brouwers and H. J. Radix, "Self-compacting concrete: Theoretical and experimental study," *Cement and Concrete Research,* vol. 35, no. 11, pp. 2116-2136, 2005.

[60] R. Jones, L. Zheng and M. Newlands, "Comparison of particle packing models for proportioning concrete constituents for minimum voids ratio," *Materials and Structures,* vol. 35, no. pp. 301-309, 2002.

[61] P. Pujadas, A. Blanco, S. Cavalaro and A. Aguado, "Performance-based procedure for the definition of controlled low-strength mixtures," *Journal of Materials in Civil Engineering,* vol. 27, no. 11, p. 06015003, 2015.

[62] EFNARC, "Specification and Guidelines for Self-Compacting Concrete," *Report from EFNARC,* vol. 44, no. February, p. 32, 2002.

[63] P. Domone, "Self-compacting concrete: An analysis of 11 years of case studies," *Cement and Concrete Composites,* vol. 28, no. 2, pp. 197-208, 1 2 2006.

[64] M. Sonebi, "Medium strength self-compacting concrete containing fly ash: Modelling using factorial experimental plans," *Cement and Concrete Research,* vol. 34, no. 7, pp. 1199-1208, 2004.

[65] G. Sua-Iam and N. Makul, "Use of increasing amounts of bagasse ash waste to produce self-compacting concrete by adding limestone powder waste," *Journal of Cleaner Production,* vol. 57, pp. 308-319, 2013.

[66] I. B. Topçu, T. Bilir and T. Uygunoğlu, "Effect of waste marble dust content as filler on properties of self-compacting concrete," *Construction and Building Materials,* vol. 23, no. 5, pp. 1947-1953, 2009.

[67] Z. J. Grdic, G. A. Toplicic-Curcic, I. M. Despotovic and N. S. Ristic, "Properties of self-compacting concrete prepared with coarse recycled concrete aggregate," *Construction and Building Materials,* 2010.

[68] S. C. Kou and C. S. Poon, "Properties of self-compacting concrete prepared with coarse and fine recycled concrete aggregates," *Cement and Concrete Composites,* vol. 31, pp. 622-627, 2009.

[69] S. C. Kou and C. S. Poon, "Properties of self-compacting concrete prepared with recycled glass aggregate," *Cement and Concrete Composites,* vol. 31, pp. 107-113, 2008.

[70] A. Turatsinze and M. Garros, "On the modulus of elasticity and strain capacity of Self-Compacting Concrete incorporating rubber aggregates," *Resources, Conservation and Recycling,* vol. 52, pp. 1209-1215, 2008.

[71] N. Ganesan, J. B. Raj and A. P. Shashikala, "Flexural fatigue behavior of self compacting rubberized concrete," *Construction and Building Materials,* vol. 44, pp. 7-14, 2013.

[72] H. Okamura and M. Ouchi, "Self-compacting high performance concrete," *Progress in Structural Engineering and Materials,* vol. 1, no. 4, pp. 378-

383, 1998.

[73] N. Su, K.-C. Hsu and H.-W. Chai, "A simple mix design method for self-compacting concrete," *Cement and Concrete Research,* vol. 31, no. 12, pp. 1799-1807, 2001.

[74] B. Felekoğlu, S. Türkel and B. Baradan, "Effect of water/cement ratio on the fresh and hardened properties of self-compacting concrete," *Building and Environment,* vol. 42, no. 4, pp. 1795-1802, 2007.

[75] L. Ferrara, Y. D. Park and S. P. Shah, "A method for mix-design of fiber-reinforced self-compacting concrete," *Cement and Concrete Research,* vol. 37, no. 6, pp. 957-971, 2007.

[76] M. Hunger and H. J. H. Brouwers, "Natural Stone Waste Powders Applied to SCC Mix Design," *Buildings,* vol. 14, no. 2, pp. 131-140, 2008.

[77] J. Kanadasan and H. A. Razak, "Mix design for self-compacting palm oil clinker concrete based on particle packing," *Materials and Design,* vol. 56, pp. 9-19, 2014.

[78] M. Nepomuceno, L. Oliveira and S. M. R. Lopes, "Methodology for mix design of the mortar phase of self-compacting concrete using different mineral additions in binary blends of powders," *Construction and Building Materials ,* vol. 26, no. 1, pp. 317-326, 2012.

[79] M. C. S. Nepomuceno, L. A. Pereira-De-Oliveira and S. M. R. Lopes, "Methodology for the mix design of self-compacting concrete using different mineral additions in binary blends of powders," *Construction and Building Materials,* vol. 64, pp. 82-94, 2014.

[80] Y.-s. Kim, T. M. Do, M.-J. Kim, B.-J. Kim and H.-K. Kim, "Utilization of by-product in controlled low-strength material for geothermal systems: Engineering performances, environmental impact, and cost analysis," *Journal of Cleaner Production,* vol. 172, pp. 909-920, 20 1 2018.

[81] G. Hüsken and H. J. H. Brouwers, "A new mix design concept for earth-moist concrete: A theoretical and experimental study," *Cement and Concrete Research,* vol. 38, no. 10, pp. 1246-1259, 2008.

[82] H. T. Le, M. Müller, K. Siewert and H.-M. Ludwig, "The mix design for self-compacting high performance concrete containing various mineral admixtures," *Materials & Design,* vol. 72, pp. 51-62, 2015.

[83] K. Wang, S. P. Shah, J. Grove, P. Taylor, P. Wiegand, B. Steffes, G. Lomboy, Z. Quanji, L. Gang and N. Tregge, "Self-Consolidating Concrete— Applications for Slip-Form Paving: Phase II," vol. 00011, no. May, p. 118, 2011.

[84] M. Pasetto and N. Baldo, "Recycling of waste aggregate in cement bound mixtures for road pavement bases and sub-bases," *Construction and Building Materials,* vol. 108, pp. 112-118, 2016.

[85] A. Katz and K. Klover, "Utilization of industrial by-products for the production of controlled low strength materials (CLSM)," *Waste Management,* vol. 24, no. 5, pp. 501-512, 2004.

[86] T. Raghavendra and B. C. Udayashankar, "Flow and strength characteristics of CLSM using ground granulated blast furnace slag,"

Journal of Materials in Civil Engineering, vol. 26, no. 9, p. 04014050, 2014.

[87] A. J. Puppala, B. Chittoori and A. Raavi, "Flowability and density characteristics of controlled low-strength material using native high-plasticity clay," *Journal of Materials in Civil Engineering,* vol. 27, no. 1, p. 06014026, 1 2015.

[88] S. Naganathan, H. A. Razak and S. N. A. Hamid, "Properties of controlled low-strength material made using industrial waste incineration bottom ash and quarry dust," *Materials & Design,* vol. 33, pp. 56-63, 1 1 2012.

[89] H. Wu, B. Huang, X. Shu and J. Yin, "Utilization of solid wastes/byproducts from paper mills in Controlled Low Strength Material (CLSM)," *Construction and Building Materials,* vol. 118, pp. 155-163, 8 2016.

[90] H.-Y. Wang and K.-W. Chen, "A study of the engineering properties of CLSM with a new type of slag," *Construction and Building Materials,* vol. 102, pp. 422-427, 1 2016.

[91] M. Etxeberria, J. Ainchil, M. E. Pérez and A. González, "Use of recycled fine aggregates for Control Low Strength Materials (CLSMs) production," *Construction and Building Materials,* vol. 44, pp. 142-148, 2013.

[92] A. Copeland, "Reclaimed Asphalt Pavement in Asphalt Mixtures: State of the Practice," *Report No. FHWA-HRT-11-021,* no. FHWA, pp. McLean, Virginia, 2011.

[93] A. C. Falchetto, K. H. Moon and M. P. Wistuba, "Microstructural analysis and rheological modeling of asphalt mixtures containing recycled asphalt materials," *Materials,* vol. 7, no. 9, pp. 6254-6280, 2 9 2014.

[94] G. Valdés, F. Pérez-Jiménez, R. Miró, A. Martínez and R. Botella, "Experimental study of recycled asphalt mixtures with high percentages of reclaimed asphalt pavement (RAP).," *Construction and Building Materials,* vol. 25, no. 3, pp. 1289-1297, 2011.

[95] A. Farina, M. C. Zanetti, E. Santagata and G. A. Blengini, "Life cycle assessment applied to bituminous mixtures containing recycled materials: Crumb rubber and reclaimed asphalt pavement," *Resources, Conservation and Recycling,* vol. 117, pp. 204-212, 2016.

[96] M. Zaumanis and R. B. Mallick, "Review of very high-content reclaimed asphalt use in plant-produced pavements: state of the art," *International Journal of Pavement Engineering,* vol. 16, no. 1, pp. 39-55, 2 1 2015.

[97] M. Arshad and M. F. Ahmed, "Potential use of reclaimed asphalt pavement and recycled concrete aggregate in base/subbase layers of flexible pavements," *Construction and Building Materials,* vol. 151, pp. 83-97, 1 10 2017.

[98] A. J. Puppala, S. Saride and R. Williammee, "Sustainable Reuse of Limestone Quarry Fines and RAP in Pavement Base/Subbase Layers," *Journal of Materials in Civil Engineering,* vol. 24, no. 4, pp. 418-429, 2012.

[99] R. Taha, A. Al-Harthy, K. Al-Shamsi and M. Al-Zubeidi, "Cement

stabilization of reclaimed asphalt pavement aggregate for road bases and subbases," *Journal of Materials in Civil Engineering,* vol. 14, no. June, pp. 239-245, 2002.

[100] S. Al-Oraimi, H. F. Hassan and A. Hago, "Recycling of reclaimed asphalt pavement in Portland cement concrete," *Journal of Engineering Research,* vol. 6, no. 1, pp. 37-45, 2009.

[101] B. Huang, X. Shu and G. Li, "Laboratory investigation of portland cement concrete containing recycled asphalt pavements," *Cement and Concrete Research,* vol. 35, no. 10, pp. 2008-2013, 2005.

[102] A. Abdel-Mohti, H. Shen and Y. Khodair, "Characteristics of self-consolidating concrete with RAP and SCM," *Construction and Building Materials,* vol. 102, pp. 564-573, 1 2016.

[103] A. J. Puppala, L. R. Hoyos and A. K. Potturi, "Resilient moduli response of moderately cement-treated reclaimed asphalt pavement aggregates," *Journal of Materials in Civil Engineering,* vol. 23, no. 7, pp. 990-998, 7 2011.

[104] M. Lachemi, K. M. A. Hossain, M. Shehata and W. Thaha, "Controlled low-strength materials incorporating cement kiln dust from various sources," *Cement and Concrete Composites,* vol. 30, no. 5, pp. 381-392, 5 2008.

[105] R. Siddique, "Utilization of waste materials and by-products in producing controlled low-strength materials," *Resources, Conservation and Recycling,* vol. 54, no. 1, pp. 1-8, 1 11 2009.

[106] M. A. Gabr and J. J. Bowders, "Controlled low-strength material using fly ash and AMD sludge," *Journal of Hazardous Materials,* vol. 76, pp. 251-263, 2000.

[107] A. G. G. Graziani, "Materiali da costruzione. I lapidei. struttura del settore e tendenze innovative (In Italian)," Centro Studi Osservatorio Fillea Grandi Imprese e Lavoro, Roma, 2005.

[108] L. Zichella, R. Bellopede, S. Spriano and P. Marini, "Preliminary investigations on stone cutting sludge processing for a future recovery," *Journal of Cleaner Production,* vol. 178, pp. 866-876, 3 2018.

[109] I. Mármol, P. Ballester, S. Cerro, G. Monrós, J. Morales and L. Sánchez, "Use of granite sludge wastes for the production of coloured cement-based mortars," *Cement and Concrete Composites,* vol. 32, no. 8, pp. 617-622, 1 9 2010.

[110] A. Souza, B. Pinheiro and J. Holanda, "Recycling of gneiss rock waste in the manufacture of vitrified floor tiles," *Journal of Environmental Management,* vol. 91, no. 3, pp. 685-689, 1 1 2010.

[111] S. Singh, S. Khan, R. Khandelwal, A. Chugh and R. Nagar, "Performance of sustainable concrete containing granite cutting waste," *Journal of Cleaner Production,* vol. 119, pp. 86-98, 15 4 2016.

[112] G. Medina, I. Sáez del Bosque, M. Frías, M. Sánchez de Rojas and C. Medina, "Granite quarry waste as a future eco-efficient supplementary cementitious material (SCM): Scientific and technical considerations,"

Journal of Cleaner Production, vol. 148, pp. 467-476, 1 4 2017.

[113] N. Careddu, G. Marras and G. Siotto, "Recovery of sawdust resulting from marble processing plants for future uses in high value-added products," *Journal of Cleaner Production,* vol. 84, pp. 533-539, 1 12 2014.

[114] M. J. Munir, S. M. S. Kazmi, Y.-F. Wu, A. Hanif and M. U. A. Khan, "Thermally efficient fired clay bricks incorporating waste marble sludge: An industrial-scale study," *Journal of Cleaner Production,* vol. 174, pp. 1122-1135, 10 2 2018.

[115] I. S. Buyuksagis, T. Uygunoglu and E. Tatar, "Investigation on the usage of waste marble powder in cement-based adhesive mortar," *Construction and Building Materials,* vol. 154, pp. 734-742, 15 11 2017.

[116] T. G. Soosan, A. Sridharan, B. T. Jose and B. M. Abraham, "Utilization of quarry dust to improve the geotechnical properties of soils in highway construction," *Geotechnical Testing Journal,* 2005.

[117] S. Raman, T. Ngo, P. Mendis and H. Mahmud, "High-strength rice husk ash concrete incorporating quarry dust as a partial substitute for sand," *Construction and Building Materials,* vol. 25, no. 7, pp. 3123-3130, 1 7 2011.

[118] H. Dehwah, "Mechanical properties of self-compacting concrete incorporating quarry dust powder, silica fume or fly ash," *Construction and Building Materials,* vol. 26, no. 1, pp. 547-551, 1 1 2012.

[119] EN 933-1, "Tests for geometrical properties of aggregates - Part 1: Determination of particle size distribution - Sieving method," CEN European Committee for Standardization, Brussels.

[120] EN 1097-6, "Tests for mechanical and physical properties of aggregates - Part 6: Determination of particle density and water absorption," CEN European Committee for Standardization., Brussels.

[121] EN 12697-39, "Bituminous mixtures. Test methods for hot mix asphalt. Part 39: Binder content by ignition," CEN European Committee for Standardization, Brussels.

[122] EN 197-1, "Cement - Part 1: Composition, specifications and conformity criteria for common cements," CEN European Committee for Standardization, Brussels.

[123] ASTM D6103/D6103M-17, "Standard test method for flow consistency of controlled low strength material (CLSM)," ASTM International, West Conshohocken, PA.

[124] AASHTO T 307-99, "Standard method of test for determining the resilient modulus of soils and aggregate materials.," American Association of State and Highway Official, Washington, DC, 2017.

[125] F. Lekarp, U. Isacsson and A. Dawson, "State of the art I: Resilient response of unbound aggregates," *Journal of Transportation Engineering,* vol. 126, no. 1, pp. 66-75, 2000.

[126] R. Pratibha, G. Sivakumar Babu and G. Madhavi Latha, "Stress–strain response of unbound granular materials under static and cyclic loading," *Indian Geotechnical Journal,* vol. 45, no. 4, pp. 449-457, 2015.

[127] J.-P. Bilodeau, C. Plamondon and G Doré, "Estimation of resilient modulus of unbound granular materials used as pavement base: combined effect of grain-size distribution and aggregate source frictional properties," *Materials and Structures,* vol. 49, no. 10, p. 4363–4373, 2016.

[128] E. Santagata, G. Chiappinelli, P. Riviera and O. Baglieri, "Triaxial testing for the short term evaluation of cold-recycled bituminous mixtures.," *Road Materials and Pavement Design,* vol. 11, no. 1, pp. 123-147, 2010.

[129] S. Fatemi and R. Imaninasab, "Performance evaluation of recycled asphalt mixtures by construction and demolition waste materials," *Construction and Building Materials,* vol. 120, pp. 450-456, 2016.

[130] R. G. Hicks and C. L. Monismith, "Factors Influencing the resilient properties of granular materials," Transportation Research Board of the National Academies, Washington, DC, 1971.

[131] J. Uzan, "Characterization of granular materials No.1022," Transportation Research Board of the National Academies, Washington, DC, 1985.

[132] Y. H. Huang, Pavement analysis and design, NJ: Pearson, 2004.

[133] CIRS, *Performance-related technical specifications for the construction and maintenance of road pavements. Interuniversity Road and Airport Research Center,,* Ancona, Italy (in Italian), 2001.

[134] ZTVE-StB, "Additional technical contractual conditions and guidelines for earthwork in road construction and technical instructions for soil and rock in road construction,," Research Society of Road and Traffic, Germany, 2004.

[135] AASHTO, "Mechanistic-empirical pavement design guide – A manual of practice," AASHTO, Washington, DC, 2008.

[136] ASTM D1633-17, "Standard Test Methods for Compressive Strength of Molded Soil-Cement Cylinders,," ASTM International., West Conshohocken, PA, 2017.

[137] C. Pierce, H. Tripathi and T. Brown, "Cement kiln dust in controlled low-strength materials, 100(6) (2003)," *ACI Materials Journal,* vol. 100, no. 6, pp. 455-462, 2003.

[138] D. Trejo, K. Folliard and L. Du, "Sustainable development using controlled low-strength material," in *Proceedings of International Workshop on Sustainable Development and Concrete Technology*, 2004.

[139] J. Funk and D. Dinger, Predictive process control of crowded particulate suspension applied to ceramic manufacturing, ISBN 978-0-7923-9409-9,Springer US, 1994.

[140] V. Senthil Kumar and M. Santhanam, "Particle packing theories and their application in concrete mixture proportioning," *Indian Concrete Journal,* vol. 77, no. 9, pp. 1324-1331., 2003.

[141] A. R. Dawson, J. Mundy M and M. Huhtala, "European research into granular material for pavement bases and subbases," *Transportation Research Record,* vol. 1721, no. 1, pp. 91-99, 2000.

[142] A. Nataatmadja and Y. L. Tan, "Resilient response of recycled concrete road aggregates," *Journal of Transportation Engineering,* vol. 127, no. 5,

pp. 450-453, 2001.

[143] P. Kumar, S. Chandra and R. Vishal, "Comparative study of different subbase materials," *Journal of Materials in Civil Engineering,* vol. 18, no. 4, pp. 576-580, 2006.

[144] L. N. Mohammad, A. Raghavandra and B. Huang, "Laboratory performance evaluation of cement-stabilized soil base mixtures," *Transportation Research Record,* vol. 1721, no. 1, p. 19–28, 2000.

[145] A. Ardah, Q. Chen and M. Abu-Farsakh, "Evaluating the performance of very weak subgrade soils treated/stabilized with cementitious materials for sustainable pavements," *Transportation Geotechnics,* vol. 11, pp. 107-119, 2017.

[146] P. Chindaprasirt, S. Hatanaka, T. Chareerat, N. Mishima and Y. Yuasa, "Cement paste characteristics and porous concrete properties," *Construction and Building Materials,* vol. 108 22, no. 5, pp. 894-901, 2008.

[147] A. Mohammadinia, A. Arulrajah, J. Sanjayan, M. M. Disfani, M. W. Bo and S. Darmawan, "Laboratory evaluation of the use of cement-treated construction and demolition materials in pavement base and subbase applications," *Journal of Materials in Civil Engineering,* vol. 27, no. 6, p. 04014186, 2015.

[148] W. Fedrigo, W. P. Núñez, M. A. Castañeda López, T. R. Kleinert and J. A. P. Ceratti, "A study on the resilient modulus of cement-treated mixtures of RAP and aggregates using indirect tensile, triaxial and flexural tests," *Construction and Building Materials,* vol. 171, pp. 161-169, 20 5 2018.

[149] M. Bassani, P. P. Riviera and L. Tefa, "Short-Term and Long-Term Effects of Cement Kiln Dust Stabilization of Construction and Demolition Waste," *Journal of Materials in Civil Engineering,* vol. 29, no. 5, p. 04016286, 5 2017.

[150] A. J. Puppala, L. N. Mohammad and A. Allen, "Engineering behavior of lime-treated Louisiana subgrade soil," *Transportation Research Record: Journal of the Transportation Research Board,* vol. 1546, no. 1, pp. 24-31, 1 1 1996.

[151] M. Rerak and P. Ocłoń, "The effect of soil and cable backfill thermal conductivity on the temperature distribution in underground cable system," in *E3S Web of Conferences 13, 02004*, 2017.

[152] A. Scola, "Method of manufacture and installation flowable thermal backfills". United States of America Patent 7581903 B1 , 2009.

[153] P. Ocłoń, P. Cisek, M. Pilarczyk and D. Taler, "Numerical simulation of heat dissipation processes in underground power cable system situated in thermal backfill and buried in a multilayered soil," *Energy Conversion and Management,* vol. 95, no. March, pp. 352-370, 2015.

[154] M. Gangadhara Rao, P. Kolay and D. Singh, "Thermal characteristics of a class F fly ash," *Cement and Concrete Research,* vol. 28, no. 6, p. 841–846, 1998.

[155] J. A. Williams, D. Parmar and M. W. Conroy, "Controlled backfill

optimization to achieve high ampacities on transmission cables," *IEEE Transactions on Power Delivery,* vol. 9, no. 1, pp. 544-552, 1994.

[156] J. C. H. Célestin and M. Fall, "Thermal conductivity of cemented paste backfill material and factors affecting it," *International Journal of Mining, Reclamation and Environment,* vol. 23, no. 4, pp. 274-290, 2009.

[157] E. C. Rusty Bascom, N. Patel and D. Parmar, "Thermal environment design considerations for ampacity of buried power cables," in *2014 IEEE PES T&D Conference and Exposition*, 2014.

[158] P. Kolay and D. Singh, "Application of coal ash in fluidized thermal beds," *Journal of Materials in Civil Engineering,* vol. 14, no. 5, pp. 441-444, 2002.

[159] S. A. Boggs, F. Y. Chu, H. Radhakrishna and J. E. Steinmanis, "Underground cable thermal backfill," in *Proceedings of the Symposium on Underground Cable Thermal Backfill*, Toronto, Canada, 1981.

[160] Electric power research institute Inc, "Increased power flow guidebook-underground cables, Final report," December 2003.

[161] L. A. Salomone and W. D. Kovacs, "Thermal resistivity of soils," *Journal of Geotechnical Engineering,* vol. 110, no. 3, pp. 375-389, 1984.

[162] IEEE 442-1981, "IEEE guide for soil thermal resistivity measurements," 2003.

[163] J. H. Neher and M. H. McGrath, "The calculation of the temperature rise and load capability of cable systems," *AIEE Transactions, Part III,* vol. 76, p. 752–772, 1957.

[164] C. Bates, K. Malmedal and D. Cain, "Cable ampacity calculations: A comparison of methods," *IEEE Transactions on Industry Applications,* vol. 52, no. 1, pp. 112-118, 2016.

[165] H. Vikan and H. Justnes, "Rheology of cementitious paste with silica fume or limestone," *Cement and Concrete Research,* vol. 37, no. 11, pp. 1512-1517, 2007.

[166] J. Côté and J.-M. Konrad, "A generalized thermal conductivity model for soils and construction materials," *Canadian Geotechnical Journal,* vol. 42, no. 2, pp. 443-458, 2005.

[167] Science education research centre, "Geochemical instrumentation and analysis,"[Online] Available:https://serc.carleton.edu/research_education/geochemsheets/techniques/SEM.html. [Accessed 14 October 2019].

[168] US EPA, "Method 3051A (SW-846): Microwave assisted acid digestion of sediments, sludges, and oils," Washington, DC, 2007.

[169] Legislative Decree 3 April 2006 n 152, "Environmental regulations," Published in the Official Gazette n. 88 of April 14th 2006 - Ordinary Supplement n. 96, 2006.

[170] US EPA, "6020A, Inductively coupled plasma-mass spectrometry," US EPA, Washington, DC, 2007.

[171] M. Huang, H. Feng, D. Shen, N. Li, Y. Chen and J. Shentu, "Leaching behavior of heavy metals from cement pastes using a modified toxicity

characteristic leaching procedure (TCLP)," *Bulletin of Environmental Contamination and Toxicology,* vol. 96, no. 3, pp. 354-360, 18 3 2016.

[172] C. S. Poon, A. I. Clark, C. J. Peters and R. Perry, "Mechanism of metal fixation and leaching by cement based fixation processes," *Waste Management & Research,* vol. 3, pp. 127-142, 1985.

[173] W. Fuller and S. Thompson, "The laws of proportioning concrete," *Transactions of American Society of Civil Engineering,* vol. 33, pp. 223-298, 1907.

[174] ASTM D5334, "Standard Test Method for Determination of Thermal Conductivity of Soil and Soft Rock by Thermal Needle Probe Procedure," ASTM International., West Conshohocken, PA, 2014.

[175] A. G. Mengistu, L. D. van Rensburg and S. S. Mavimbela, "The effect of soil water and temperature on thermal properties of two soils developed from aeolian sands in South Africa," *Catena,* vol. 158, pp. 184-193, 2017.

[176] J. H. Neher and M. H. McGrath, "The calculation of the temperature rise and load capability of cable systems," *Transactions of the American Institute of Electrical Engineers. Part III: Power Apparatus and Systems,* vol. 76, no. 3, pp. 752-764, 1957.

[177] I. Türkmen, R. Demirboğa and R. Gül, "The effects of different cement dosages, slumps and pumice aggregate ratios on the freezing and thawing of concrete," *Computers and Concrete,* vol. 3, no. 2-3, pp. 163-175, 1 5 2006.

[178] K.-H. Kim, S.-E. Jeon, J.-K. Kim and S. Yang, "An experimental study on thermal conductivity of concrete," *Cement and Concrete Research,* vol. 33, no. 3, pp. 363-371, 2003.

[179] M. I. Khan, "Factors affecting the thermal properties of concrete and applicability of its prediction models," *Building and Environment,* vol. 37, no. 6, pp. 607-614, 2002.

[180] B. Shinghan-Roy, "Research on several physico-mechanical properties of lightweight aggregate concrete. 2(4), ()," *International Journal of Cement Composits and Lightweight Concrete,* vol. 2, no. 4, pp. 185-191, 1980.

[181] B. J. Kim, J. G. Jang, C. Y. Park, O. H. Han and H. K. Kim, "Recycling of arsenic-rich mine tailings in controlled low-strength materials," *Journal of Cleaner Production,* vol. 118, pp. 151-161, 2016.

[182] S.-Y. Hong and F. Glasser, "Alkali sorption by C-S-H and C-A-S-H gels: Part II. Role of alumina," *Cement and Concrete Research,* vol. 32, no. 7, pp. 1101-1111, 1 7 2002.

[183] M. Adresi, A. khishdari, A. Ahmadi and H. Rooholamini, "Influence of high content of reclaimed asphalt on the mechanical properties of cement-treated base under critical environmental conditions," *International Journal of Pavement Engineering,* vol. 20, no. 9, pp. 1098-1105, 2 9 2019.

[184] S. Singh, K. Monu and G. D. Ransinchung R. N., "Laboratory investigation of RAP for various layers of flexible and concrete pavement," *International Journal of Pavement Engineering,* pp. 1-14, 24 1 2019.

[185] F. Bell, “Lime stabilization of clay minerals and soils,” *Engineering Geology,* vol. 42, no. 4, pp. 223-237, 1 7 1996.

[186] A. K. Jha and P. Sivapullaiah, “Mechanism of improvement in the strength and volume change behavior of lime stabilized soil,” *Engineering Geology,* vol. 198, pp. 53-64, 23 11 2015.

[187] M. Rosone, C. Celauro and A. Ferrari, “Microstructure and shear strength evolution of a lime-treated clay for use in road construction,” *International Journal of Pavement Engineering,* pp. 1-12, 20 9 2018.

[188] E. Choorackal, P. P. Riviera and E. Santagata, “Mix design and mechanical characterization of self-compacting cement-stabilized mixtures for paving applications.,” *Construction and Building Materials,* vol. 229, 2019.

[189] M. Uysal and K. Yilmaz, “Effect of mineral admixtures on properties of self-compacting concrete,” *Cement and Concrete Composites,* vol. 33, no. 7, pp. 771-776, 2011.

[190] ASTM C231/C231M-17a, “Standard test method for air content of freshly mixed concrete by the pressure method,,” ASTM International, West Conshohocken, PA, 2017.

[191] DIN 18134: 2012-4, “Determining the deformation and strength characteristics of soil by the plate loading test.,” Technical Committee 05.03.00 Baugrund, Versuche und Versuchsgeräte of the Normenausschuss Bauwesen, 2012.

[192] EN 12390-2 Part 2, “Testing hardened concrete - Part 2, Making and curing specimens for strength tests,” European Committee for Standardization, Brussels:, 2009.

[193] EN 12390 Part 3, “Testing hardened concrete - Compressive strength of test specimens,” European Committee for Standardization, Brussels, 2009.

[194] S. Fatemi and R. Imaninasab, “Performance evaluation of recycled asphalt mixtures by construction and demolition waste materials,” *Construction and Building Materials,* vol. 120, pp. 450-456, 1 9 2016.

[195] J.-K. Kim, Y.-H. Moon and S.-H. Eo, “Compressive strength development of concrete with different curing time and temperature,” *Cement and Concrete Research,* vol. 28, no. 12, pp. 1761-1773, 1 12 1998.

[196] A. Mohammadinia, A. Arulrajah, J. Sanjayan, M. M. Disfani, M. Win Bo and S. Darmawan, “Stabilization of demolition materials for pavement base/subbase applications using fly ash and slag geopolymers: laboratory Investigation,” *Journal of Materials in Civil Engineering,* vol. 28, no. 7, p. 04016033, 7 2016.

[197] A. R. Dawson, M. J. Mundy and M. Huhtala, “European research into granular material for pavement bases and subbases,” *Transportation Research Record: Journal of the Transportation Research Board,* vol. 1721, no. 1, pp. 91-99, 1 1 2000.

[198] A. Nataatmadja and Y. L. Tan, “Resilient Response of Recycled Concrete Road Aggregates,” *Journal of Transportation Engineering,* vol. 127, no. 5, pp. 450-453, 10 2001.

[199] K. H. Mamatha and S. V. Dinesh, "Evaluation of strain modulus and deformation characteristics of geosynthetic-reinforced soil – aggregate system under repetitive loading," *International Journal of Geotechnical Engineering,* pp. 1-10, 7 4 2017.

[200] Y.-J. Choi, D. Ahn, T. Nguyen and J. Ahn, "Assessment of field compaction of aggregate base materials for permeable pavements based on plate load tests," *Sustainability,* vol. 10, no. 10, p. 3817, 22 10 2018.

[201] H. Theyse and M. Muthen, "Pavement analysis and design software (PADS) based on the South African mechanistic-empirical design method.," SATC, 2000.

[202] RVS, "Projektierungsrichtlinien - Bauliche Gestaltung - Tunnel," Bundesministerium für Verkehr, Innovation und Technologie,, 2001.

[203] P. E. Stephen Tofler, "Review of Overseas Tunnels," Austroads, Sydney, 2015.

[204] FEHRL, "Making best use of long-life pavements in Europe, ELLPAG PHASE 2: A guide to the use of long-life semi-rigid pavements," FEHRL Secretariat, Brussels, Belgium, 2009.

[205] ASTM C 490, "Standard practice for use of apparatus for the determination of length change of hardened cement paste, mortar, and concrete," ASTM International, West Conshohocken, PA;, 2017.

[206] M. Nataraja and Y. Nalanda, "Performance of industrial by-products in controlled low-strength materials (CLSM)," *Waste Management,* vol. 28, p. 1168–1181, 2008.

[207] N. Lee, J. Jang and H. Lee, "Shrinkage characteristics of alkali-activated fly ash/slag paste and mortar at early ages," *Cement and Concrete Composites,* vol. 53, pp. 239-248, 1 10 2014.

[208] ASTM D 560-16, "Standard test methods for freezing and thawing compacted soil-cement mixtures.," ASTM International, West Conshohocken, PA;, 2016.

[209] S. Achtemichuk, J. Hubbard, R. Sluce and M. H. Shehata, "The utilization of recycled concrete aggregate to produce controlled low-strength materials without using Portland cement," *Cement and Concrete Composites,* vol. 31, no. 8, pp. 564-569, 1 9 2009.

[210] J. Canto-Perello, J. Curiel-Esparza and V. Calvo, "Analysing utility tunnels and highway networks coordination dilemma," *Tunnelling and Underground Space Technology,* vol. 24, no. 2, pp. 185-189, 1 3 2009.

[211] CNR, "Catalogo delle Pavimentazioni Stradali, CNR-BU 154," Consiglio Nazionale delle Ricerche, Rome, Italy., 1995.

[212] Shell (1998) BISAR 3.0. Shell International Oil Products BV, The Netherlands

[213] WSDOT, "Everseries user's guide – pavement analysis computer software and case studies," Washington State Department of Transportation, USA, 2005.

[214] F. Bonnaure, G. Gest, A. Gravois and P. Uge, "A new method of predicting the stiffness of asphalt paving mixtures," in *Proceedings of the*

Association of Asphalt Paving Technologists, 1977.